Aalto University
School of Electrical Engineering
Degree program in Communications Engineering

Teemu Veijalainen

Beam steering in millimeter wave radio links for small cell mobile backhaul

Master's Thesis
Espoo, 17.5.2014

Supervisor: Professor Jukka Manner
Instructor: M.Sc. (Tech.) Pekka Wainio

Author: Teemu Veijalainen

Subject of the thesis: Beam steering in millimeter wave radio links for small cell mobile backhaul

Date: Language: English Number of pages: 92+9

Department of Communications and Networking

Professorship: Communications Engineering
Code of professorship: S-72

Supervisor: Prof. Jukka Manner

Instructor: M.Sc. (Tech.) Pekka Wainio

The mobile data volumes are constantly increasing setting new challenges for the networks to keep up with the demand. One source of improved network performance comes with the extreme cell densification also known as small cells.

The small cell deployment creates new challenges for the backhaul. As the small cells are located in city areas of high demand in unconventional installation sites such as lamp posts and building walls; the provisioning of the conventional wired backhaul might be unreasonable.

Potential solutions for the small cell backhaul are technologies utilizing millimeter-wave frequencies on 60, 70/80 GHz providing several gigahertz of low cost spectrum. The millimeter-wave frequencies need narrow antenna beams, less than a few degrees, to compensate the high signal attenuations on these frequencies. The narrow beam radio links need vibration compensation mechanisms to compensate the sways and twist of the installation structure caused by wind. Additionally, the narrow beam radio links should automatically establish the connection to avoid time consuming and expensive manual link alignment. Therefore, beam steering is needed denoting that the device can switch the direction of the antenna beam.

The main scope of this master's thesis is to identify the possibilities, challenges and limitations of the potential beam steering methods. The practical part of this thesis included implementation of the beam steering functionalities to a proof-of-concept millimeter-wave small cell backhaul system developed by Nokia Solutions and Networks. The author's conducted tests confirmed the functionality of the methods and provided suggestions for the future development of the system.

Keywords: small cell, millimeter-wave, beam steering, vibration compensation, backhaul

Tekijä: Teemu Veijalainen

Työn nimi: Millimetrialueen taajuuksien antennikeilan ohjausmenetelmät piensoluverkkojen runkokytkennälle
Päivämäärä: Kieli: englanti Sivumäärä: 92+9

Tietoliikenne- ja tietoverkkotekniikan laitos

Professuuri: Tietoliikennetekniikka
Koodi: S-72

Valvoja: Prof. Jukka Manner

Ohjaaja: DI Pekka Wainio

Mobiiliverkkojen dataliikenne kasvaa jatkuvasti. Tulevaisuuden mobiiliverkot kohtaavat uusia haasteita täyttääkseen jatkuvan kasvun asettamat vaatimukset. Yksi mahdollinen tapa parantaa mobiiliverkkojen suorituskykyä on piensoluverkkojen hyödyntäminen, joissa tukiasemat sijaitsevat lähellä toisiaan.
Piensoluverkkojen tukiasemat asennetaan epätavallisiin sijainteihin kuten katuvaloihin ja rakennusten seiniin. Piensoluverkkojen tukiasemien epätyypilliset sijainnit asettavat uusia haasteita verkon runkokytkennän toteuttamiselle.
Potentiaalinen ratkaisu piensoluverkkojen runkokytkennän toteuttamiseksi on millimetrialueen taajuuksien hyödyntäminen. Millimetrialueen taajuuksilla tarkoitetaan tässä yhteydessä 60 ja 70/80 GHz taajuuksia jotka tarjoavat usean gigahertsin lisensoimatonta ja kevyesti lisensoitua taajuuskaistaa.
Millimetrialueen taajuuksilla on korkeat signaalivaimennukset. Teknologiat näillä taajuuksilla tarvitsevat korkean antennivahvistuksen vaimennusten kompensoimiseen. Tämä tarkoittaa sitä että antennin keilanleveys on erittäin kapea.
Kapeat antennikeilat tarvitsevat antennikeilan ohjausmenetelmiä muun muassa tuulesta aiheutuvan vibraation kompensoimiseen ja yhteyden muodostamiseen automaattisesti toisen kapeakeilaisen laitteen kanssa, jotta radiolinkkiä ei tarvitse kohdistaa manuaalisesti.
Tämän opinnäytetyön päätavoite on kehittää antennikeilan ohjausmenetelmiä Nokia Solutions and Networksin kehittämään millimetrialueen taajuuksilla toimivalle piensoluverkon runkokytkentälaitteelle. Työn tulokset vahvistivat konseptin toimivuuden ja antoivat lupaavia tuloksia antennikeilan ohjausmenetelmien jatkokehitykselle.

Avainsanat: piensolu, millimetrialueen taajuudet, antennikeilan ohjaus, vibraatiokompensointi, mobiiliverkon runkokytkentä

Preface

This Master's Thesis completes my studies in the Aalto University School of Electrical Engineering. The work has been done for Nokia Solutions and Networks between September 2013 and April 2014.

I want to thank Professor Jukka Manner and M.Sc (Tech.) Pekka Wainio for the valuable feedback, guidance and for the opportunity of making this thesis. Additionally, I want to thank M.Sc (Tech.) Juha Nurmiharju and everyone else from Nokia Solutions and Networks who gave me feedback and guidance for the writing of this thesis and for supporting my contribution to the system development.

Finally, special thanks go to my fellow students Antti, Ville, Joonas and Riikka who supported me throughout the years in the University.

Espoo, April 2014
Teemu Veijalainen

Contents

List of abbreviations

1G	First Generation Mobile Network
2G	Second Generation Mobile Networks
3G	Third Generation Mobile Networks
3GPP	Third Generation Partnership Project
4G	Fourth Generation Mobile Networks
AC	Authentication Center
ADSL	Asymmetric Digital Subscriber Line
AMPS	Advanced Mobile Phone System
ATM	Asynchronous Transfer Mode
BICN	Bearer Independent Core Network
BSC	Base Station Controller
BSP	Beam Steering Processor
BSS	Base Station Sub-System
BTS	Base Transceiver Station
CDMA	Code Division Multiple Access
CN	Core Network
CoMP	Coordinated Multi-Point
EDGE	Enhanced Data rates for GSM Evolution
EIR	Equipment Identity Register
EIRP	Equivalent Isotropically Radiated Power
eNode-B	Evolved Node-B
EPS	Evolved Packer Core
E-UTRAN	Evolved UTRAN
FDMA	Frequency Division Multiple Access
GGSN	Gateway GPRS Support Node
GNSS	Global Navigation Satellite System
GPRS	General Packer Radio Service
GSM	Global System for Mobile Communications
GUI	Graphical User Interface
HLP	Higher Layer Protocols
HLR	Home Location Register

HSDPA	High Speed Downlink Packet Access
HSPA	High Speed Packet Access
HSS	Home Subscriber Server
HSUPA	High Speed Uplink Packet Access
ILA	Integrated Lens Antenna
IMS	IP Multimedia Sub-System
IMT-2000	International Mobile Telecommunications 2000
IMT-A	International Mobile Telecommunications Advanced
IP	Internet Protocol
IS-95	Interim Standard 95
ITU	International Telecommunication Union
LOS	Line-Of-Sight
LTE	Long Term Evolution
MBH	Mobile Backhaul
MC-HSPA	Multi Carrier HSPA
MIMO	Multiple Input Multiple Output
MME	Mobile Management Entity
MPLS	Multiprotocol Layer Switching
MSC	Mobile Switching Center
NGMN	Next Generation Mobile Networks
NLOS	Non-Line-Of-Sight
NMT	Nordic Mobile Telephone
NSN	Nokia Solutions and Networks
NSS	Network Sub-System
OFDMA	Orthogonal Frequency Division Multiple Access
PCRF	Policy and Charging Control Function
PCU	Packet Control Unit
PDC	Personal Digital Cellular System
PDH	Plesiochronous Digital Hierarchy
P-GW	PDN-Gateway
RNC	Radio Network Controller
RNS	Radio Network Sub-System
RSSI	Received Signal Strength Indicator

SAE	System Architecture Evolution
SDH	Synchronous Digital Hierarchy
SGSN	Serving GPRS Support Node
S-GW	Serving Gateway
SON	Self-Organizing Network
Sonet	Synchronous Optical Networking
TACS	Total Access Communications Systems
TDD	Time Division Duplexing
TDD	Time Division Duplexing
TDM	Time Division Multiplexing
TDMA	Time Division Multiple Access
TCO	Total Cost of Ownership
UART	Universal Asynchronous Receiver Transmitter
UE	User Equipment
UMTS	Universal Mobile Telecommunications System
UTRAN	Universal Terrestrial Radio Access Network
VLR	Visitor Location Register
W-CDMA	Wideband-CDMA
WLAN	Wireless Local Arena Network
WPAN	Indoor Wireless Personal Area Network

1 Introduction

The mobile data volumes keep increasing while continuously demanding more from the mobile networks. Constant technological improvements and innovations are required to keep up with the growth. Small cells located on close proximity in city areas of high demand improve the network performance; however, creating a challenge for the backhaul. Due to the high number and unconventional locations of the small cell base stations, wireless backhaul solutions become in question. Potential technologies for the small cell backhaul are the millimeter-wave frequencies on 60 and 70/80 GHz providing a great deal of low cost spectrum. Due to the features of these frequencies, the antenna beams are narrow, requiring beam steering capabilities from the system to automatically align the radio link and to compensate temporary misalignments caused by the vibrations of the installation structure. The main scope of this master's thesis is to identify the challenges, possibilities and limitations of beam steering methods in millimeter-wave small cell backhaul. Additionally, the beam steering methods are implemented into a proof-of-concept system provided by Nokia Solutions and Networks to study and verify the implemented methods and to give suggestions for future work.

1.1 Background

The mobile data volumes experienced an exponential increase during the past few years and are expected to continue the growth in the near future. The forecasted data volumes [1] [2] [3] [4] suggests that the current mobile networks fall short of capacity and performance. A variety of different technological enhancements and innovations has been proposed to fulfill the demands of future networks, one of which is the cell densification also known as small cells. In a typical small cell scenario, the base stations are located in city areas of high demand with the distance ranging from tens of meters to a few hundreds of meters from each. Typical installation sites for the small cell base

station are for instance building walls and light poles. The high number of small cells in unconventional locations sets new challenges for the small cell backhaul. [5] [6]

1.2 Problem statement

Due to the untypical installation structures and high number of small cells, the extension of a conventional wired backhaul to a typical small cell site might become unreasonable. Therefore, wireless solutions play an important role when selecting the small cell backhaul solution. New problems arise when implementing reliable, low cost and high capacity backhaul. First, the high speed radio links require a great deal of spectrum. Second, due to the high number of base stations, the total cost of ownership (TCO) should be kept at minimum level; including expenses generated from the backhaul device, spectrum licensing, installation and maintenance. Third, interference between the closely located devices should be kept at minimum level. [5] [6] [7]

In the context of small cell backhaul, millimeter-wave frequencies denote the 60 and 70/80 GHz frequencies. These frequencies provide promising features to fulfill the requirements of the small cell backhaul. Depending on the nation, millimeter-wave frequencies provide several gigahertz of unlicensed or lightly licensed spectrum denoting that the high speed radio links are deployable with minimum effort and cost. The millimeter-wave frequencies suffer from high signal attenuations due to free space path loss, atmospheric absorption and rain. To overcome the attenuations, high antenna gain is required. For instance, to achieve a radio link of a few hundred meters in distance, antenna gain over 30 dBi might be required. Antenna gain of this magnitude decreases the antenna beam width to less than a few degrees. The high signal attenuation and the narrow beam width decreases the interference generated to other nearby devices on the same frequency. [8] [9] [10] [11]

Despite the promising features of millimeter-wave frequencies, some challenges are included. The narrow antenna beams get easily misaligned; especially if the devices are mounted on a structure like lamp post that might experience sways

and twists due to wind that vibrates the installation structure. Additionally, to keep the installation and maintenance costs low, the device should provide a plug and play feature connecting the narrow beam radio links automatically when the power of the device is switched on. Afterwards, the small cell backhaul should automatically connect to devices that are brought within its reach. The automatic link alignment and vibration compensation require the capability of changing the direction of the narrow antenna beam. The switching of the beam direction is called beam steering. This thesis investigates the problems and solutions of millimeter-wave beam steering for small cell backhaul including the investigation of beam steerable antennas, automatic link alignment and vibration compensation. [5] [6] [7]

1.3 Authors contribution and test result overview

The main scope of this master's thesis is to identify the possibilities, challenges and limitations of the potential beam steering methods. The practical part of this thesis included implementation of the beam steering functionalities to a proof-of-concept millimeter-wave small cell backhaul system developed by Nokia Solutions and Networks. The main author's contribution in the system has been:

- drafting the limitations, challenges and possibilities of the beam steering methods in the millimeter-wave small cell backhaul concept
- the software development, implementation and testing of the automatic link alignment and author's invented vibration compensation methods implemented on the beam steering processor
- the creation and software development of the MATLAB functions and graphical user interface for the development and visualization of the beam steering methods

The beam steering tests included the automatic link alignment test and vibration compensation test with three different methods implemented. Overall, the test of the proof-of-concept system showed promising results. Despite the non-idealities of the system still under development, the automatic link

alignment and the vibration compensation tests demonstrated that the system has potential to fulfill the long term objectives of the project.

1.4 Structure

This master's thesis consists of five main chapters. Chapter 2 gives the data forecasts of the future mobile networks to justify the need for the enhancements of the future mobile networks. Additionally, the evolution of the mobile networks is introduced from the first generation networks towards the emerging fourth generation networks and beyond. Chapter 3 introduces the concept of small cell backhaul with its requirements, challenges and deployment possibilities. Chapter 4 discusses the millimeter-wave frequencies as a solution for the small cell backhaul. The features of these frequencies are introduced giving their advantages and disadvantages for the small cell backhaul. Additionally, the beam steering concept is introduced giving suggestions for the implementation of automatic link alignment and vibration compensation methods. Chapter 5 introduces the proof-of-concept small cell backhaul beam steering system with the author's contribution. Finally, Chapter 6 introduces the author's conducted tests and test results of the proof-of-concept system with suggestion for future work.

2 Mobile traffic and network evolution

This chapter provides an overview of mobile network evolution and examines the future outlook of the networks. First, the expansion of mobile data volumes with the future data forecast is studied. Second, the evolution of mobile networks is provided explaining the evolution from analog voice services to emerging all IP mobile broadband networks. Third, the future outlook of mobile networks is investigated with possible solutions to fulfill the requirements of future mobile networks.

2.1 Mobile traffic evolution

Due to the increasing number of mobile subscriptions together with the increasing amount of data consumed by each user, data volumes in mobile networks experienced an exponential growth during the past few years. The growth is enabled by the widespread adoption of wireless broadband technologies together with the success of smart devices such as smartphones, tablets and mobile PCs. The versatile features of these smart devices enable users to consume larger amounts of data through music and video streaming, social networks, cloud-based synchronization, Web applications, Web browsing, content downloading etc.

Various studies indicate that the mobile traffic volumes continue the exponential growth in the near future [1] [2] [3] [4]. Figure 1 illustrates a mobile traffic forecast by the year 2018 from Ericsson Mobility Report [3]. According to the report, mobile data exceeded voice traffic in 2009 and the data consumption is growing in a steady state while the growth of the voice traffic remains moderate. The mobile data traffic is expected to grow around 50 percent each year from 2012 to 2018; resulting in approximately a 12-fold increase by the year 2018. Similar evidence is provided by Cisco's white paper [4] forecasting a 13-fold increase in the mobile data traffic by the year 2017 with a 7-fold increase in the average network speeds (from 526kbps to

3.9Mbps) and 8-fold increase in the average consumed data by user (from 342MB per month to 2.7GB per month). Another data traffic forecast is provided by Nokia Solutions and Networks (NSN) claiming that mobile networks should prepare to support up to a 1000-fold increase in total mobile traffic by the year 2020 [2]. The magnitude of the data growth varies between the different data forecasts. However, there is a consensus with the fast data growth in the near future requiring research and development effort to cope with the future mobile data volumes.

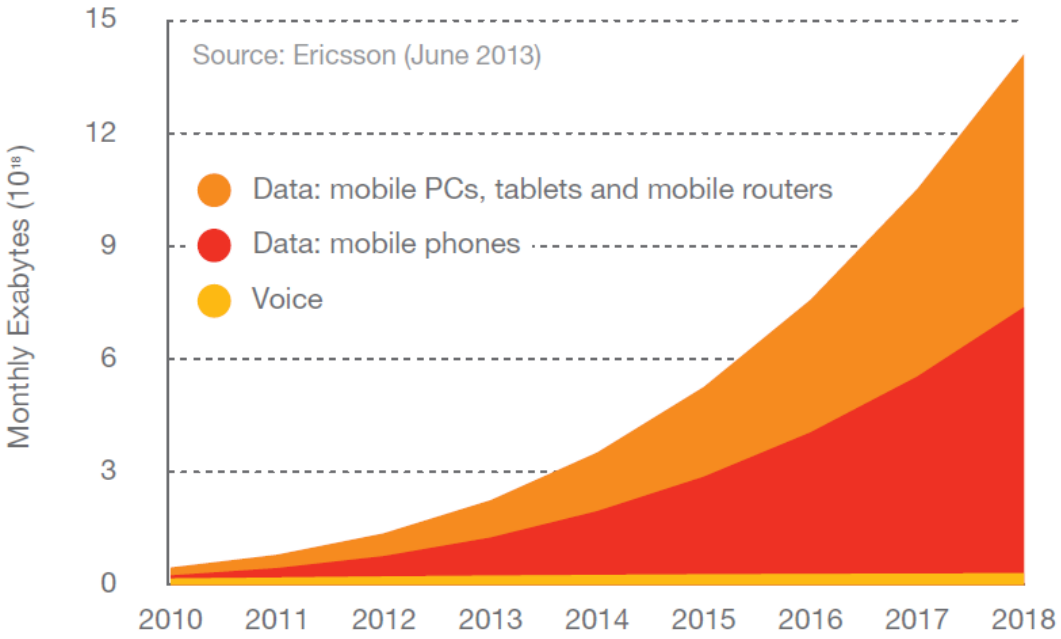

Figure 1: Global mobile data traffic forecast [3].

Although it might seem that better technologies, providing higher capacity for mobile networks, would resolve the need for better mobile network performance. Improved network performance encourages new behavior patterns increasing the demand even further. For example, enhanced networks speed provided by HSPA and LTE with ever improving smart devices creates new opportunities for better applications and services taking advantage of the enhanced network speeds and eventually pushing the mobile network to its limits. In other words, users will take advantage of the improved performance of mobile networks and smart devices. For example, the larger screen sizes and

resolutions enable users to watch high definition and eventually ultra-high definition video content. In fact, video is the largest growing segment in mobile data traffic. According to Ericsson mobility report [3] video is currently the largest growing segment of the mobile data traffic and by 2018 it is expected to take around half of the global mobile data traffic. Similar evidence is provided by Cisco's white paper [4] stating that two thirds of mobile data traffic will be video by the 2017. Cisco's mobile traffic forecast by application is presented in Figure 2.

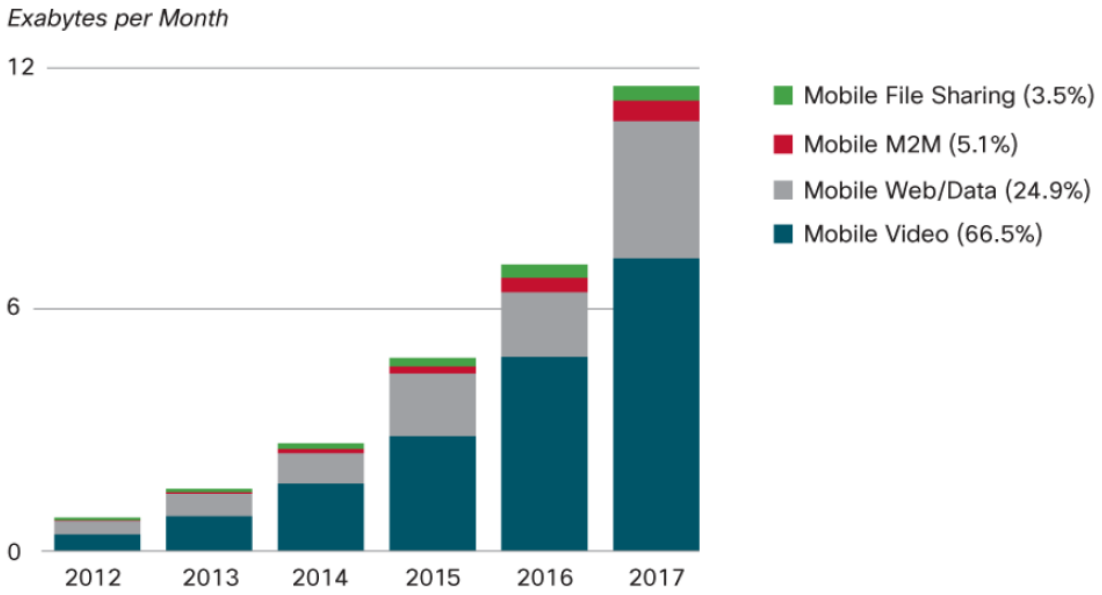

Figure 2: Mobile data traffic forecast by application [4].

2.2 Mobile network evolution

This section gives an overview of the mobile network evolution including steps from the first generation networks towards the emerging fourth generation networks. Although the mobile network architecture has changed from the first generation networks, all generations of mobile network share common architectural properties shown in Figure 3. The functionality of a mobile network is divided between the radio access network and the core network. The radio access network handles the radio resources and tries to maintain a good signal between the radio network and user equipment. The Core Network (CN) is free from radio related functionalities maintaining subscriber information,

authentication, charging, mobility and interfacing with other networks such as Internet and telephone network. [12]

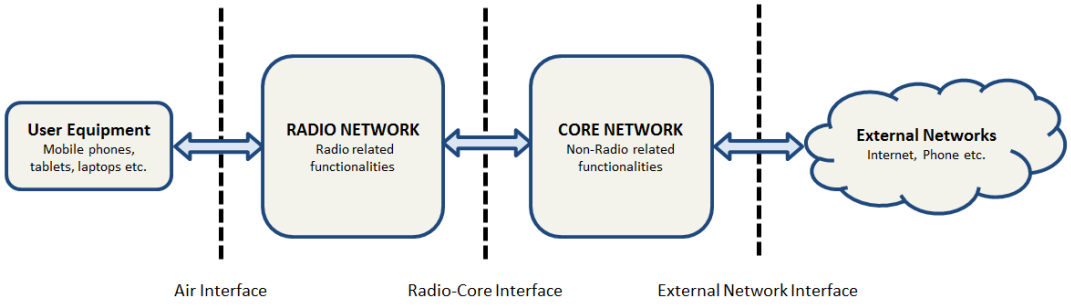

Figure 3: High level abstraction of mobile network architecture [12].

2.2.1 First generation networks

The evolution of mobile networks started in the 1980s with the first generation (1G) mobile standards. Many different standards were deployed in different countries such as Nordic Mobile Telephone (NMT) in Europe, Advanced Mobile Phone System (AMPS) in the United States, and Total Access Communications Systems (TACS) in United Kingdom. All the 1G standards provided analog voice services through a circuit switched network by using Frequency Division Multiple Access (FDMA). For each voice call, a frequency segment from the mobile operator's frequency band is allocated, limiting the number of simultaneous voice calls. Due to the analog transmission, the voice quality drops as the received signal level decreases due to distance and obstacles on the radio path. In addition, the first generation standards had unreliable handover and they were unable to interoperate within different countries. Eventually, the popularity of the 1G technologies became their downfall because of the capacity limitations and lack of global unity [13] [14] [15] [16].

2.2.2 Second generation networks

Second generation (2G) mobile systems were introduced in the late 1980s. The most significant difference between 1G and 2G cellular technologies is the digitalization. The 2G mobile systems use Time Division Multiple Access (TDMA) or Code Division Multiple Access (CDMA) that allow multiple

connections on a shared frequency. In TDMA simultaneous voice calls are separated by time slots, while in CDMA the users are separated by codes. Digitalization and the multiple access techniques provided more capacity and better spectral efficiency than the 1G networks. Additionally, 2G networks had better handover capabilities. The most successful 2G standard is the TDMA based Global System for Mobiles (GSM) and is today the most widely used wireless technology worldwide with over 3 billion subscribers. Other competing standards were CDMA based Interim Standard 95 (IS-95) used in the United States and Personal Digital Cellular System (PDC) in Japan. [16]

The high level architecture of GSM network is illustrated in Figure 4. The main elements of GSM network are the Base Station Subsystem (BSS) and Network Sub System (NSS). The main components of BSS are Base Transceiver Stations (BTS) and Base Station Controller (BSC). The main components of NSS are Mobile Switching Center (MSC), Visitor Location Register (VLR), Home Location Register (HLR), Authentication Center (AC) and Equipment Identity Center (EIR). BSS is the radio access part of GSM including all the possible functionalities connecting mobile users to the network. NSS is the core network of GSM including all the necessary functionalities to manage call switching, mobile management, subscriber management etc. [14] [16]

Initially, GSM was developed as a circuit switched network for voice. In the 1990s Internet became popular while the GSM standard did not provide any sufficient data services. To send packet-switched data over the existing GSM network, General Packet Radio Service (GPRS) was developed to enhance the GSM. With GPRS, the GSM network can achieve data rates around 50 kbps. Later, data rates were further enhanced with the development of Enhanced Data rates for GSM Evolution (EDGE). With EDGE, the transmission speeds were boosted up to 250 kbps. The deployment GPRS and EDGE required new network elements to enable packet-switched data transmission in the circuit-switched GSM network. The added network elements were Packet Control Unit (PCU), Serving GPRS Support Node (SGSN) and Gateway GPRS Support Node (GGSN). The new GSM network architecture is presented in Figure 5. PCU is located

between the radio and core network deciding if the data is destined to circuit-switched part of the network (standard GSM) or to the packet switched part (GPRS/EDGE) of the network. SGSN and GGSN provide the required functionalities to route the packets to external networks. [14] [16]

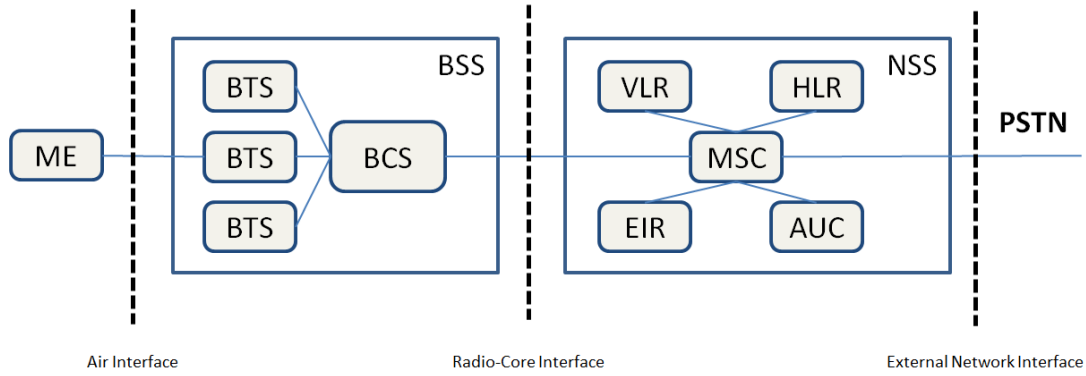

Figure 4: GSM network architecture.

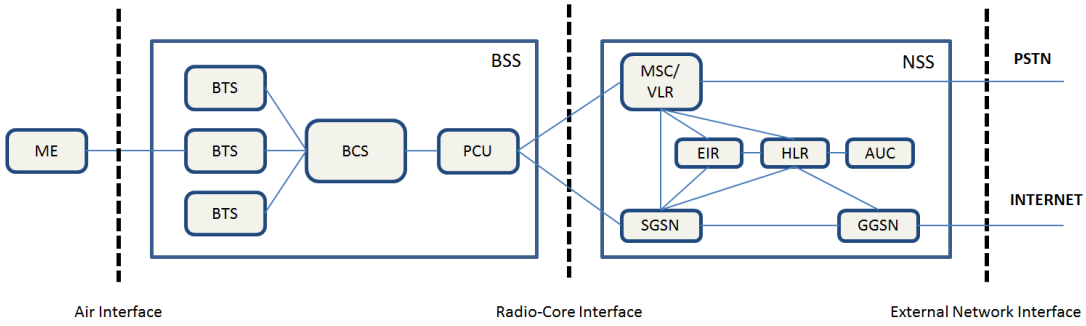

Figure 5: GSM architecture with GPRS/EDGE.

2.2.3 Third generation networks

When, the Internet first came popular in mid 1990s the fixed-line transmission speeds were around 50 kbps with circuit-switched modems. Later on, with technologies like Asymmetric Digital Subscriber Line (ADSL) modems and cable the fixed-line transmission speeds were in terms of megabytes per second. Meanwhile GSM provided the transmission speeds of 50 kbps with GPRS and around 250 kbps with EDGE. Improving the data rates of GSM beyond the capabilities of EDGE is challenging due to the limitations of GSM, such as time slot structure and narrow band transmission. Therefore, new technologies were required to boost up the network performance. Since the development of GSM,

the computing power and memory capacity of hardware have improved tremendously allowing more efficient and sophisticated wireless technologies than was possible during the development of GSM. International Mobile Telecommunications – 2000 (IMT-2000) is a project of International Telecommunication Union (ITU) which goal was to specify requirements for third generation (3G) mobile systems. A collaboration of telecommunication associations known as Third Generation Partnership Project (3GPP) was founded to specify a global 3G mobile networking system that fulfills the requirements of IMT-2000. Universal Mobile Telecommunications System (UMTS) was developed by the 3GPP to be the 3G standard. Later, 3GPP took responsibility of evolving GSM, UMTS and LTE standards. The 3GPP standards are known as 'Releases'. The first release is the UMTS also known as Release 99 referring to its release year; later releases are in numerical order starting from Release 4. [14]

The most significant improvement of Release 99, compared with 2G networks, was the complete redesign of the radio interface. The air interface in UMTS is Wideband CDMA (W-CDMA). For each user, a unique code is assigned separating the users and allowing simultaneous transmission on the same frequency band. Furthermore, the bandwidth was increased to 5MHz allowing download speed up to 384kbps and upload speed to 64-128kbps. UMTS network reuses many features from the GMS/GPRS/EDGE combining the properties of circuit-switched voice network and packet-switched data network. The high level network architecture of GSM/UMTS is demonstrated in Figure 6. The core network of UMTS did not include any significant changes compared with GSM, only software updates and new interface cards is required for the interoperation of GSM and UMTS. The radio access network in UMTS is called Terrestrial Radio Access Network (UTRAN) introducing new component names and functionalities. Radio Network Subsystem (RNS) is corresponding BSS in GSM architecture. Radio Network Controller (RNC) and Node B are corresponding BSC and BTS in GSM architecture. In addition, mobile stations are called User Equipment (UE).

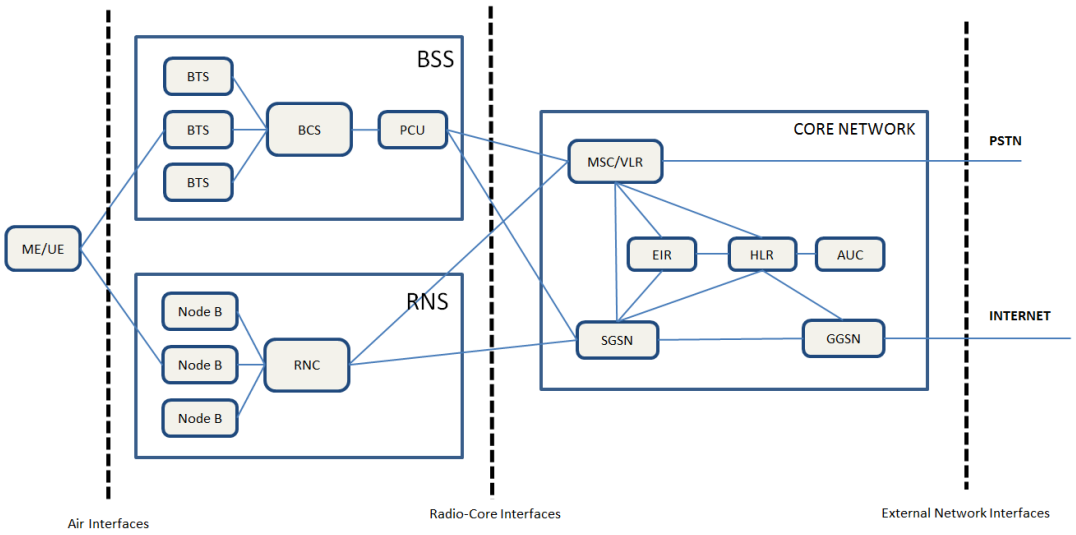

Figure 6 GSM/UMTS network architecture.

After the Release 99, 3GPP has published new releases in a steady state, introducing major enhancements for the core and radio network. The core network has evolved towards Internet Protocol (IP) based packet switched network while the air interface enhancement has increased the data speed up to tens of megabytes per second. For the core network, Release 4 introduced Bearer-Independent Core Network (BICN) enabling IP-routing in the core network instead of traditional E1 connections. Another major enhancement for the core network came with the Release 5 introducing IP Multimedia Subsystem (IMS) handling circuit-switched services via packet-switched part of the network. The most significant radio access improvement for UMTS is the High Speed Downlink Packet Access (HSDPA) and High Speed Uplink Packet Access (HSUPA), together known as High Speed Packet Access (HSPA). HSDPA was introduced in Release 5 increasing the download speeds up to 14.4 Mbps. Release 6 introduced HSUPA with significant improvement in uplink capabilities. With later releases, the HSPA is further enhanced by improving spectral efficiency with advanced Multiple Input Multiple Output (MIMO) antenna systems, higher order modulation and dual carrier transmission schemes. In Release 11, the maximum data rate of HSPA reaches 100 Mbps. [14]

2.2.4 Fourth generation networks

Although the constant evolution of UMTS, the 3GPP decided once again to completely redesign the radio and core network. ITU's project called International Mobile Telecommunications – Advanced (IMT-Advanced) specified the requirements for fourth generation (4G) networks, due to similar reasons why UMTS was developed to improve the downsides of GSM. These requirements include for example: an all-IP based network, interoperability with existing standards, over 100 Mbps data rate, low delay, scalable bandwidth and high spectral efficiency. [14]

Long Term Evolution (LTE) is specified in 3GPP's Release 8 and is considered as the first 4G mobile technology. One of the main improvements of LTE compared with UMTS is the air interface. In UMTS, the bandwidth is fixed to 5 MHz limiting the transmission speed and scalability. In addition, due to the single carrier transmission scheme the symbol time of W-CDMA is short making it vulnerable to multipath fading. LTE uses Orthogonal Frequency Division Multiple Access (OFDMA) where data is transmitted using several 180 kHz narrowband carriers orthogonal to each other. This decreases the effect of multipath fading compared with UMTS as the symbol duration is considerably longer. In addition, multicarrier transmission enables sufficiently easy bandwidth scaling. In Release 8 the bandwidth is standardized from 1.25 MHz to 20 MHz. With the 20 MHz bandwidth the maximum download speed is 100 Mbps. The second major enhancement in LTE is the adoption of an all-IP approach to the core network. While UMTS uses a circuit-switched core network for voice services inherited from GSM, LTE relies on all-IP core network. Moreover, in LTE the protocols below IP are open creating flat network architecture. The radio access part of LTE is called Evolved UTRAN (E-UTRAN). The non-radio access part of LTE is known as System Architecture Evolution (SAE) including the Evolved Packet Core (EPS). The high level abstraction of LTE network is illustrated in Figure 7. LTE radio access consists of Evolved Node B's (eNode-B) that can communicate with each other without any other network components. The core network in

LTE consists of a MME (Mobility Management Entity), S-GW (Serving Gateway), P-GW (PDN-Gateway), HSS (Home Sub-scriber Server) and PCRF (Policy and Charging Control Function). MME is the control node that processes the signaling between UE and the core network. S-GW acts like a router between the base stations and P-GW. P-GW Communicates with the external networks, having a similar role as the SGSN and GGSN in GSM and UMTS networks. HSS is a database including information about networks subscribers. PCRF is responsible for policy control decision-making, [17] [18]

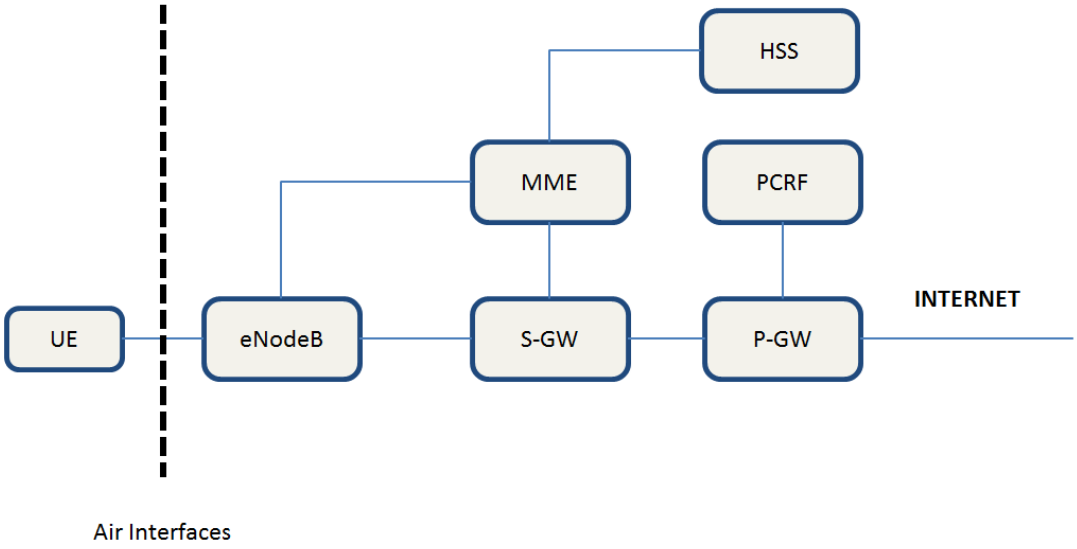

Figure: 7 EPS network elements [18].

2.3 Future mobile networks

The mobile data volumes are increasing exponentially and new technological innovations and enhancements are required to fulfill the future demand. According to various studies [1] [2] [19], the future improvements of mobile networks can be broadly categorized into three segments: spectral efficiency improvements, spectrum innovations, and cell densification.

One important source of improved network performance is the enhancements in digital processing powers allowing the utilization of advanced devices and technologies with high spectral efficiency. For example, the latest 3GPP releases enable MIMO and multicarrier transmission with the HSPA (MC-HSPA). In Release 11 MC-HSPA can combine eight 5 MHz carriers providing peak

downlink data rates up to 336Mbps and 69 Mbps in uplink. With 100 MHz bandwidth LTE-Advanced can provide peak data rates up to 1 Gbps in downlink and over 375 Mbps in uplink. As the spectrum efficiency is reaching its theoretical limits, another source of capacity for mobile networks is to use more spectrum. However, this would require the re-organization of existing spectrum allocations as well as allocation of new spectrum blocks. New spectrum arrangements would require global co-operation by the governments and regulators around the world to find harmony with the spectrum innovations. Another promising source of performance for the future networks is the extreme cell densification also known as small cells. Traditionally, base stations are covering an area from a few hundreds of meters to tens of kilometers in diameter. Small cells base stations are most likely placed densely in city areas of high demand, where a typical base station installation site is for example a lamp post or a building wall. With the densely located base stations that are brought closer to the user, the base stations are less congested and are able to provide better signal quality for the users. [1] [2] [19]

2.4 Summary

The driving force behind the evolution of mobile networks has been the increasing popularity of Internet together with the improvements of hardware and computing power. The mobile networks have evolved from the 1G circuit-switched analog voice networks towards the 4G all-IP data-networks providing date rates are up to hundreds of megabits per second. However, with the success of the smart devices and with the increasing number of mobile subscriptions, the data forecasts suggest that further research and development of mobile networks are required to address the future demand. The proposed solutions to increase the network performance include: spectral efficiency improvements, spectrum innovations, and cell densification. The spectral efficiency is enhanced by continuously improving hardware that allows the utilization of more sophisticated technologies. With the global re-arrangement of radio frequency spectrum, more spectrum would be available. The cell densification is also known as small cells. The closely located base stations

provide higher throughputs as the users are closer the network and the congestion of the cells is lower.

3 Mobile backhaul

This chapter provides an overview of mobile backhaul and small cell backhaul. First, an overview of the current mobile backhaul systems is provided. Second, small cell backhaul is introduced with its requirements, challenges and deployment possibilities. This chapter should provide sufficient preliminary knowledge for the next chapter where millimeter-wave beam steering for small cell backhaul is discussed. In the context of this thesis, the mobile backhaul denotes the transport infrastructure from base stations to the core network. Small cell backhaul indicates the first mile access from a small cell base station to the local aggregation gateway.

3.1 Mobile backhaul in current systems

Traditionally mobile networks consist of thousands of base station sites. The base stations are connected to a core network. The number of core networks is significantly less than the number of base station sites. The responsibility of Mobile Backhaul (MBH) is to offer transport infrastructure from base station sites to the core network. The high level abstraction of MBH is presented in Figure 8. Usually, backhaul is illustrated as a single line between the mobile networks elements. However, the MBH can be divided into three basic elements including the access tier, aggregation tier and backbone tier. Access tier is the first mile access combining the geographically close base station sites to an access gateway. The topology of an access tier is usually a tree as the 2G and 3G base stations do not provide any cooperative functionality. The data of several access tiers is combined in an aggregation tier. Next, data from the aggregation tier is combined into the backbone. The number of access tiers is large in comparison with the number of backbone tiers. Consequently, data speeds in access tiers are lower than in the backbone tiers. The data speeds and number of aggregation tiers lies somewhere between access and backbone tiers. [12]

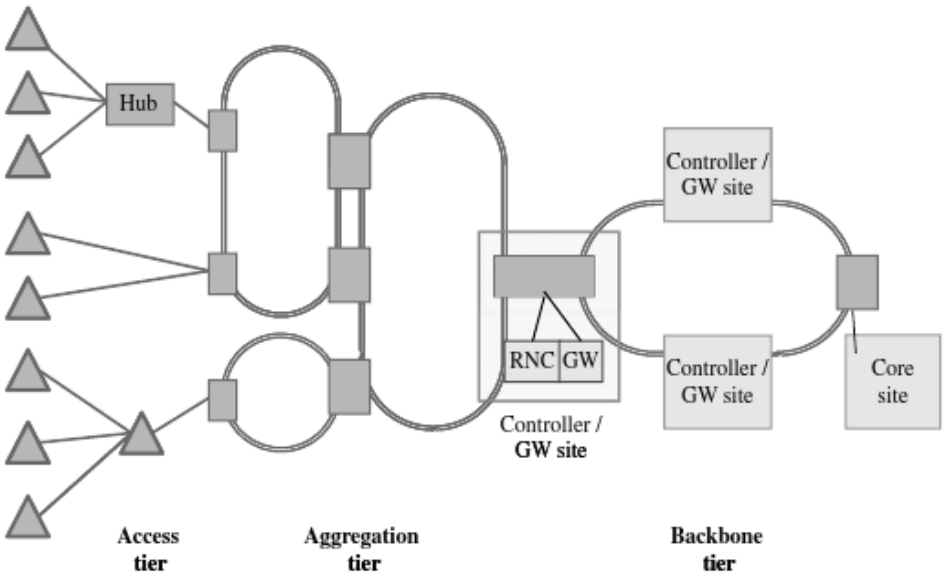

Figure 8: High level abstraction of MBH architecture [12].

Most of the existing backhaul infrastructures have been designed for 2G and 3G mobile networks. Therefore, the backhaul connections are initially optimized to support low capacity voice services requiring usually only a few 2 Mbps connections. Due to the time slot nature of GSM, the backhaul connections are usually deployed by Time Division Multiplexing (TDM) transport technologies such as PDH (Plesiochronous Digital Hierarchy) and SDH/Sonet (Synchronous Digital Hierarchy/ Synchronous Optical Networking). Networks designed for 3G might contain ATM (Asynchronous Transfer Mode) connections, especially on the aggregation and backbone tier. MBH designed for packet-switched technologies, such as HSPA and LTE, use packet switches and routers for example Ethernet switches and IP/MPLS (Multiprotocol Layer Switching) solutions. As explained in Chapter 2, the enhancements of UMTS allow packet-based connections using IP routing. Furthermore, LTE is fully IP based technology. However, the deployment of fully packet-based MBH might not be possible as the MBH has to support older generation technologies such as GSM. This sets new challenges for the backhaul design because the legacy networks might not be compatible with the packet-based network components. Figure 9 illustrates the high level abstraction of the possible evolution steps of MBH from TDM based circuit-switched technologies towards fully packet-based MBH. First

scenario demonstrates a legacy network where access and backbone are using ATM over TDM. In the second scenario, the access supports a transparent circuit and packet-switched transport while the backbone is fully packet-based. The third scenario demonstrates a fully packet-based UMTS network. The last example is all-IP packet-based LTE network. [12]

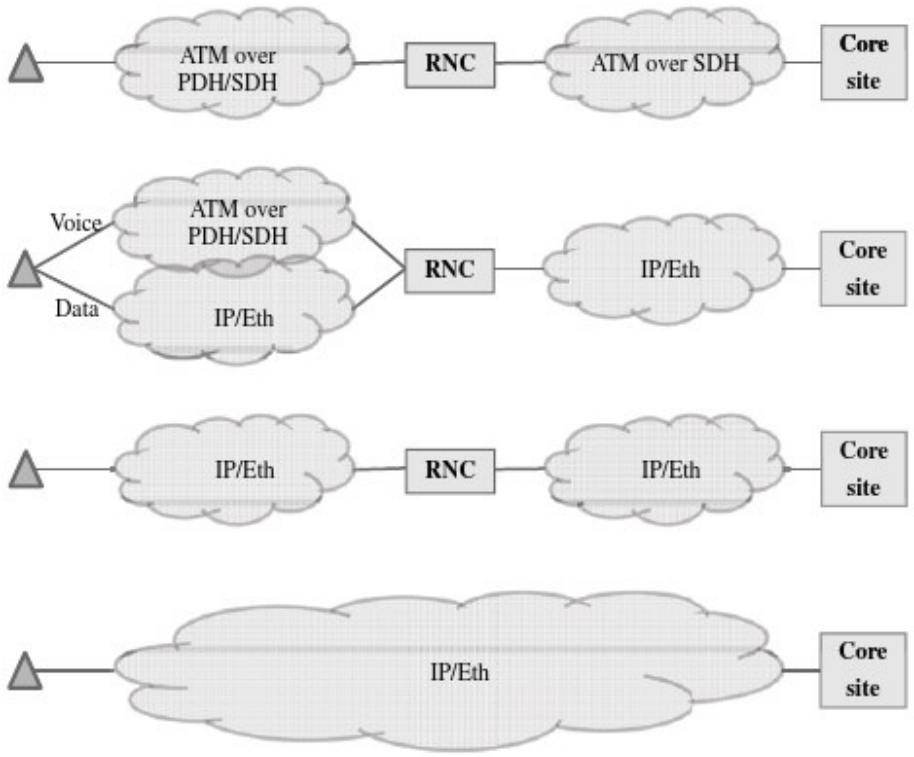

Figure 9: An example of MBH deployment [12].

3.2 Small cell backhaul

As outlined in Chapter 2, cell densification is one of the technological enhancements of the future mobile networks. The densely placed base stations are also known as small cells. By definition, a small cell is operator-controlled, low-powered radio access node operating in licensed spectrum whose coverage is ranging from tens of meters to a few hundreds of meters [7]. The small cells will be most likely located in city areas of high demand where the small cell base stations are installed for example on lamp posts, building walls and utility poles [6]. A small cell scenario is illustrated in Figure 10. The green circles illustrate

the small cell base stations. The overlaying macro cell is demonstrated with the red circle.

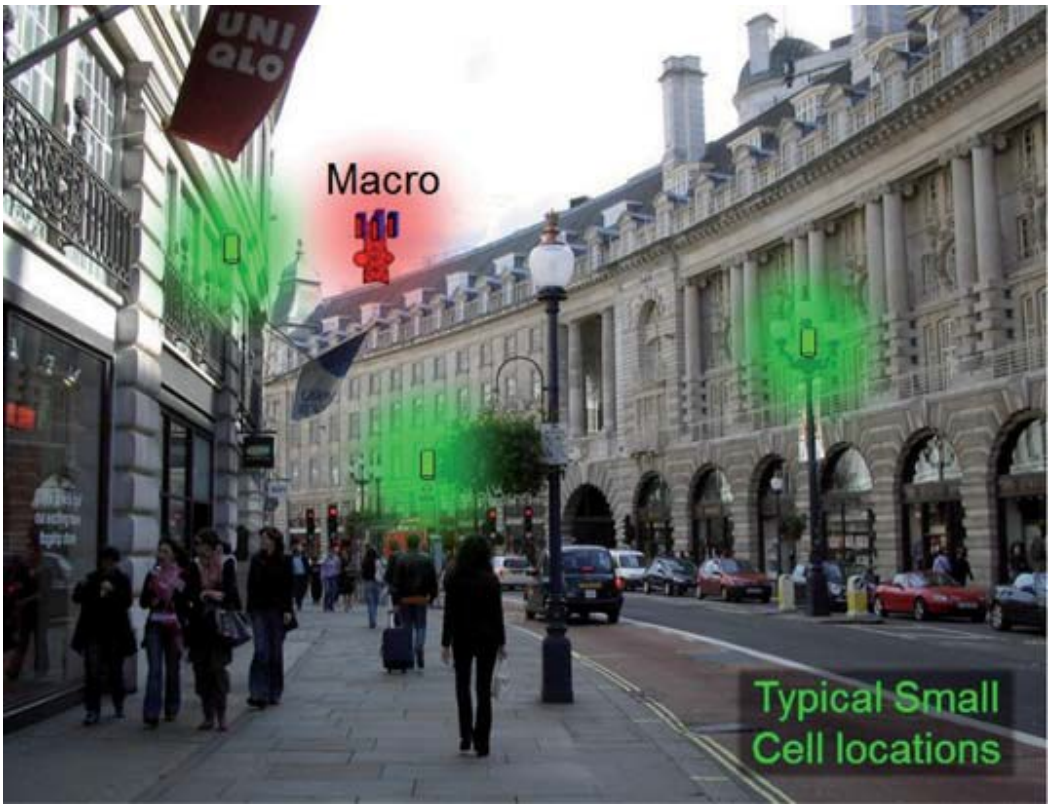

Figure 10: A typical small cell scenario [6].

The dense network of high speed small cells creates new challenges for the backhaul. Due to the unconventional location areas of small cells, provisioning of traditional wired backhaul for the small cell might be unreasonable. The backhaul solution for small cells is a debated topic. Rather than having an optimal answer, the small cell backhaul solutions form a toolbox of different technologies [6] [7]. Selection of the small cell backhaul technology depends on factors such as motivation behind the small cell deployment, requirements, and available resources. For instance, motivation behind the small cell acquirement might include: targeted capacity enhancements for hot-spots, non-targeted capacity enhancements to uplift overall performance, offloading macro cell traffic, or increasing coverage. Furthermore, the available resources such as existing wired connections and available wireless spectrum, affects the selection of the technology. [5] [6] [12] [20] [21] [22] [23]

This chapter introduces wireless small cell backhaul technologies for the toolbox of solutions, each with individualizing features. First, the requirements and challenges of small cell backhaul are introduced. Second, different wireless backhaul technologies are discussed. Finally, the technology possibilities for different deployment scenarios are illustrated.

3.2.1 Requirements and challenges

The untypical locations, the density of sites and high data volumes of small cells sets new requirements and challenges for the backhaul. This sub-section gives an overview of the requirements and challenges of wireless small cell backhaul.

Cost of ownership: As the number of small cells is high, the total cost of ownership should be considerably lower in comparison with more traditional base station deployment. The expenses generated for example from installation, maintenance, and the device should be as low as possible. These requirements lead to a plug and play solution where the low cost backhaul device is placed on a desired location with minimum configuration and network design. The wireless small cell backhaul devices should automatically find other nearby devices and align the radio links without a need for human effort. Furthermore, the devices should include remote management features to monitor network operation, update firmware and troubleshoot the network. The mentioned characteristics imply to a Self-Organizing Network (SON) features that are for example specified for LTE in Release 8. [6]

Availability and resiliency: The small cell backhaul should provide adequate levels of availability and resiliency. Availability is the time that backhaul connection is fully functional while resiliency is capability to recover quickly from temporary outages. The availability of small cell backhaul should be 99.9% - 99.99% when small cells add coverage to the existing network and do not have failback connection to the macro cell site. When small cells are deployed to ease the congestion from the overlaying macro cell, the availability requirement can be reduced to 99%-99.9%. With the lower availability requirement, network design can be eased to reduce the cost and complexity of the network. Due to

street level deployment, temporary blockages such as busses and construction yards decrease the availability of wireless links. By adding backup connections with network topologies such as mesh, the availability and resiliency increases; thus requiring some intelligence from the devices. Another challenge comes with the wind induced movement of the small cell sites. Backhaul nodes mounted on lamp posts or other similar structures are vulnerable to pole sway caused by wind. During heavy wind, the lamp posts might experience significant vibration that misaligns the radio link thus reduces availability. For the compensation of sways and twists the backhaul device should implement a vibration compensation method in order to achieve adequate levels of availability during the periods of heavy wind. [5] [6] [7]

Synchronization: Small cell backhaul should provide sufficiently accurate synchronization. For example, HSPA and LTE require frequency synchronization. Additionally, technologies such as the time division duplexing (TDD) version of LTE, and Coordinated Multi-Point (CoMP) require phase synchronization. Global Navigation Satellite System (GNSS) provides frequency and phase synchronization with adequate accuracy. However, indoor environment or bad weather conditions might block the signal. Another synchronization option is to use packet-based synchronization including technologies such as IEEE1588v2, NTP and synchronous Ethernet. [6]

Physical structure of the device: Due to the visibility of the small cell devices, the appearance of the device should be unobtrusive and small. The device should be protected from any kind of intervention such as the weather and unauthorized persons contact. Additionally, the connection between the backhaul device and the small cell base station should be reasonably implemented. The backhaul functionality could be integrated on the small cell base station hardware or vice versa. Alternatively, the small cell and backhaul could have separate hardware. [6]

Delay: 3GPP TS 23.023 recommends one way delay budgets for different quality classes for LTE/EPC. For example from UE to the PCEF, gaming has the most

demanding recommendation for delay of 50 milliseconds. In practice, denoting 100 milliseconds delay summed to delay from the Internet or other external networks. According to the round-trip-time delay budget estimations provided by Small Cell Forum, the small cell backhaul have a margin over 60 milliseconds to fulfill the delay recommendation. However, the delay recommendations represent the worst case scenarios rather than the typical performance. [7]

Capacity: White paper provided by Next Generation Mobile Networks (NGMN) [6] gives guidelines for the capacity requirements of the small cell backhaul. The data traffic in a small cell is assumed to consist of busy times and quiet times. During a busy time, several users are sharing the resources of a small cell while in a quiet time one user is utilizing all the resources. Figure 11 illustrates the mean throughput of LTE with various configurations that a single user generates for the backhaul. The data rates exceed the maximum capacity of the device because the values include the overheads generated by signaling in the backhaul. A simple estimate for the required backhaul traffic is provided by the NGMN white paper; the required backhaul capacity is the maximum between the peak data rate of the small cell, or the number of small cells multiplied with the mean of busy time data rate.

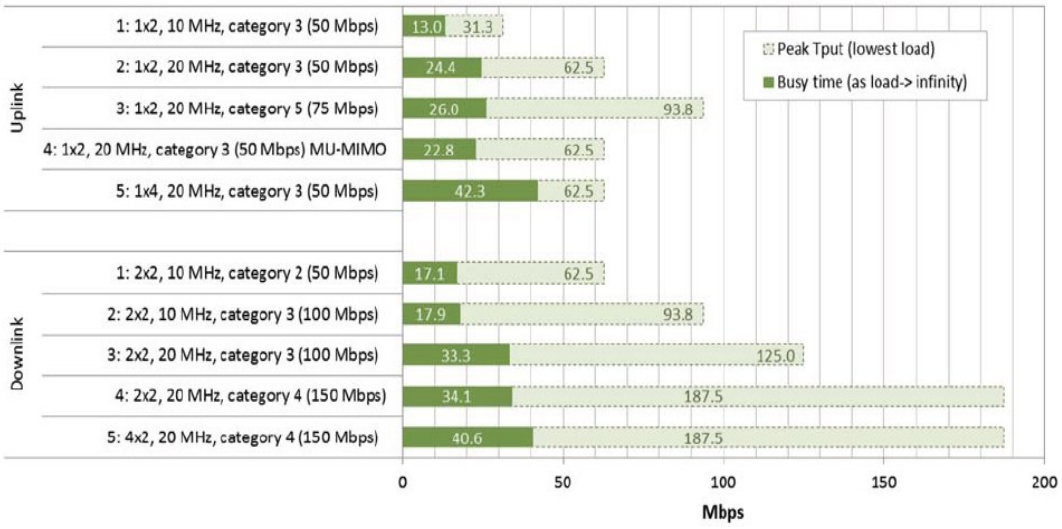

Figure 11: Backhaul characteristics for LTE in various configurations [6].

3.2.2 Technology choice

The small cell backhaul solutions include variety of different wireless and wired technologies. Wired connections are an obvious choice when the deployment is reasonable. As illustrated in Figure 10, extending the wired connections to a typical small cell location might be unreasonable. Therefore, wireless technologies are playing an important role as part of the toolbox of small cell backhaul solutions. The performance features of wireless small cell backhaul can be broadly evaluated based on: frequency, Line-Of-Sight (LOS) and Non-Line-Of-Sight (NLOS) capabilities, spectrum licensing, and connectivity. Furthermore, wireless small cell backhaul technologies are categorized into four different groups based on the features given above: millimeter-wave 60, 70/80 GHz band, Microwave 6-60 GHz band, sub-6 GHz licensed and unlicensed bands. [5] [6] [7]

Performance features: Due to the physical features, the cost of deployment and available spectrum of given frequency, the frequency of choice is the most influencing factor of the small cell backhaul technology. In general, the attenuation of a radio signal increases as a function of frequency. Therefore, high frequencies require higher gains than lower frequencies. Additionally, antenna size is proportional to the wavelength of the given frequency allowing higher antenna gain in smaller size when the frequency increases. On the other hand, as the antenna gain increases the directivity of an antenna increases. Narrow antenna beams have to be carefully aligned at both ends of the radio link and they are vulnerable to antenna misalignment and outages. Although lower frequencies might appear to have better performance characteristics as higher frequencies, generally higher frequencies have more available spectrum with light licensing making them an attractive option for high speed and low cost small cell backhaul. Additionally, narrow beams and high attenuation increases the frequency reusability and reduces the risk of interfering nearby devices. Non-Line-Of-Sight (NLOS) capability denotes that the radio link can penetrate through obstacles on the radio path. Consequently Line-Of-Sight (LOS) indicates that the path between the transmitter and receiver must be

clear of obstacles. Generally NLOS radio links are deployable on frequencies below 6 GHz. Spectrum licensing is another important factor as some parts of the spectrum are more expensive than others. Spectrum licensing schemes can be broadly categorized into four different categories. License exempt bands are free to use with some restrictions. Link licensed bands are parts of the spectrum that can be used on a specific geographical location for point-to-point communication. Area licensed spectrum can be used anywhere within defined geographical area. Light licensed spectrum can be licensed easily, quick and cheap. [5] [6] [7]

Millimeter-wave frequencies: In the context of small cell backhaul the millimeter-wave frequencies stand for 60 and 70/80 GHz frequency bands, also known as the V- and E-band. As the capacities are increasing and the base station distances are decreasing, millimeter-wave frequencies offer a very potential option for a number of reasons. Generally V- and E-bands are unlicensed or lightly licensed reducing the cost of the radio link. Depending on the national rule, V-band has 4-9 GHz of unlicensed spectrum available and E-band has two lightly licensed 5 GHz bands available. With the huge amount of spectrum, transmission speeds can be boosted up to few gigabits per second with very modest transmission methods. Additionally, high frequency allows small antenna design, high antenna gain, and low production costs. The radio signal attenuation due to distance and obstacles are extremely high for the millimeter-wave frequencies in comparison with greater degrees of lower frequencies. Furthermore, oxygen causes peak attenuation at 60 GHz limiting the range of E-band below V-band. To cope with the high path loss, high gain antennas with narrow beams are required. Therefore, millimeter-wave frequencies enable only short range point-to-point LOS radio links and the connection to the local aggregation gateway might require a number of hops. However, the high path loss and narrow beams reduce the risk of interfering with other millimeter-wave radio links. The huge amount available low cost spectrum, low interference, and the possibility to develop small and low cost

devices, makes the millimeter-wave frequencies a potential candidate for a LOS point-to-point small cell scenarios. [5] [6] [7]

Microwave frequencies: Microwave frequencies from 6-60 GHz have been used for wireless backhaul links for many decades. For example, in the United Kingdom around 16 GHz of spectrum is available. Microwave channel size is typically 7 MHz and modern microwave radios can combine multiple channels up to 56 MHz. With modern transmission methods the capacity of a microwave radio link can be boosted up to 1 Gbps. Depending on the frequency and link budget, microwave frequencies allow coverage ranging from a few hundreds of meters to a few kilometers. Similarly with millimeter-wave frequencies, the microwave frequencies require narrow beams to cope with the path loss. However, the beams are wider than millimeter-wave beams requiring less accurate antenna alignment. The licensing on microwave frequencies is usually link based or area based. Link based licensing allows point-to-point connections whereas area based licensing allows point-to-multipoint connections. In a point-to-multipoint scenario the backhaul node can operate as a hub for several backhaul devices. While the millimeter-wave frequencies are suitable for densely placed base stations, microwave frequencies are more suitable for long distance rooftop-to-rooftop connections due to less available spectrum and lower path loss. [5] [6] [7]

Sub-6 GHz: The sub-6 GHz spectrum is divided into two categories: licensed and unlicensed frequency bands. The unlicensed bands include generally the 2.4 and 5 GHz bands that are widely used by the Wireless Local Area Network (WLAN). The available bandwidth is typically 100 and 150 MHz in the 2.4 and 5.8 GHz bands respectively. The channel bandwidth is up to 40 MHz and by aggregating channels the capacity of a few hundred megabits per seconds is achievable. An obvious drawback of the WLAN-bands is the interference generated by other applications on the same frequency. However, most technologies utilizing the unlicensed spectrum rely on contention based protocols that allow interoperability and co-existence with other technologies. Due to the limited transmission power of the sub-6GHz licensed bands;

coverage is limited to some tens of meters. Therefore, these frequencies could provide backhaul connection for example for isolated locations or Wi-Fi access points. The sub-6 GHz licensed spectrum has been primarily used for mobile access. However, many of the bands are under-utilized providing a potential opportunity for small cell backhaul. For example, LTE specifies an in-band LTE mesh-and-rely specifying how to use access and backhaul on the same frequency. Available spectrum is generally ranging from 5 to 20 MHz. The sub-6 GHz licensed bands has potential to achieve the capacity of hundreds megabytes per seconds. Additionally, sub-6GHz frequencies can achieve NLOS coverage of some kilometers. [5] [6] [7]

3.2.3 Deployment possibilities

Depending on the backhaul technology, connections from the small cell towards the local aggregation gateway may have a variety of topologies such as point-to-point, point-to-multipoint, tree, ring or mesh. Some topology scenarios are demonstrated in Figure 12. In the upper scenarios, the overlaying macro cell is performing as the local aggregation point. In the lower scenarios, the aggregation gateway is some other point in the geographical area. The demonstrated topologies in Figure 12 are point-to-point, point-to-multipoint or mesh. In point-to-point topology, all of the small cells are connected by an individual link to the aggregation point. In point-to-multipoint, several small cells share the transport medium. A suitable technology could be for example an area licensed microwave radio link. In a mesh topology, the small cells form a network where the data is routed to a specific small cell that is connected to the aggregation point. The mesh topology is suitable for example when millimeter-wave radio links are deployed in a city where only a few small cells have LOS connectivity to the aggregation point.

Figure 13 demonstrates the toolbox of backhaul solutions. At the street level small cells are located on lamp posts. These small cells are closely placed and have LOS thus suitable for 60 GHz due to very short range and requirement for low interference. On the right side of the figure, trees are blocking the LOS;

therefore, sub-6 GHz technology is used to cope with the NLOS. In the example, two aggregation points exist. On the left side of the figure, a small cell performs as an aggregation point by providing a wired connection towards the core network. The two other nearby small cells route their data to the aggregation site using 60 GHz technology. On the right side of the figure macro cell base station is operating as an aggregation point. Two small cells are connected to the macro site by point-to-point 60 GHz links. At the roof-level Microwave and 70 GHz radio links connect other nearby macro cells, routing the data towards the core network. [7]

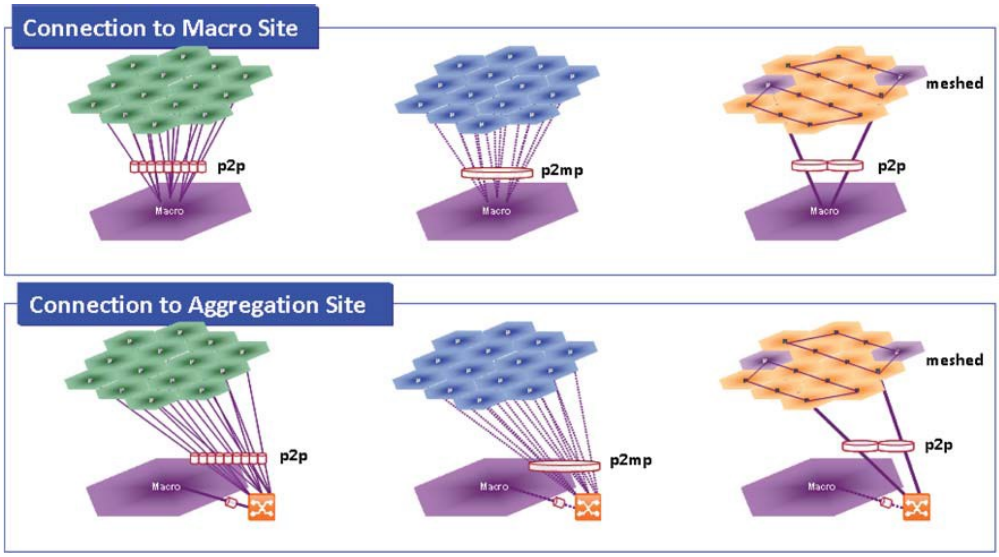

Figure 12: Small cell backhaul topologies.

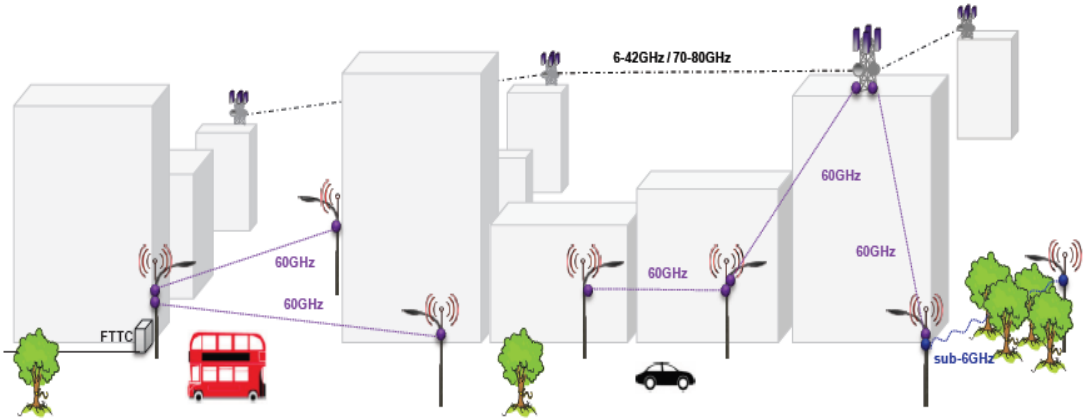

Figure 13: Small cell backhaul deployment possibilities.

3.3 Summary

Responsibility of MBH is to offer transport infrastructure from base station sites to the core network. In the context of small cells, backhaul denotes the 'first mile connection' from the small cell to the local aggregation point connecting to the core network. In a typical small cell scenario, the small cell base stations are located in city areas of high demand and installed for example on lamp posts, bus stops or building walls. The high number and the untypical locations of small cells create new design challenges and requirements for the backhaul. The backhaul solution for small cells is a debated topic and do not include an optimal solution. Instead, the small cell backhaul solutions include a toolbox of solutions, each having individualizing features. Wireless technologies are an important part of the toolbox of small cell backhaul solution, as extending the wired connection to a typical small cell location might become unreasonable. The most important factor in the design of wireless small cell backhaul is the cost of ownership; including expenses generated from spectrum, the device, installation, maintenance etc. To provide the low cost requirement the backhaul device should implement SON features including self-configuring, self-optimizing and self-healing.

The wireless backhaul technologies are summarized in Figure 14. The millimeter-wave frequencies provide great potential for LOS point-to-point short distance high speed backhaul connections due to the high amount of available spectrum, high signal attenuation and low interference. Additionally, the millimeter-wave frequencies are usually unlicensed or lightly licensed reducing the cost of ownership. Microwave frequencies provide point-to-point and point-to-multipoint radio links. The licensing is usually link or area based. A typical deployment scenario for Microwaves is a roof-to-roof backhaul radio links. Sub 6-GHz bands are categorized as licensed and unlicensed bands. The unlicensed bands are generally the WLAN frequencies that operate on 2.4 GHz and 5 GHz. The licensed bands are usually deployed by mobile access but in some cases are not fully utilized. For example, in LTE specifications in-band

backhaul is specified to implement backhaul and radio access on the same frequency.

Category name	Carrier Frequency	LOS or Non LOS	Spectrum Licensing	Connectivity
Millimetre 70-80 GHz	70-80 GHz	LOS	Light licensed	Point-to-point
Millimetre 60 GHz	56-64 GHz	LOS	Unlicensed	Point-to-point
Microwave point-to-point	6-56 GHz	LOS	Link licensed	Point-to-point
Microwave point-to-multipoint	6-56 GHz	LOS	Area licensed	Point-to-multipoint
Sub 6 GHz unlicensed	2.4 GHz, 3.5, 5 GHz	Non LOS	Unlicensed	Point-to-multipoint
Sub 6 GHz licensed	800MHz-6 GHz	Non LOS	Area licensed	Point-to-multipoint

Figure 14: Categories of wireless small cell backhaul solutions.

4 Beam steerable millimeter wave radio link in small cell backhaul

Millimeter-wave radio links are part of the tool box of small cell backhaul technologies. In Chapter 3 it was noted that the millimeter-wave frequencies provide great potential for the small cell backhaul. This chapter provides more detailed explanation of millimeter-wave frequencies for small cell backhaul with the focus on beam steering; that is used for automatic beam alignment and vibration compensation of the narrow beam millimeter-wave radio links. First, the physical features of millimeter-wave radio links are presented with its advantages and disadvantages. Second, beam steerable antennas are studied. Third, the concept of automatic beam alignment is described for supporting the plug and play requirement. Finally, beam steering methods are discussed for compensating the wind induced movement of the installation site.

4.1 Millimeter wave radio links

In the context of small cell backhaul, millimeter-wave frequencies refer to the 60 and 70/80 GHz frequencies, also known as V- and E-band. Millimeter-wave frequencies have the following individualizing features making them attractive for small cell backhaul: a great deal of unlicensed or lightly licensed spectrum, high frequency re-use, low interference and small radio frequency components. This section discusses the characteristics of millimeter-waves that enable these features.

Spectrum: One major advantage of millimeter-wave frequencies is the large amount of available spectrum. Figure 15 demonstrates the available spectrum on V- and E-band. The V-band has been allocated worldwide for unlicensed wireless communication systems. Depending on the region, the available spectrum varies from 4 to 9 GHz. The E-band denotes the 71-76 GHz and 81-86 GHz frequency bands that are worldwide available with light licensing. Usually, the deployment of E-band requires a short visitation at the regulator's website

with a low admission cost. With the huge amount of available spectrum, millimeter-wave radios provide the capacity of a few gigabits per second with very modest transmission schemes. The transmission parameters such as, bandwidth, transmission power and antenna gain are regulated. In the USA for instance, the minimum antenna gain in E-band is 50 dBi and in Europe 38 dBi. In V-band in Europe, the maximum EIRP (Equivalent Isotropically Radiated Power) is 57 dBm with the maximum antenna gain of 37 dBi. Whereas in the USA the maximum EIRP is 43 dBm and the maximum antenna gain is not specified [8].

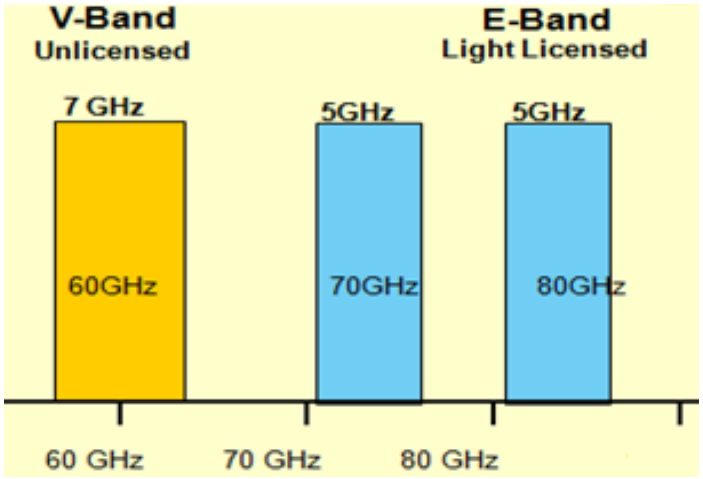

Figure 15: Available spectrum in V- and E-band.

Attenuations: The hop lengths of millimeter-wave radio links are limited by the attenuation caused by distance, atmospheric absorption and rain. For the millimeter-wave frequencies, path loss is high in comparison with greater orders of lower frequencies. Due to free space path loss for example, after one kilometer the millimeter-wave frequencies have attenuated around 130 decibel while 2.4 GHz experiences approximately 30 decibel less attenuation. Another range limiting factor for millimeter-waves is the attenuation caused by atmospheric gasses. Figure 16 demonstrates the oxygen and water vapor attenuation in different frequencies [9]. At 60 GHz oxygen causes a peak of 15 decibel per kilometer attenuation while the oxygen absorption for 70 and 80 GHz is nearly nonexistent. However, water vapor attenuation for 70 and 80 GHz can reach a few decibel when the humidity of air is high. Although E-band is

higher in frequency than V-band, due to the oxygen absorption E-band experience less attenuating as the distance increases. However, the high attenuation of the millimeter-wave frequencies gives some advantages to small cell backhaul deployment, especially for the E-band. The absorptions attenuate the signal over distance so that the signal cannot travel far beyond the intended recipient. Therefore, the radio signal is quickly reduced to a level not interfering with other nearby radio links on the same frequency. [10]

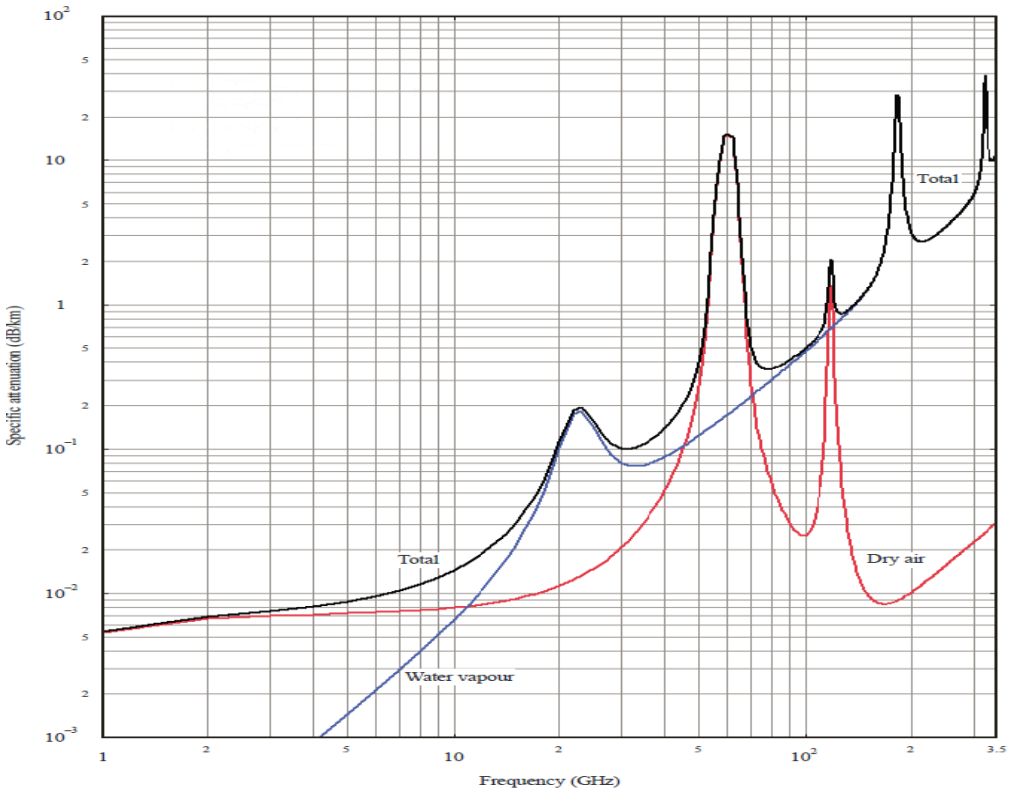

Figure 16: Atmospheric attenuation on different frequencies [9].

Rain and availability: As mentioned in Chapter 3, small cell backhaul should provide sufficient availability. Rain limits the range and availability of millimeter-wave radio links. The amount of signal loss due to rain depends on the rain rate, measured in millimeters per hour. The attenuation of specific rain rate can be estimated using ITU's recommendation [24]. In addition, ITU has developed a model for computing the probability of rain rates in various geographical locations [25]. Figure 17 demonstrates the ITU's defined rain fall regions around the world. Table 1 presents the percentage of time that some

rain fall rate appears in different rain fall regions [25]. The availability of a millimeter-wave radio link is tied to the rainfall characteristics of the geographical area. A high availability requirement decreases the hop length of a millimeter-wave radio link or consequently increases the additional gain requirement. Southern Finland for example belongs to rain region E. To achieve the availability of 99.999 percentages the radio link has to tolerate a rain rate of 70 millimeters per hour. The corresponding rain attenuation is around 20 decibel per kilometer. Therefore, the millimeter-wave radio link has to tolerate additional attenuation around 20 decibel per kilometer to achieve the 99.999 percentage availability. If the availability requirement is decreased to 99.9 percentages, the rain fall margin is decreased to around ten decibel per kilometer. Respectively, southern India belongs to rainfall region M, to achieve the availability of 99.999 percentages; the radio link should tolerate a rain rate around 120 millimeters per hour that results in attenuation more than 30 decibel per kilometer.

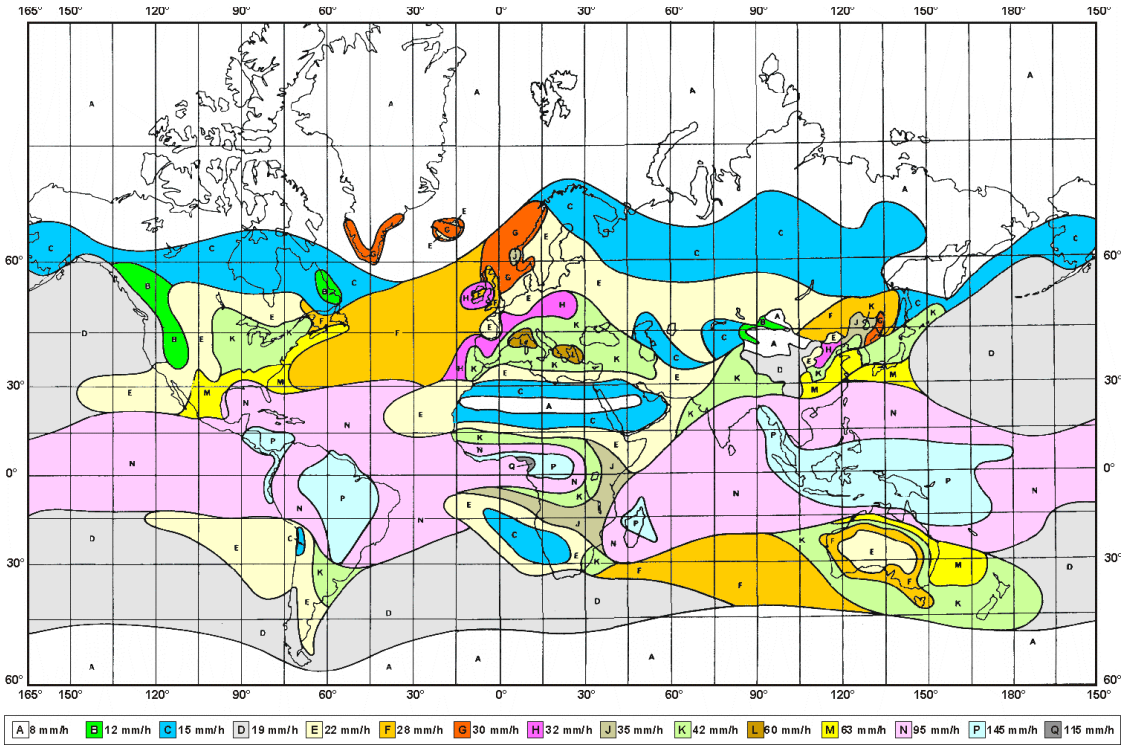

Figure 17: ITUs defined rainfall regions [25].

Table 1: Rainfall rates in different geographical regions [25].

Percentage of time (%)	A	B	C	D	E	F	G	H	J	K	L	M	N	P	Q
1.0	<0.1	0.5	0.7	2.1	0.6	1.7	3	2	8	1.5	2	4	5	12	24
0.3	0.8	2	2.8	4.5	2.4	4.5	7	4	13	4.2	7	11	15	34	49
0.1	2	3	5	8	6	8	12	10	20	12	15	22	35	65	72
0.03	5	6	9	13	12	15	20	18	28	23	33	40	65	105	96
0.01	8	12	15	19	22	28	30	32	35	42	60	63	95	145	115
0.003	14	21	26	29	41	54	45	55	45	70	105	95	140	200	142
0.001	22	32	42	42	70	78	65	83	55	100	150	120	180	250	170

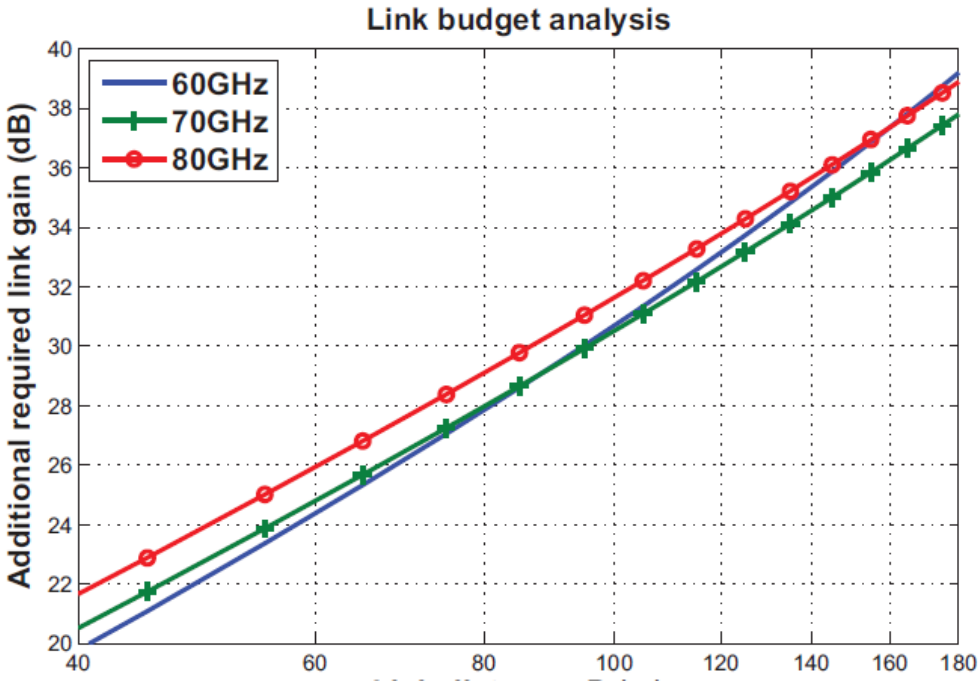

Figure 18: Additional link gain versus distance [11].

Additional link gain: Millimeter-wave radio links need additional link gain to cope with the high attenuations. Figure 18 demonstrates suggestive numbers for the additionally required link gain versus link distance [11]. To achieve for example 100 meter hop length, the additional gain is around 30 decibel. The most important source of additional link gain comes from the antennas. With more traditional frequencies, the gain of this magnitude would result in unreasonably large antennas. Luckily, the antenna size decreases as a function of frequency. Therefore, the millimeter-wave frequencies enable adequate

antenna gain in compact size. With the antenna gain of this magnitude, the beam width of an antenna decreases to less than a few degrees. Narrow beams decrease interference thus increases the frequency reusability allowing the deployment of multiple radio links in close proximity. With the narrow beams and strong signal attenuation, different network topologies are deployable such as point-to-point mesh while other wireless technologies often reach their scalability limit due to the cross interference. [10]

4.2 Beam steerable antennas

Due to the high gains required by the millimeter-wave small cell backhaul, the antenna beams are narrow. Traditionally, the narrow beam radio links are manually aligned at both ends. As explained in Chapter 3, the small cell backhaul devices should automatically find other nearby devices in any direction. In addition, the device should compensate temporary misalignments caused by the sways and twists of the installation site. Therefore, beam steering capabilities are needed, meaning that the device can change the direction of transmission and reception. This section gives an overview of technologies that provide suitable beam steering capabilities for the described scenarios. The investigation of beam steerable antennas concentrates on two technologies: beamforming and integrated lens antennas (ILA). Although several beam steering technologies exist, these technologies are selected because by the author's knowledge they are the most commonly referred technologies in the context of beam steering for millimeter-wave small cell backhaul.

Beamforming is an antenna array technology using phase-arrays. Phase-array is an array of antennas, each having adjustable gain and phase. By shifting the phase of each antenna element to a certain value the signals can be added constructively in the desired direction and destructively in other direction. Thereby, the gain of the antenna and direction of the transmission or reception can be adjusted. The principle of beamforming is demonstrated in Figure 19. The dots illustrate antennas transmitting a sine wave. A circle with a specific color illustrates the phase of the sine wave. The arrows demonstrate the point

when the sine waves are in the same phase and the signals add constructively. In other directions, the signals are out of phase adding destructively. By changing the phase of an antenna, the direction of the gain changes as the point when the signals are in phase is elsewhere. The maximum antenna gain is proportional to the number of antennas and number of phase-shift alternatives per antenna. To increase the antenna gain and accuracy of directivity, an increasing number of antennas and phase-shifts per antennas are required. Thus, the complexity of the systems increases exponentially as the potential phase-shift combinations grow. Beamforming techniques for millimeter-waves have been defined in standards such as IEEE 802.15.3c (TG3c) for Indoor Wireless Personal Area Networks (WPAN), IEEE 802.11 ad (TGad) and Wireless Gigabit Alliance (WiGi) on WLAN. However, these technologies are targeted for indoor environments and extending their capabilities for the outdoor small cell scenarios would reach beyond their limits. [11]

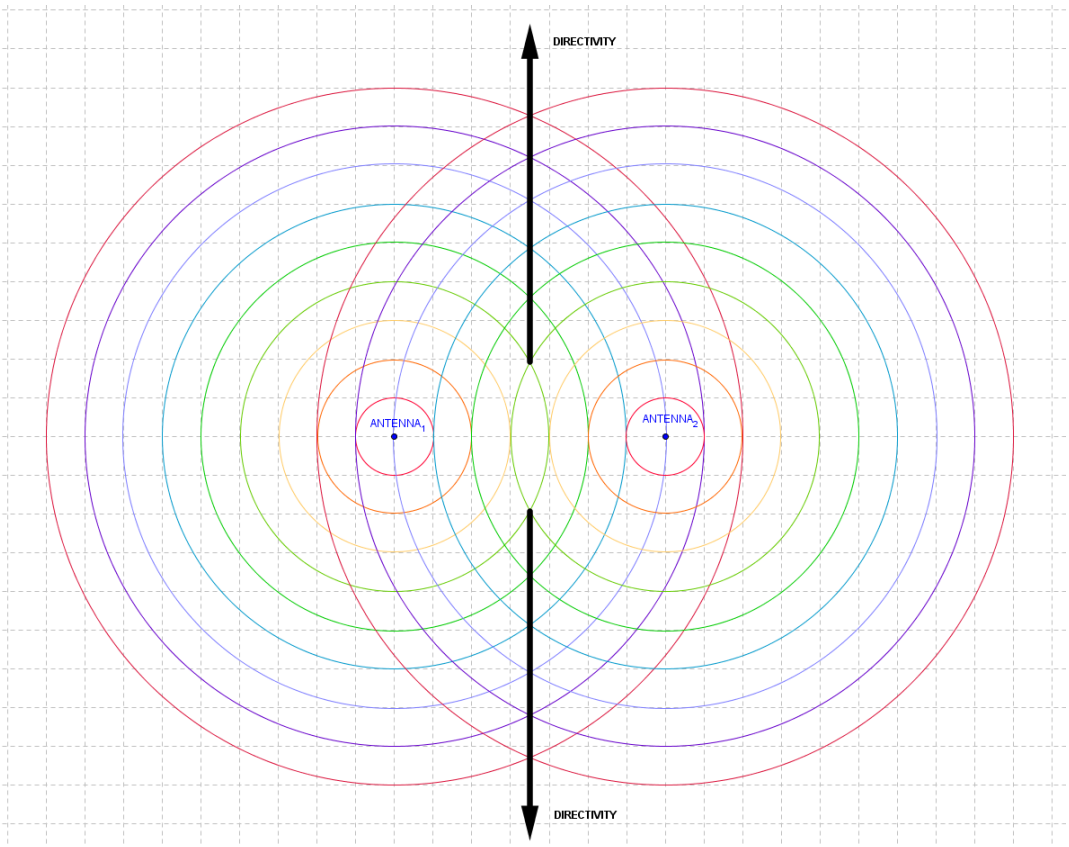

Figure 19: A simple beamforming illustration.

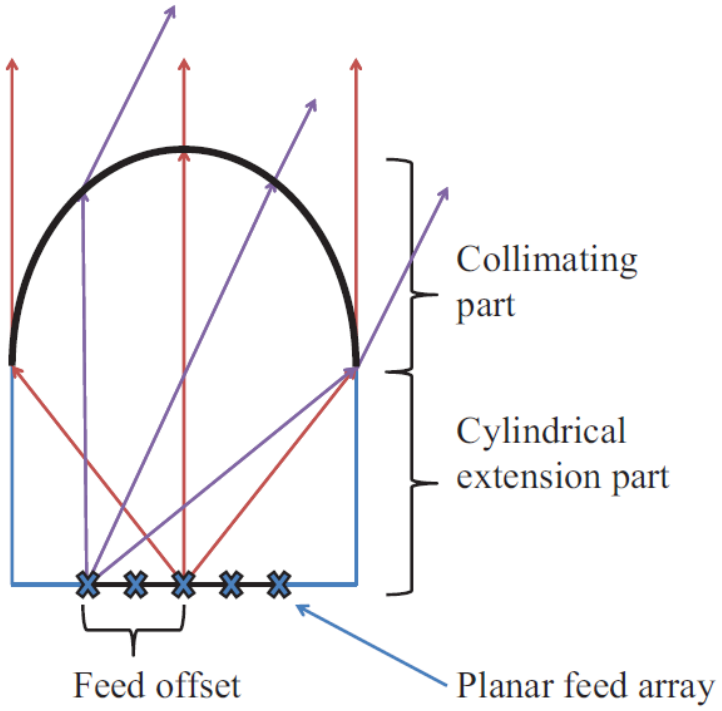

Figure 20: Integrated lens antenna with feed array [26].

Another option for beam steering is to use integrated lens antennas (ILA). Figure 20 demonstrates the principle of ILA. An array of feed antennas is placed on the back surface of a lens. The lens has an elliptical or hemispherical shape that collimates the radiation from the feed array. Only one antenna element is active at a time and beam steering is achieved by switching between the antenna elements. The direction of the beam depends on the location of the active antenna element. The gain of the ILA depends on the size of the lens, lens material and length of the cylindrical part called an extension. The extension length for different lens materials is optimized for maximum directivity. [26] Various studies show promising results for the beam steering capabilities of integrated lens antennas [27] [28] [29]. Beam widths of 2 – 2.5 degree with antenna gain around 28 dBi were achieved on 77 GHz by using extended hemispherical lens with a diameter of 100 mm and extension of 85 mm [27]. In another study for 73-94 GHz, the gain of 16 and 20 dBi were achieved with the lens diameters of 15 and 25 mm and with the extensions lengths of 5.5 and 9 mm respectively [28]. Finally, the antenna gain of 37 and 43 dBi were achieved with beam widths below two and one degrees respectively. In the study, the diameters of the lens antennas were 120 and 246 mm [29]. The presented

studies confirmed that the integrated lens antennas provide potential for the beam steering of millimeter-wave small cell backhaul.

The beamforming and ILA provide potential for the small cell backhaul beam steering. The beamforming techniques provide different beam widths in any direction; however the complexity is extremely large in comparison with the ILA. The lens antenna technology enables simplified beam steering with a low cost implementation, where just the direction of the transmission is changeable and beam width is fixed.

4.3 Automatic link alignments

The goal of the automatic link alignment is to find the best possible transmit and receive beam-pairs that maximizes the radio link quality with less protocol overhead as possible [30]. As explained in Chapter 3, the small cell backhaul device should automatically find other nearby devices in any direction. Therefore, the devices need a procedure that updates the status of neighboring devices. For example, this could be carried out by periodically scanning different directions with some coordinated manner. This sub-section provides discussion about automatic link alignment methods for the millimeter-wave small cell backhaul.

The beam steering capabilities of the antenna affect to the design of the automatic link alignment method. For example, lens antennas can search only one narrow discrete direction at a time while with beamforming the beam width can be increased or decreased. With the most simplified link alignment method, known as the exhaustive method, every possible beam pair between the transmitter and receiver is tested. If the nodes have N beams, the number of required beam searches is N to the power of two. Therefore, the alignment time increases exponentially as the number of beam directions increase. The lens antenna technology has to rely on similar methods like the exhaustive method, because only one discrete direction can be used at a time. However, some information such as the coordinates of the other nodes would most probably

decrease the number of searches. This could be provided for example by Omni-directional antennas that transmit some low data rate information.

Beamforming technologies allow the use of multi-level beam searching, denoting that wide beams are used to estimate the initial direction of the radio link and the beam width is narrowed as the approximate direction is found. For example, the 802.11ad and 802.15.3c utilizes beamforming with a similar principle. Simplified, the methods deploy two stages; sector level search and normal beam search. At sector level search, both ends of the radio link transmit training symbols in different directions using wide and exchange the measurement information to determine the approximated direction of the connection. After which the devices transmit narrow beams in the estimated direction and exchange information to determine the best possible beam-pair. This kind of method decreases the number of beam searches compared with the exhaustive method. However, the number of searches still increases exponentially as the beams get narrower. Various studies propose more advanced beam alignment methods for beamforming to minimize the search time [11] [30] [31]. In [31] a beam alignment method using beamforming for millimeter-wave wireless backhaul is proposed. The method utilizes tree-structured beamforming codebooks where different levels of the tree have different beam widths. This is demonstrated in Figure 21. A beamforming codebook means that the parameters of the phase-array are predefined thus single code in the codebook has a fixed direction and gain. The search is performed by sounding the system using progressively narrower beams at the transmitter and receiver. Based on the received signal, the receiver sends back a limited amount of feedback information to inform the transmitter which branch should be taken during the next level of sounding. The simulation results show that the amount of searches with 32 antennas decreased from 4096 searches to 48 searches compared with the exhaustive method. A similar beam alignment method was introduces in [11]. The results show that especially with large antenna arrays the search time is reduced significantly compared with the exhaustive method or the 802.11ad standard.

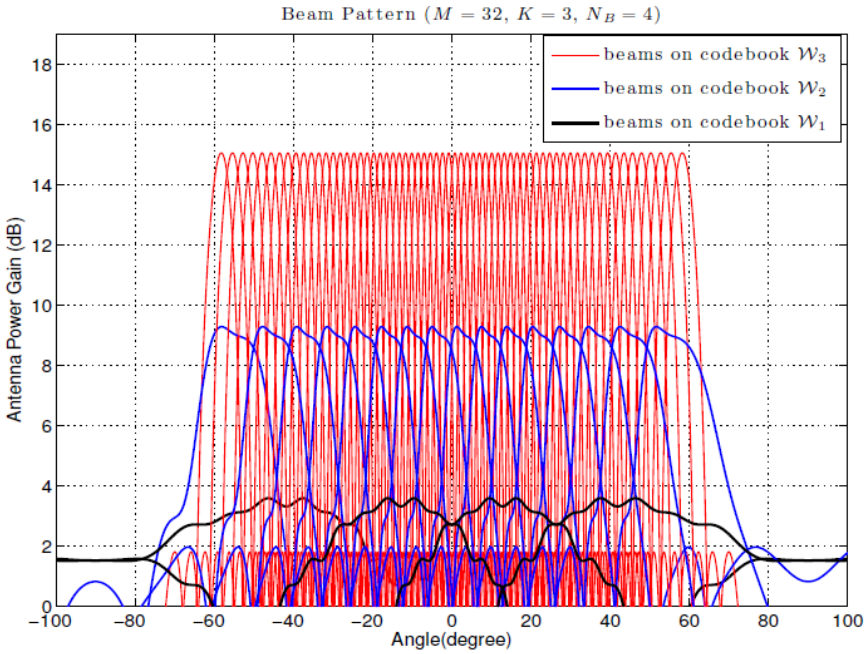

Figure 21: Tree structured beamforming codebooks [31].

4.4 Vibration compensation

The narrow beam millimeter-wave radio links are vulnerable to antenna miss alignment due to wind induced movement. This section investigates the worst case scenarios of lamp post movement to give suggestive figures for vibration compensation methods. First, the worst case scenarios are investigated. Second, potential vibration compensation methods are discussed.

4.4.1 Worst case pole sway scenarios with mathematical considerations

A typical small cell location is for example a lamp post. Because the beams are narrow, wind might sway the pole misaligning the radio link. This sub-section provides the worst case scenarios of a pole sway with mathematical considerations to introduce the possible limitations and problems of millimeter-wave vibration compensation methods. The calculations and examples give suggestive figures for lamp post-kind-of vibration. It is assumed that the pole does not bend or twist and therefore the sway takes place on a spherical

surface. The derived calculations are part of the author's contribution in this thesis.

Horizontal sway: Figure 22 illustrates pole sway in a horizontal direction when only one node is swaying. The figure is a top view of two nodes. Initially, both nodes uses beam number one. When the left side node sways the beams are misaligned. Both nodes should change the beam to compensate the misalignment. However, the devices require some information for changing the beam. The swaying node could change the beam in the correct direction with knowledge of its movement. However, the stationary node only realizes that the signal quality has dropped and without any feedback or measurements the node can only guesstimate the correct beam. Figure 23 demonstrates a pole sway scenario where the nodes are simultaneously swaying in an opposite direction. In the previous example, the moving node could compensate the misalignment by knowing its movement. However, in this scenario the knowledge of node's movement becomes insignificant, because the beam number one of both nodes is yet pointing to the initial position of the other node. Therefore, the beam switching requires measurements or feedback.

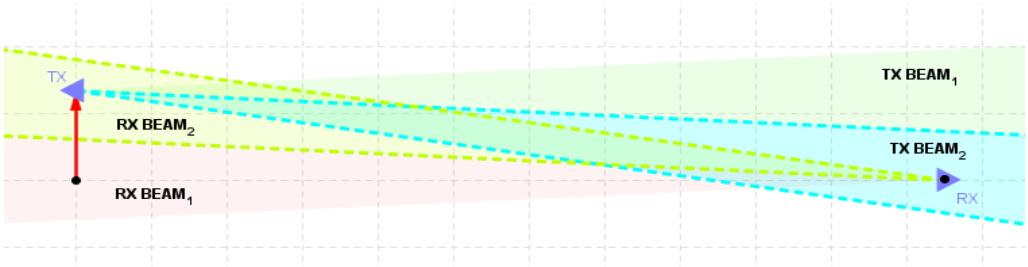

Figure 22: Horizontal pole sway scenario with one node swaying.

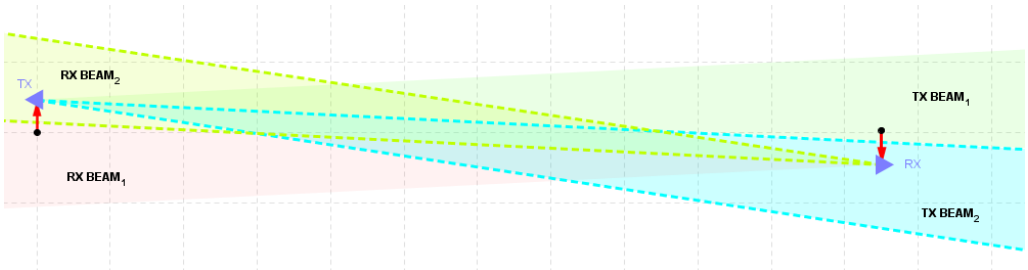

Figure 23 Horizontal pole sway scenario with both nodes swaying.

Next, the horizontal pole sway is examined mathematically. Figure 24 demonstrates the horizontal pole sway looked from behind of the node. The larger circle is the surface on which the backhaul device is swaying and the smaller circle demonstrates the area that the beam covers on the receiving side. Point $R_x(x_{rx},z_{rx})$ is the receiving device where x_{rx} and z_{rx} are the x- and z-coordinates of the demonstration. Point $T_x(\Delta x,r-\Delta z)$ is the transmitting node where Δx is the nodes x-coordinate and $r-\Delta z$ is the nodes z-coordinate. Origin is in base of the receiving nodes lamp post. The length of the horizontal sway in x- and z-dimension is denoted by Δx and Δz. The coverage radius of the beam at the received side is denoted by r_β. The swaying angle in horizontal direction is denoted by ρ. The maximum swaying angle leading to miss alignment is calculated by finding the value of ρ when the distance between T_x and R_x is equal to r_β. The equation is given below:

$$(x_{rx}-\Delta x)^2+\left(z_{rx}-(r-\Delta z)\right)^2=r_\beta^2 \qquad (1)$$

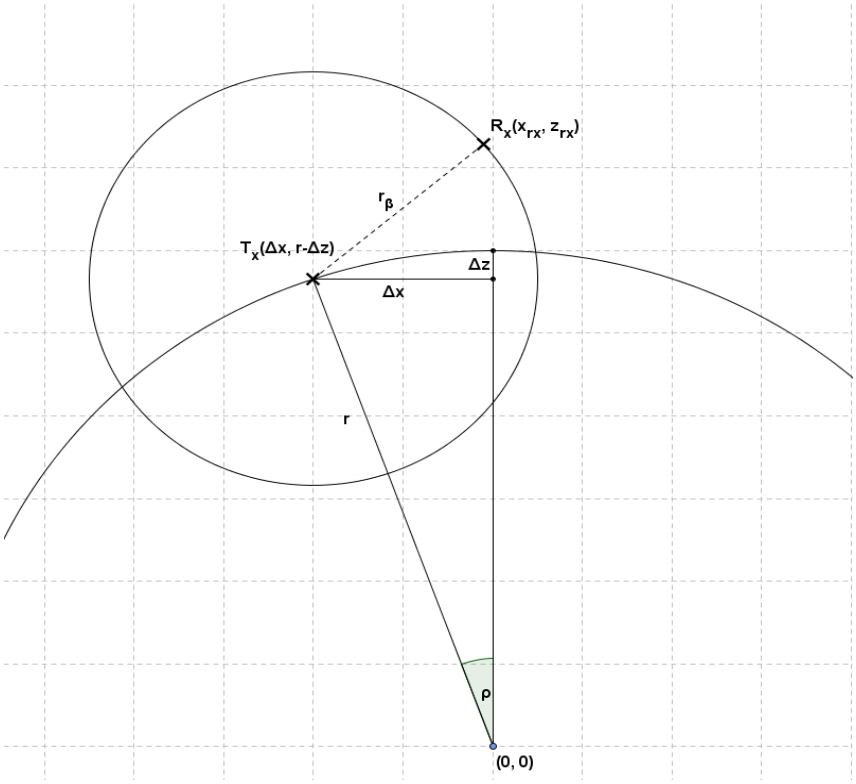

Figure 24: The horizontal pole sway with mathematical consideration.

Figure 25 demonstrates the maximum horizontal pole sway derived from equation (1). The ratio of the link distance and pole radius on the x–axis and y-axis demonstrates the maximum pole sway in degrees. In the calculations x_{rx} is zero and z_{rx} equals r meaning that the nodes are perpendicular to each other. The beam widths of 0.5, 1 and 2 degrees are used in the calculation. The figure shows that as the distance increases the maximum swaying increases. Obviously, the maximum swaying angle is smaller for the narrower beam widths. The maximum sway is approximately the ratio of link distance and pole radius multiplied with the beam width in degrees. This applies to small angles, because when Δz is small the maximum horizontal sway is approximately the same as shifting the node on a flat surface. The results show that vibration compensation in the horizontal direction might only be needed with short link distances and very narrow beams. For example, for the calculated beam widths with the minimum link distance of 50 meters and maximum pole height of 5 meters, the maximum tolerable pole sways in the horizontal direction are 5, 10 and 20 degrees.

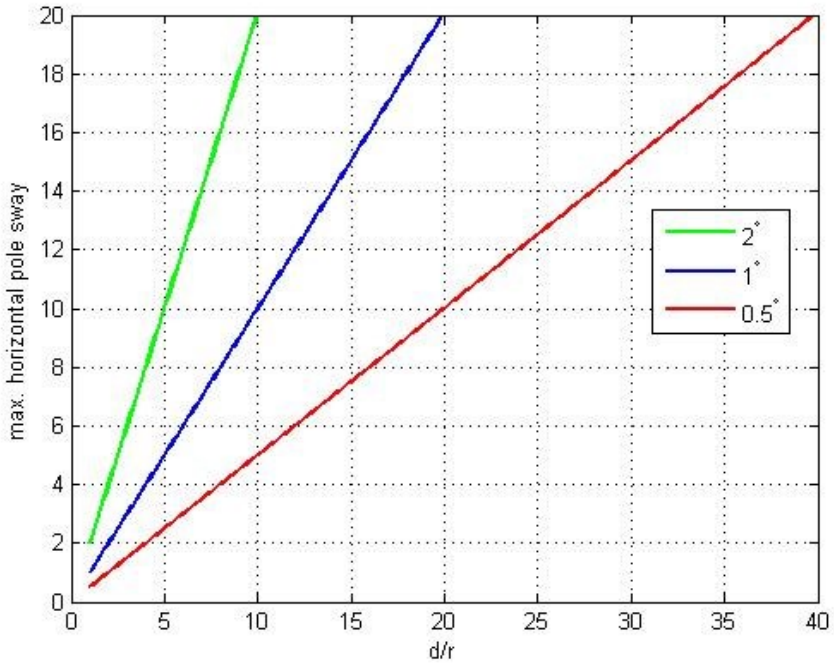

Figure 25: The maximum horizontal pole sway angle.

Vertical sway: Figure 26 illustrates the pole sway in the vertical direction. The vertical misalignment takes place when the pole tilts towards or away from the other node. The figure is a side view of the pole sway scenario. As with the horizontal pole sway, due the geometry of the movement, the downwards movement, denoted by Δz, is small. Therefore, for the device to sway outside of other node's service area, the tilting angle should be unrealistically large. Therefore, in the vertical direction the swaying node needs only information about its own movement to compensate the misalignment.

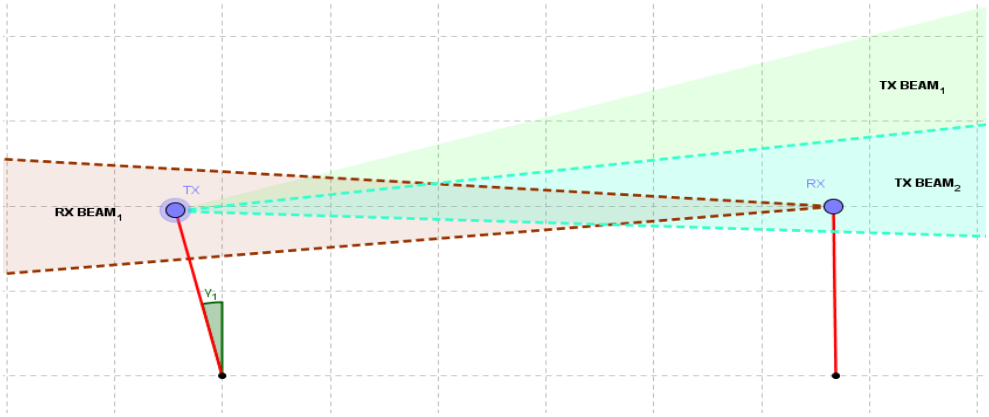

Figure 26: A vertical pole sway scenario.

Next, the vertical pole sway is examined mathematically. Figure 27 shows a side view of the vertical pole sway. Point $R_x(d, z_{rx})$ is the receiving node with its coordinates where d is the distance between the nodes and z_{rx} is the height of the receiving node. Point $T_x(\Delta y, r - \Delta z)$ is the transmitting node with its coordinates. The movement towards or away from the other node is denoted by Δy, and Δz is the movement downwards. The coverage radius of the beam at the received side is denoted by r_β, and φ is the swaying angle in the vertical direction. The maximum angle that the node can tilt is found by calculating the tangent when either of the beam edges crosses the point R_x. The equation is given in (2). Approximation for r_β is given in (3).

$$\tan(\gamma \pm \beta n) = \frac{z_{rx} - (r - \Delta z)}{d + \Delta y} \qquad (2)$$

$$\tan(\beta) = \frac{r_\beta}{d_\beta} \rightarrow r_\beta = \tan(\beta)\, d_\beta \qquad (3)$$

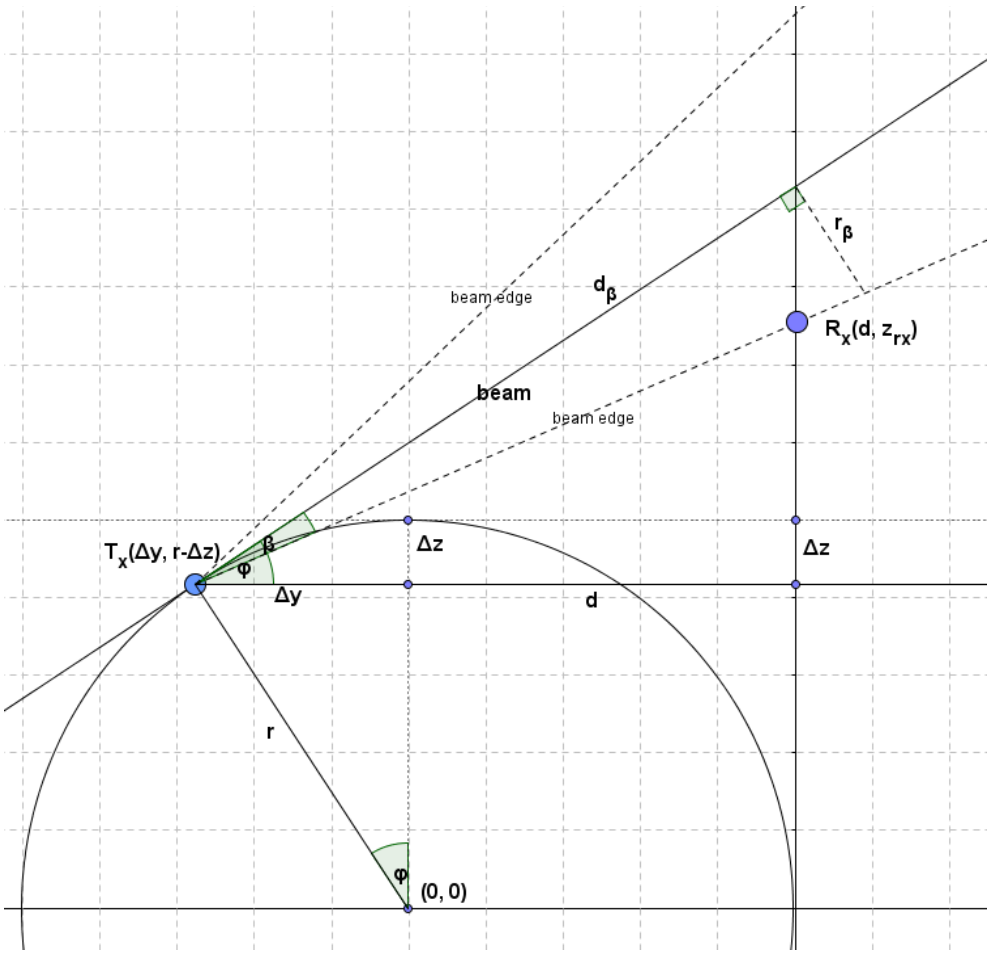

Figure 27: the vertical pole sway with mathematical consideration.

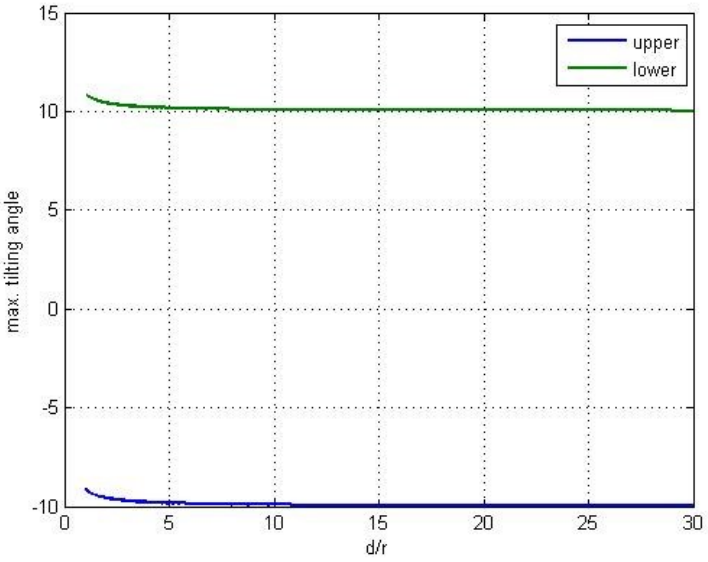

Figure 28: maximum vertical pole sway angle.

Figure 28 demonstrates the maximum vertical swaying angles derived from (3). On the x-axis is the ratio between distance and pole radius, on y-axis is the maximum swaying angle. In the calculation x_{rx} is zero and z_{rx} equals r, meaning that the nodes are perpendicular to each other. The beam width is 10 degrees that is unrealistically large but it provides more illustrative results than a realistic beam width. The results show that the maximum swaying angle in the vertical direction is approximately the same as the beam width. The maximum swaying angle deviates significantly from the approximation, only with unrealistically short distances.

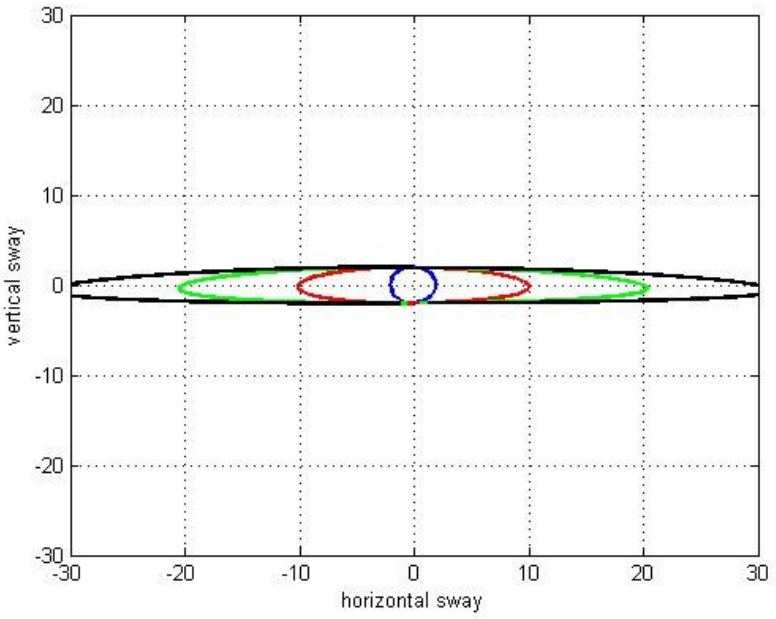

Figure 29: Joint vertical and horizontal sway.

Joint movement: Figure 29 demonstrates the maximum swaying angles when the device sways simultaneously in the vertical and horizontal direction. The results are obtained by combining equations (1) and (2). The figure demonstrates four different ratios of the link distance and pole radius. The blue, red, green and black denotes the ratios of 1, 5, 10 and 15 respectively. The beam width is set to two degrees. The results confirm the assumption that horizontal pole sway is insignificant with long distances and the maximum vertical swaying angle is approximately the beam width. Only on the edges of the

horizontal sway the vertical sway is significantly less than the beam width; however, on the edges the horizontal sway is unrealistically large.

Conclusions: The demonstration of horizontal pole sway showed that the swaying is significant only for very narrow beams at short distances. The swaying can be modeled as if the node is moving horizontally sideways on a flat surface. Thereby, the maximum horizontal swaying is approximately the ratio of link distance and pole radius multiplied with the beam width. If the horizontal compensation is necessary, measurement or information about the movement of the other node with its coordinates should be available. The vertical pole sway demonstration showed that swaying towards or away from the other node can be treated as if the node is vertically tilted on a stationary position. Therefore, the compensation of vertical beam sway can be handled without any information about the other node. The joint movement analysis verified the results obtained for the horizontal and vertical pole sway.

4.4.2 Vibration compensation

Due to the narrow beams and untypical locations of small cells the millimeter-wave radio links are vulnerable to wind induced movement. In the previous sub-section, worst case scenarios of a lamp post vibration were simplified. The demonstration provided suggestive figures to illustrate the influence of wind induced movement. The results showed that narrow beams are easily misaligned. Similar evidence is provided by simulation of narrow beam millimeter-wave small cell backhaul links [11], showing that availability of the radio link can reduce significantly with high wind speeds. Therefore, the narrow beam radio links need vibration compensation methods to improve the availability of the radio link. This sub-section discusses the possible vibration compensation methods. It is assumed that the vibration compensation is similar for lens and beam forming technologies, denoting that the beam steering antenna in use has some predefined discrete directions where the transmission or reception can be targeted. The discussion of this chapter concentrates on recognizing different vibration compensation methods and identifying their

pros and cons. The vibration compensation methods described in this sub-section includes orientation estimation method, RSSI (Received Signal Strength Indicator) measurement method and hybrid of those two. In the orientation estimation method, the vibration is compensated with an orientation sensor that measures the angels of the device's orientation. The RSSI measurement method compensates the vibration by measuring different directions and trying to find the best possible beam pair. The methods use feedback or not. The hybrid of the orientation and RSSI measurement methods denotes that the methods are combined.

Orientation estimation method: The small cell backhaul devices could be located on a variety of different locations. Different installation sites might sway differently in similar wind conditions. For example, a building wall might provide a solid mounting without significant vibration, whereas different lamp post models might sway differently in case of a gust of wind. If the vibration trajectory of the device is modeled with reasonable accuracy, simple orientation estimation could be used to compensate the temporary misalignment. For instance, in the previous sub-section the pole sway is modeled with the assumption that the device sways on a spherical surface. It was realized that with long enough distances, only the vertical sway is significant. The effect of the vertical sway is approximately the same as tilting the device vertically with the same angle that the pole is tilted. Therefore, the vibration could be compensated by switching to the upper or lower beam when the angle of vertical sway reaches the beam width of the antenna. This simple sway direction estimation would definitely address the low cost requirement of the small cell device and the beam steering would take place without any complex and time consuming calculations, signal measurements or feedback. However, the provision of a sufficiently accurate orientation sensor and a pole sway model for different installation sites might include some practical challenges. In addition, when the ratio of link distance and pole radius is small, less than five, compensation of horizontal sway might be needed. As explained in the previous sub-section, the horizontal vibration compensation requires knowledge of the

coordinates of the devices and information about the other node's orientation. Therefore with short link distances, the sway direction estimation needs a feedback channel that increases the complexity of the system.

RSSI measurement method: Ideally, a vibration compensation method should operate in any possible swaying scenario from a light pole to a palm tree. A vibration compensation method utilizing measurements in different directions could provide installation site independent vibration compensation unlike the orientation estimation method. The measurements should be carried out periodically in sufficiently short intervals commensurate to the vibration frequency and speed of the swaying device, in a manner that the beam is switched before the link quality drops significantly. This would require training periods in the transmission frames or capability to measure multiple directions while the main beam is active. For example, measuring the neighboring beams of the active beam during the training periods the beam could be switched if the measurements indicate that better beam has found. However, as mentioned in the previous sub-section, in some cases the transmitting node has to change the beam to compensate the misalignment. This could be overcome by TDD transmission scheme if the transmission direction changes with sufficiently short intervals. Another way is to use feedback that would provide more accurate vibration compensation. For example, a similar principle could be applied as in the link alignment procedure of 802.11 ad. By transmitting periodical training signals, the devices could measure all combinations of beam pairs. Therefore, with feedback the devices could decide the best possible beam pair that maximizes the signal quality. However, the training periods decreases the capacity of the radio link but increases the availability. Therefore, the measurement based vibration compensation is a trade-off between capacity and availability.

RSSI measurement with orientation estimation: Using orientation estimation together with the measurements, the amount of required feedback and training could be reduced. For example, with orientation estimation the

beam measurements could be performed on the direction of the sway thus decreasing the required measurement produced protocol overhead.

4.5 Summary

In the context of small cell backhaul the millimeter-wave frequencies refer to the 60 and 70/80 GHz frequencies also known as V- and E-band. The most attractive feature of these frequencies is the large available bandwidth that provides unlicensed or lightly licensed spectrum; allowing the data rates of several gigabits per second with low a cost and easily deployable spectrum. Millimeter-wave bands are range limited by high attenuation due to distance and rain. Additionally, V-band experiences high atmospheric attenuation limiting the range even further. However, the high attenuations decrease interference between the neighboring backhaul radio links. To cope with the high path losses of millimeter-wave frequencies, high antenna gain, the order of 30 to 40 dBi, is required. Therefore the antenna beam widths are less than a few degrees. The narrow beams reduce the interference even further and allow high frequency reuse.

The small cell backhaul devices should provide plug and play features where the backhaul devices automatically find other devices in any direction. Furthermore, to achieve high availability the radio device should compensate temporary misalignments caused by sways and twists of the installation site. The automatic link alignment with the vibration compensation requires beam steerable antennas. Beam steerable antennas can change the transmission or reception direction of the device. Antenna technologies called the integrated lens antenna and beamforming provide the beam steering capabilities. With beamforming, the beam width and the direction of the antenna are adjustable. However, the complexity of the system increases exponentially with narrow beams. To decrease the complexity of beamforming, predefined codebooks for different beam widths and directions are proposed in many studies, to simplify and speed up the system. The lens antenna provides simple beam steering capabilities in predefined discrete directions and with fixed beam width.

For the automatic link alignment the beamforming technology provides more versatility than the lens antenna technology, due to the adjustable beam width. Without any prior information of the searched devices, ILAs has to rely on the exhaustive search method when finding other devices; resulting an exponentially increasing beam alignment time as the number of possible search directions increases. With the beamforming technology, wide beams can initially determine the approximate direction of the radio link. After the approximate direction is found, the narrower beams can be used in the direction of the estimated direction, reducing the number of beam searches.

The presented vibration compensation methods included three methods: orientation estimation method, RSSI measurement method and a hybrid method. If the wind induced behavior of the installation structure, such as a lamp post, could be modeled with reasonable accuracy, the vibration compensation could be performed simply by the orientation estimation. The method utilizes an orientation sensor estimating the tilting angles of the device and the beam is switched based on the angles. Measurement based vibration compensation could provide installation site independent functionality. By applying training periods, the method measures the neighboring beams during the training periods and determines if a better beam is found. Furthermore, with a feedback channel the devices could jointly decide the best possible beam pair that maximizes the signal quality. However, the training periods and feedback decrease the capacity of the radio link but increase the availability. Therefore, the measurement based vibration compensation is a trade-off between capacity and availability. Combining the measurements with the orientation estimation, the number of required training periods would decrease. For example, requesting training periods only when the movement of the device is detected or when the signal quality decreases, the measurements could be applied less frequently and in the direction of the sway. Therefore, the number of training periods would decrease thus still enhancing the capacity and availability of the radio link.

5 The system description

This chapter provides the system description and the author's contribution to the proof-of-concept beam steerable millimeter-wave small cell backhaul system developed by Nokia Solutions and Networks. The main author's contribution in the project has been:

- drafting the limitations, challenges and possibilities of beam steering methods for the system
- mathematical analysis of a pole sway for vibration compensation (Chapter 4)
- the software development, implementation and testing of the automatic link alignment and author's invented vibration compensation methods implemented on the beam steering processor (BSP)
- creation, software development and implementation of the MATLAB functions and graphical user interface (GUI) for the development, visualization and debugging of the beam steering methods
- development and implementation of the auxiliary components of the BSP including beam control, RSSI measurements, orientation sensor, Led-matrix and LCD-display

This chapter introduces the system overview together with the implemented beam steering methods. First, the proof-of-concept system is introduced. Second, the automatic link alignment procedure is explained. Third, the vibration compensation methods are described. In the next chapter, the test setup and the test results for the system are introduced.

5.1 Explanation of the system

The high level overview of the proof-of-concept beam steerable millimeter-wave small cell backhaul system is provided in Figure 30. The antenna system provides beam steering capabilities by utilizing an integrated lens antenna with a feed-array. Modem handles the baseband data of transmission and reception.

The Higher Layer Protocols (HLP) on separate hardware coordinates the communications between multiple devices. The HLP and the modem are connected with an Ethernet interface. The HLP add commands to the Ethernet frame and the modem extracts the necessary data for the BSP. As the name implies, the beam steering processor handles the beam steering functionalities. The beam steering decisions are made based on the HLP's commands, orientation estimation and RSSI measurements. Additionally, the BSP is connected to LED-Matrix, LCD-Display and MATLAB GUI on PC, which are used for debugging and demonstration purposes.

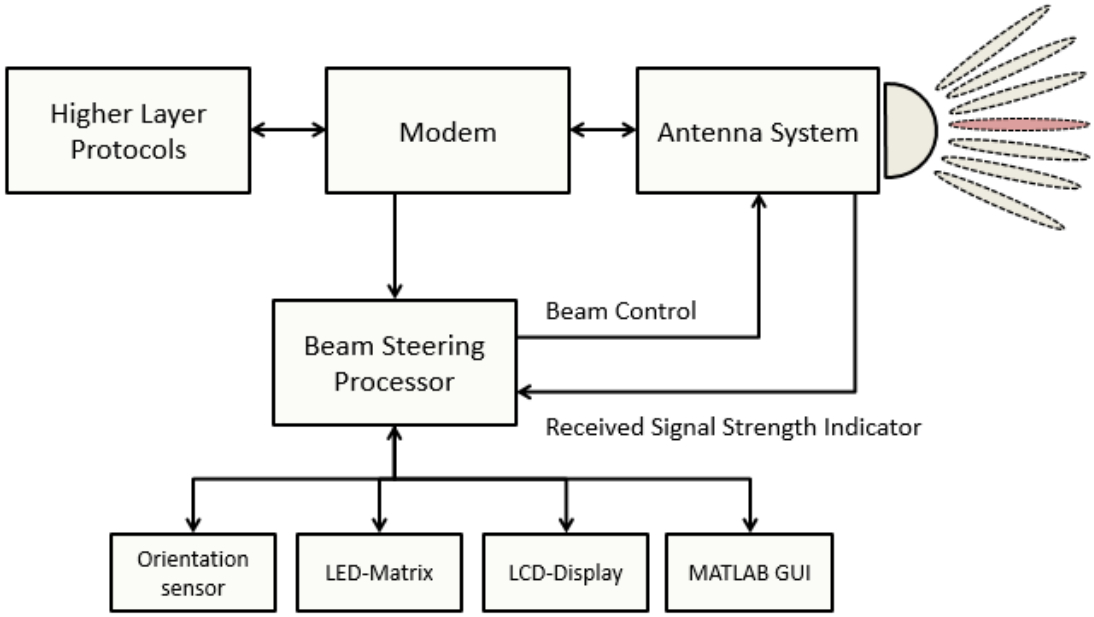

Figure 30: High level overview of the proof-of-concept millimeter-wave beam steering system for small cell backhaul.

Antenna system: The antenna system is developed for E-band. The system includes the beam steerable antenna and the necessary radio frequency components for the millimeter-wave communications. The antenna is an integrated lens antenna whose diameter is 95 millimeters and the material is Rexolite. The beam steering is realized by 4x16 feed-array. Thereby, the system has 64 beams in total, 16 beams on each of the four rows. One antenna element is active at a time and each antenna element has a fixed beam direction. The three decibel beam width of the system is around two and a half degrees;

resulting in approximately a beam steering range of ±4 degrees in the vertical direction and ±17 degrees in the horizontal direction. Figure 31 demonstrates the three decibel beam widths of the system. The antenna gain of the system is ranging from 18 to 20 dBi, depending on the beam. The antenna system is connected to the modem and BSP. The modem feeds the baseband data for the antenna system and vice versa. The beam is switched by a control signals transmitted from the BSP to the antenna system. Additionally, the antenna system performs RSSI measurements which are forwarded to the BSP.

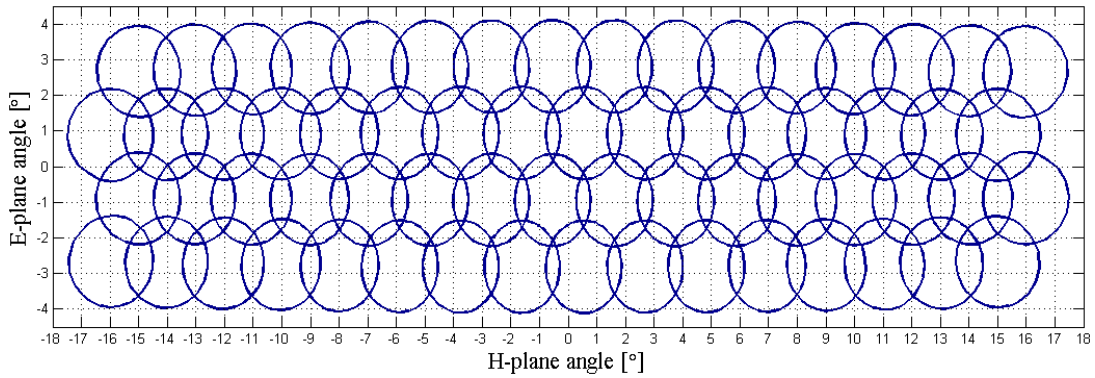

Figure 31: Three decibel antenna beam widths of the antenna system.

BSP: The beam steering software is implemented on chipKIT Max32 Prototyping Platform [32] utilizing a Microchip 32-bit microcontroller [33]. The responsibility of the BSP is to change the active beam according to HLP commands and independently compensate the temporary misalignments of the radio link. The HLP commands are transmitted from the modem to the BSP. The beam is changed by transmitting a signal to the antenna system. Vibration compensation algorithms are implemented independently by the BSP. The vibration compensation is based on the RSSI measurements and orientation estimation. The RSSI measurements are provided by the antenna system and the orientation estimation is handled by a separate sensor connected to the BSP. Other peripherals devices connected to the BSP are LCD-Display, LED-Matrix and MATLAB GUI.

Orientation sensor: UM6 Ultra-Miniature Orientation Sensor [34] is connected to the BSP. The sensor is connected to the BSP via Universal Asynchronous

Receiver Transmitter (UART). The sensor utilizes rate gyros, accelerometers and magnetic sensors to estimate the orientation angles of the device. For instance, the BSP uses the orientation estimations with vibration compensation.

LED-Matrix: Four 8x8 LED-matrixes [35] are connected via Serial Peripheral Interface (SPI) to the BSP for demonstration and debugging purposes. For instance, at the center of the LED-matrix a 4x16 area of LEDs are allocated to indicate the current beam.

LCD-Display: A LCD-display [36] is connected to the BSP via UART. The display is used for instance to show the current RSSI or the orientation of the device. The display includes four 20 character rows.

Modem: The modem is a TDD modem developed by Xilinx for millimeter-wave backhaul radio links. All the baseband functionalities of the system are handled by the modem. The modem is connected to the HLP, BSP and antenna system. The HLP and the modem are connected via Ethernet Interface. The modem extracts the beam steering commands from the Ethernet frames for the BSP. Additionally, the modem handles the transmission and reception control of the BSP.

Higher Layer Protocols: The higher layer protocols are located on separate hardware and are responsible for coordinating the communication between multiple small cell backhaul radio links. The functions of HLP that are related to beam steering are for example the neighbor discovery algorithm that connects all of the devices within the reach of the radio link.

MATLAB GUI: The BSP and MATLAB GUI on a computer are connected using UART. The MATLAB GUI is presented in Figure 32. All the features of the MATLAB GUI are implemented to support the beam steering software development. Next, the GUI is introduced with more detail. The most important parts of the GUI are the three graphs:

- The left upper graph shows the orientation estimates of the orientation sensor. The values include yaw, pitch and roll.

- The left lower graph shows the RSSI. Additionally, the graph shows with red numbers when a beam is changed and with start and stop markers when the automatic link alignment procedure is started.
- The lower right curve shows the beam graph similarly as in Figure 31. The current beam is rounded with the blue circle around the beam. The beams have different colors to demonstrate the current RSSI. White color denotes that the RSSI of the beam is around the noise level and red color denotes high RSSI.

Another important part of the GUI is the pop-up menu on the right hand side of the GUI. From the pop-up menu, a command is selected that is transmitted to the orientation sensor. The sensor executes the commands and the result is displayed below the pop-up menu. For instance, in the figure the communication register of the sensor is read and displayed below the pop-up menu.

The GUI has variety of different labels denoting the boxes that include pop-up menus and buttons:

- Serial port connection label handles the functionalities needed to connect MATLAB and the BSP. The pop-up menu includes the serial ports of the PC and therefore the port connected to the BSP should be selected. The connect button connects the MATLAB and the BSP. The read data button starts the communication between MATLAB and BSP. The ping button checks if the connection has been established and queries the current parameters of the BSP.
- Data recording label includes the record and the analyze buttons. The record button starts the data collection of the RSSI, current beam and orientation angles. The analyze button plots the statistics of the recorded data that are used to analyze the vibration compensation methods.
- The commands label shows the status of an executed command and show the receive buffer status of the MATLAB. The buffer size is printed to the GUI to show that data from BSP is not lost due to buffer overflow.

- The Tx frequency label includes buttons to change the BSP's transmission frequency of the RSSI and orientation estimations. By controlling the transmission frequency, the receive buffer of MATLAB is kept stable.
- The angle information label includes a pop-up menu to select what angle estimation the BSP transmits. The selection is between Euler angles, quaternions and no angle transmission. Additionally the angle offset of the BSP can be reset and the plotted angels can be selected.
- The beam selection label includes a button to disable or enable RSSI transmission from the BSP, a pop-up menu to switch the current beam, a button to find the best beam and a pop-up menu to select the vibration compensation method.
- From the beamwidth label the assumed three decibel beam width of the vibration compensation methods can be changed.
- From the measurements label the threshold values of the RSSI measurement method and the hybrid method of RSSI measurement and orientation estimation can be changed. The two values below the buttons show the percentage of time that the measurements occupy and the frequency of the neighbor beam measurements.
- The sensor steering label includes the buttons to change the parameters of the orientation estimation based vibration compensation methods. The parameters are the amount reduced RSSI measurements before the beam switch and threshold to determine when the RSSI is decreased.

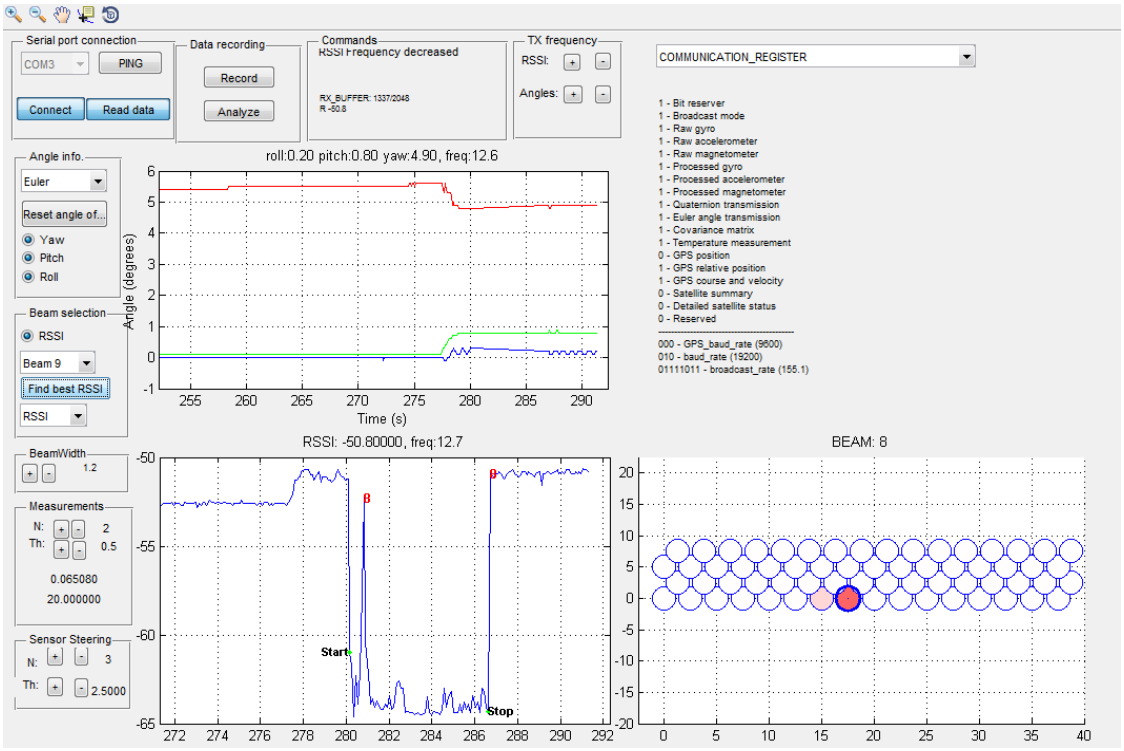

Figure 32: MATLAB GUI.

5.2 Automatic link alignments

The goal of the automatic link alignment is to establish the connections automatically between the backhaul devices within the reach of the radio link. The automatic link alignment is coordinated by the HLP. The modem extracts the HLP commands from the Ethernet frames and sends them to the BSP. According to the commands, the BSP changes the beam. The method realizes the so called brute force method. During predefined time intervals, both end of the radio link scan through all the possible beam pairs. A backhaul device is in a slow mode or a fast mode. Initially, a new device in the network is in the fast node and an existing device is in the slow mode. In the slow mode, the device sends predefined training messages during predefined time intervals. The duration of the training message is adequate time for the device in fast mode to can scan through all the possible beam directions. After the device in slow mode has completed sending the training messages, it moves to the receive mode for detecting a acknowledge message from the fast mode devices. If the device in fast mode detects the training messages, it responses with acknowledge packets

to establish a connection. After every cycle time of the slow mode, the slow mode devices switch to the next beam direction. Thereby, after the slow mode device has gone through the beam direction it has created the connection to its nearby devices.

5.3 Vibration compensation

This section introduces the vibration compensation algorithms implemented in the BSP. The implemented methods are:

- orientation estimation method
- RSSI measurement method
- the hybrid method that utilizes RSSI measurement method with orientation estimation

Orientation estimation method: The orientation estimation method utilizes the UM6 Ultra-Miniature Orientation Sensor. The principle of the method is demonstrated in Figure 33. The BSP continuously reads the orientation angles from the sensor. The beam is changed if the calculations based on the orientation angles suggest switching the beam and if the RSSI have been below the given threshold in N consecutive measurements. However, if the previous beam was better than the new beam, the beam is switched back to the previous beam and the procedure starts over. This property is implemented to provide protection from bad decisions due to the difficulty of estimating the exact point of the radio link inside a beam and the exact direction of the vibration.

The methods calculations are based on the mathematical analysis provided in Chapter 4. As explained in Chapter 4, the assumption is that the device is installed on a lamp post kind of a structure where the vibration of the device takes place on a spherical surface. The mathematical consideration showed that the horizontal pole sway is insignificant and the worst case vertical sway is equal to half of the three decibel beam width. The beam width of the antenna is approximately 2.5 degrees. Therefore, 1.25 degree sway in the vertical direction is the threshold value for changing the beam. The rotation of the device is taken

into account to determine the direction of the vertical sway. If the device is only rotating, 1.25 degrees is the threshold values for changing the beam. Figure 34 illustrates the orientation estimation. The red x-sign is the active beam and the black arrow is the estimated direction and magnitude of the vibration. The red dashed line demonstrates the beam change. The beam is switched when the black arrow reaches some other beam.

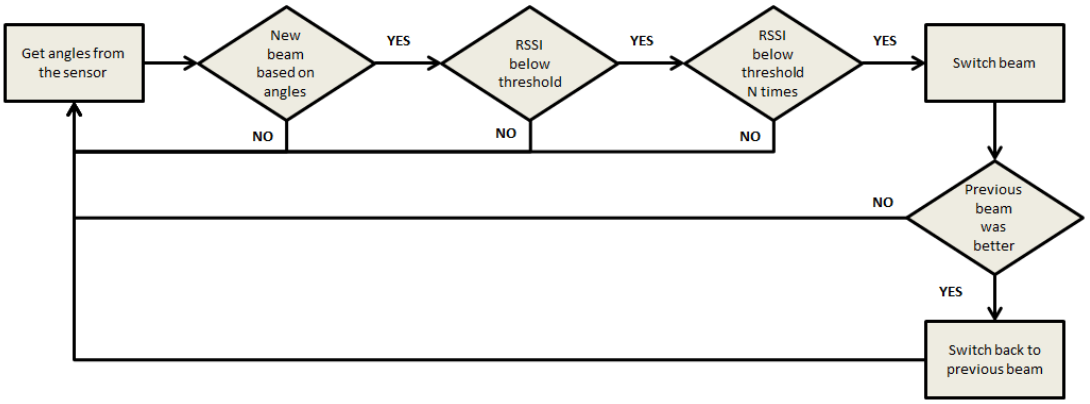

Figure 33: Vibration compensation utilizing orientation estimation.

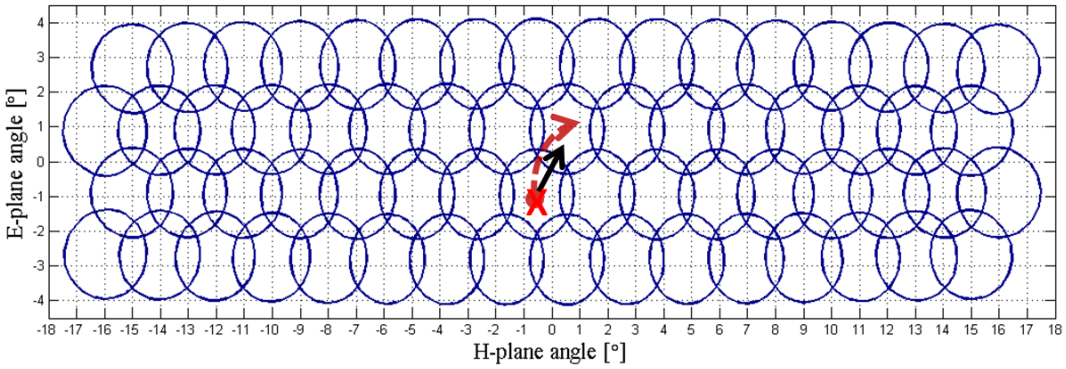

Figure 34: Orientation estimation based vibration compensation.

RSSI measurement method: In the RSSI measurement method, neighboring beams of the current beam are measured periodically. The measurements must take place with sufficient intervals in comparison with the vibration magnitude and frequency of the installation site. Additionally, predefined training periods are required from the transmitter and receiver to determine the time slots of the measurements. Figure 35 demonstrates the principle of the method. First, the neighboring beams are measured. The beam is changed if the same beam

has had better RSSI in N consecutive measurements. The neighbor beam measurement is illustrated in Figure 36, where the red x-sign represents the active beam and the dashed circle shows the direction of the neighbor measurements. Unlike the orientation estimation method, the RSSI measurement method provides installation site independent vibration compensation as the features of the installation site's vibration surface are not required.

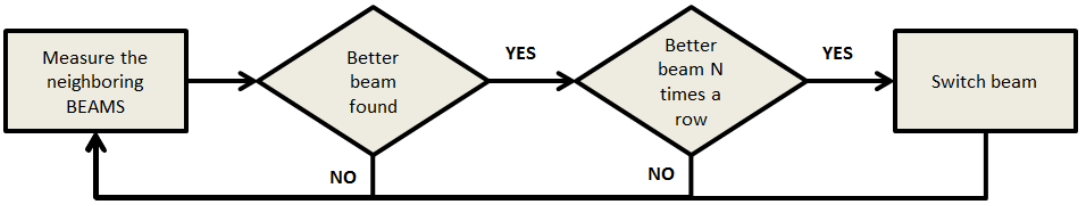

Figure 35: Illustration of the RSSI measurement based vibration compensation.

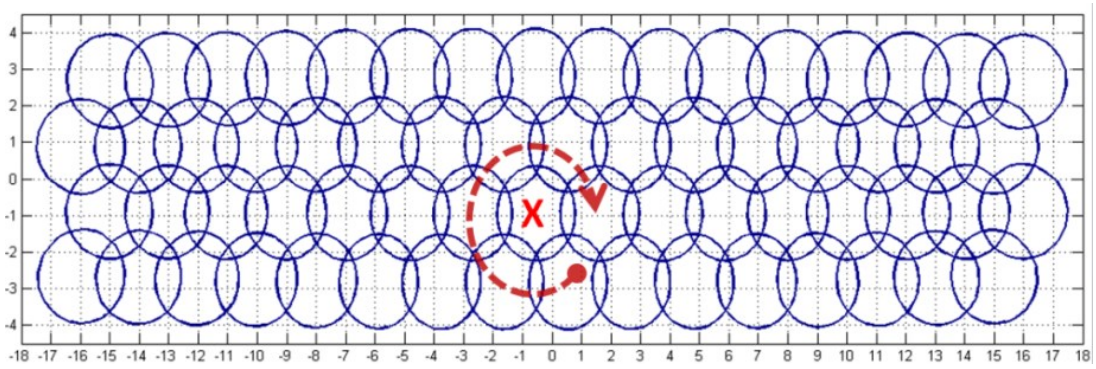

Figure 36: Neighbor beam measurements of the RSSI measurement method.

Without any prior information about the installation site's vibration, the adequate frequency of the measurements can only be estimated. By assuming that the installation site vibrates with the maximum frequency of 5 hertz and the vibration takes place between two beams resulting in 10 beam changes in a second. Additionally, by assuming that sufficiently working vibration compensation requires four neighbor scans before changing the beam. Therefore, the number of required neighbor scans is around 40 per second. The frame length of the HLP is ranging from 30 to 300 microseconds resulting 1200 to 12000 frames per second. If the neighbor scan is carried out during the HLP frame, every 30^{th} to 300^{th} frame should be allocated for the neighbor

measurements creating a 0.3 to 3 percentage extra overhead taken by the measurements.

The hybrid method: The hybrid method combines the RSSI measurement method with the orientation estimation method. The method is described in Figure 37. Similarly as with the orientation estimation method, the hybrid method uses the orientation angles for calculating whether the beam should be switched. When the calculations suggest switching the beam, the RSSI is measured from the beams in the direction of the movement. Therefore, the number of measurements is reduced as measurements take place only when the device is vibrating. Additionally, the measurements reduce the inaccuracy of the orientation estimation method. The measurements in the direction of the movement are demonstrated in Figure 38. The red x-sign demonstrates the current beam. The black arrow is the estimated direction of the movement. The red dashed arrow shows the beams that are measured. The calculated new beam is measured and the neighboring beams of the calculated beam are measured, similarly as with the RSSI measurement methods neighbor measurement. The current beam is included in the neighbor measurement to verify that the beam is not switched to a worse beam.

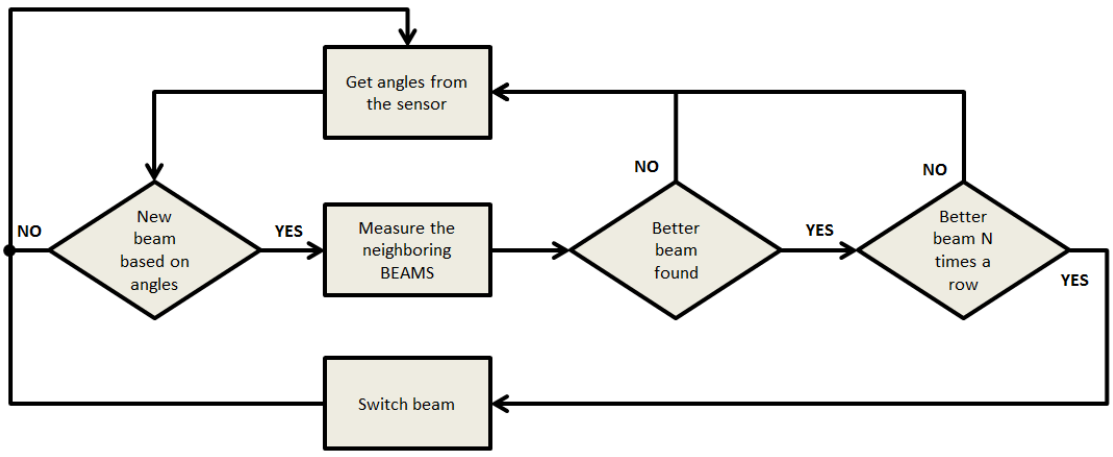

Figure 37: Illustration of the hybrid method.

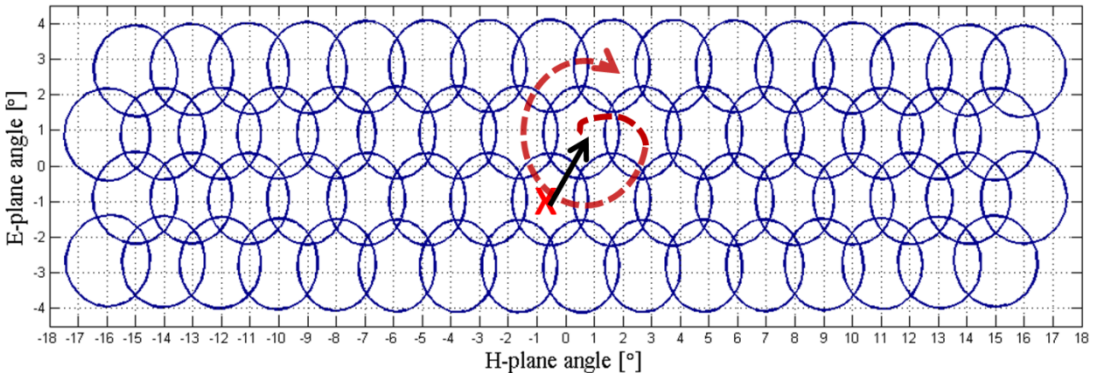

Figure 38: Neighbor beam measurements of the hybrid method.

To determine when the measurements frames should take place, the communicating devices need to exchange information. When the movement is detected, the moving device could send a request for N measurement frames in specific time slots. When the movement stops, the communicating devices agree to stop the measurements.

5.4 Summary

This chapter introduced the proof-of-concept millimeter-wave small cell backhaul system with the millimeter-wave beam steering algorithms. The main components of the system are the beam steering processor, orientation sensor, antenna system, modem and the higher layer protocols. Additionally, other auxiliary components of the system that are used for debugging and demonstration purposes include LCD-display, LED-Matrix and MATLAB GUI. The author's contribution of the system includes:

- drafting the limitations, challenges and possibilities of beam steering methods for the system
- mathematical analysis of a pole sway for vibration compensation (Chapter 4)
- the software development, implementation and testing of the automatic link alignment and author's invented vibration compensation methods implemented on the beam steering processor (BSP)

- creation, software development and implementation of the MATLAB functions and graphical user interface (GUI) for the development, visualization and debugging of the beam steering methods
- development and implementation of the auxiliary components of the BSP including beam control, RSSI measurements, orientation sensor, Led-matrix and LCD-display

The antenna system is designed for E-band and utilizes an integrated lens antenna with 4x16 feed-array. The antenna beam widths are approximately 2.5 degrees with the antenna gain ranging from 18 to 20 dBi. The beam steering is handled by the beam steering processor. The implemented beam steering algorithms are automatic link alignment and three different vibration compensation methods. The automatic link alignment is coordinated by the HLP and the BSP changes the beams according to the HLP commands. The implemented vibration compensation methods include:

- orientation estimation method
- RSSI measurement method
- the hybrid method that utilizes RSSI measurement method with orientation estimation

The orientation estimation method utilizes the UM6 Ultra-Miniature Orientation Sensor connected to the BSP. Together with the orientation angles provided by the sensor the method calculates the correct beam using the mathematical analysis given in Chapter 4. The RSSI measurement method periodically measures the RSSI of the neighboring beams and changes the beam if the measurements suggest that a better beam was found. The hybrid method combines the orientation estimation and the RSSI measurement method. The beams are measured only in the direction of the movement and only when the movement is detected. Therefore, the number of required measurements is reduced thus reducing the extra overhead created by the measurements.

6 Tests and test results

This chapter explains the test setup and provides the test results for the proof-of-concept beam steerable millimeter-wave small cell backhaul system introduced in the previous chapter. The tests include the automatic link alignment tests and the vibration compensation tests for the implemented methods. The goal of the tests is to verify and study the performance of the methods for further development. The content of this chapter is the following; first, the test setup is described; second, the test results are provided; finally, the results are analyzed with suggestions for future work.

Due to the early stage of the project, hardware limitations limit the testing of the system with the described configuration. For instance, the HLP is excluded from the tests, the TDD scheme of the modem is modified, the measurement periods of the vibration compensation methods are artificial and the test are carried out with the beams 1 to 16.

6.1 Test setup

The test setup is described in Figure 39. The setup contains two backhaul nodes. The node in the left hand side of the figure is equipped with the beam steering hardware described in the previous chapter. The node in the right hand side of the figure uses a horn antenna instead of the lens antenna. The horn antenna transmits in a fixed direction. The three decibel beam width of the horn antenna is around 10 degrees and the antenna gain is around 20 dBi. The modems operate in TDD. However, due to the hardware limitations of the system, the transmission and reception channels of the modems are divided between wireless and wired transport medium. The horn antenna transmits over air at 70 GHz and the lens antenna system receives the wireless signal. Connections to opposite direction go through wired media. Thereby, the beam steering tests take place in the lens antenna node that is only receiving during the reception periods of the TDD.

The nodes are installed in a pole, specially designed for the beam steering tests, with height around one meter. The pole can be rotated or tilted in any direction. The distance between the devices, installed in the poles, is approximately four meters. The lens antenna node is connected to MATLAB that records the RSSI, orientation and current beam of the device. The recorded data is analyzed after the tests to evaluate the performance of the methods.

The lens antenna system has a known fault limiting the tests. The beams on the lowest row of the antenna-array, denoting the beams from 1 to 16, have substantially higher antenna gain than the rest of the beams. This is illustrated in Figure 40 showing a lens antenna measurement, where some of the beams are shown with their relative antenna gain. For instance, the beams at the lowest row have approximately 5 to 15 decibel higher gain than the beams at the second row. Therefore, the horn antenna is pointed towards the lowest beam row of the lens antenna and the tests take place with those beams. This limitation prevents the testing of the vibration compensation methods with vertical pole sway. However, by rotating the device parallel to the beams at the lowest row, the situation is similar when tilting the device vertically.

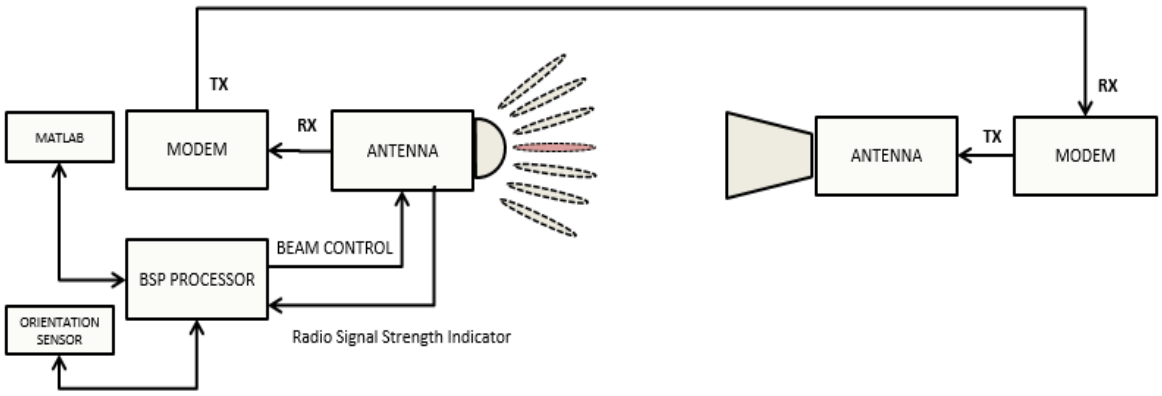

Figure 39: Test setup.

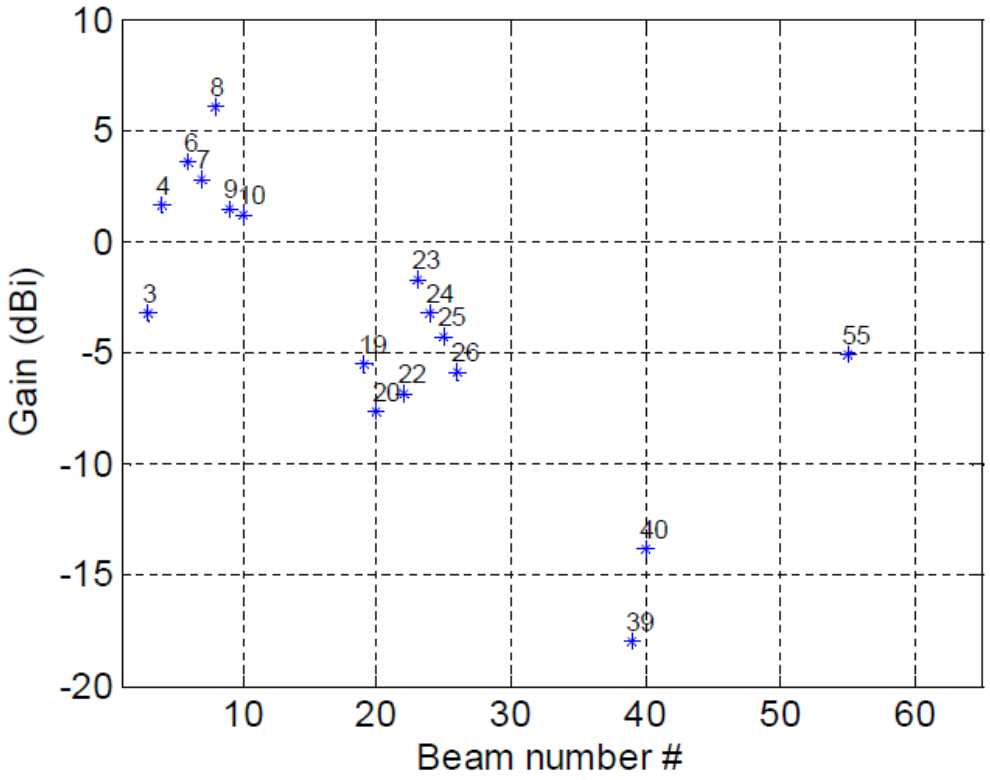

Figure 40: Relative antenna gain measurement.

6.1.1 Automatic link alignment

Due to the hardware limitations of the system, the automatic link alignment test is carried out without the HLP. However, the test is performed similarly like with the HLP, simply by scanning through all the beams and connecting to the best-found beam. The test setup is illustrated in Figure 41 where the receiving device with the beam steering capabilities is rotated with different angles. With the different orientations of the device, the automatic link alignment procedure is started. The different test cases are investigated with the RSSI graph and beam color map provided by the MATLAB GUI. The results will show that the system finds the best beam in the expected direction and can connect to the beam, as it was designed to do. This is illustrated in Figure 41 where the lens antenna device finds the beam that is pointing towards the transmitting device.

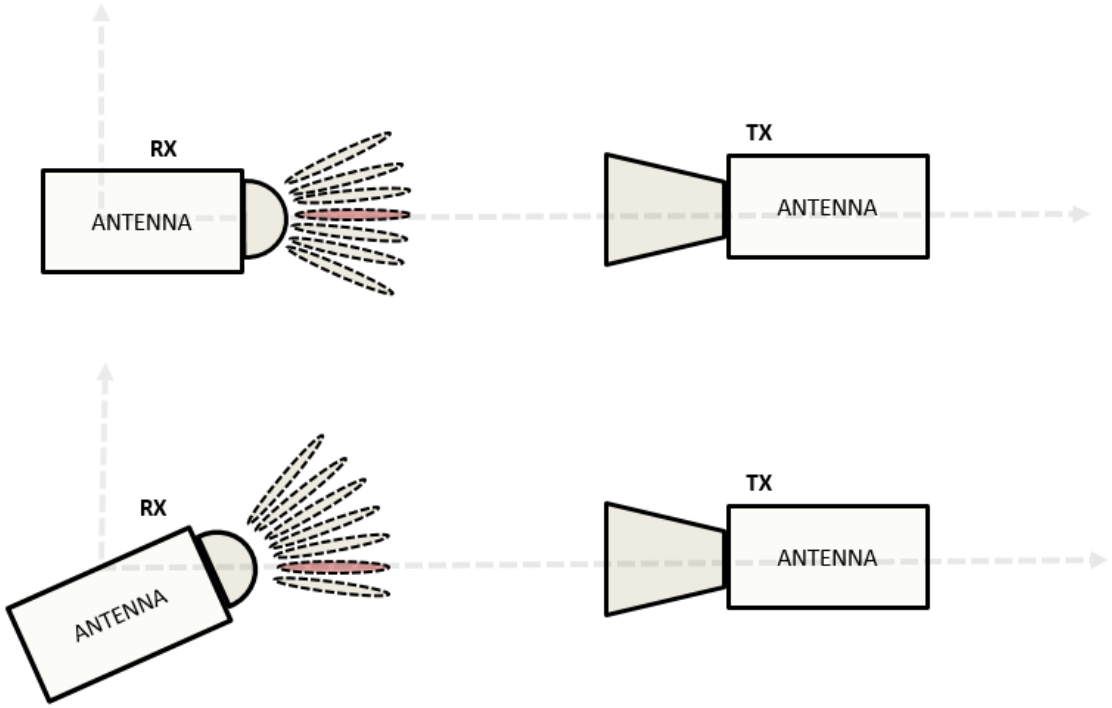

Figure 41: Automatic link alignment test.

6.1.2 Vibration Compensation

The vibration compensation tests include the testing of the three methods described in the previous chapter: the RSSI measurement method, the orientation estimation method, and the hybrid method. The vibration compensation methods are tested by vibrating the receiving device from side to side. Additionally, the test is performed without any vibration compensation method in order to illustrate the achieved gain of the methods. During the tests, the MATLAB GUI records the RSSI, the orientation angles and the current beam. With the data, the methods are evaluated with:

- angle versus RSSI graph to show the average RSSI with different orientation angles
- probability density functions (PDF) of the RSSI
- cumulative distribution functions (CDF) of the RSSI
- RSSI graph in the time domain showing the beam switches and demonstrating the performance of the method.

Due to the limitations of the hardware, the measurement periods of the RSSI measurement method and the hybrid method are carried out during the regular frames of the modem. Therefore, the RSSI shows insignificant values during the neighbor beam measurement. However, the measurement periods are excluded from the test results showing performance as if the measurement periods would be included in some protocol.

The main objective of the tests is to provide knowledge of the advantages and disadvantages of the vibration compensation methods for further development before complete the testing with HLP and proper antenna hardware.

6.2 Test results

6.2.1 Automatic link alignment

The automatic link alignment was tested with six different orientations of the lens antenna device. The results are shown in Figures 42 to 47. Each figure is taken from the MATLAB GUI representing the different orientations. The graph on the left hand side of a figure is the RSSI in the time domain where x-axis is time in seconds and y-axis is the RSSI value in dBm. The numbers in the graph are the scanned beams with RSSI above -55 dBm that is considered as a limit for sufficient signal quality. The noise level in the system is around -65 dBm. The start and stop markers in the graph indicate the start and stop instants of the automatic link alignment. The right hand side of a figure is the beam graph similarly as in Figure 31. The x- and y-axis demonstrates the beam width in degrees. The color of a beam is from white to red. A white color demonstrates RSSI around noise and red indicates good signal strength.

In Figure 42, the device is rotated to its other extreme, towards the beam number 16. The RSSI graph and the beam graph shows that the beam number 16 was found with RSSI around -46 dBm. Additionally, the beam number 15 had RSSI slightly above the -55 dBm. Excluding the found beam, the RSSI of the beams are around noise level which is close to the ideal performance of the system. Figure 43 shows the alignment test when the node is rotated a few

degrees in relation with the previous test. Beam number 14 was found with RSSI around -53 dBm. The beam graph of the test shows that the beams around the found beam had RSSI slightly above the noise level. This is also seen from the RSSI graph with the peaks on the graph. The next test is demonstrated in Figure 44; the beam number 10 was found with RSSI around -49 dBm. Three beams in the neighborhood of the found beam had RSSI above the -55 dBm. Additionally, the beam graph demonstrates that a few beams in random positions had RSSI slightly above the noise level. In the fourth test demonstrated in Figure 45, the beam number 7 was found with RSSI around -43 dBm. Two neighboring beams have RSSI above the -55 dBm. Otherwise, the test shows good performance as the rest of the beams have RSSI around the noise level. In Figure 46, demonstrating the fifth test, the beam number 4 was found with RSSI around -45 dBm. Additionally, several beams above -55 dBm were found in the vicinity of the found beam and a few beams with RSSI slightly above noise was found in random positions similarly as in Figure 44. In the final test demonstrated in Figure 47, the beam number 2 was found with RSSI around -43 dBm. Several neighboring beams had RSSI above -55 dBm and a few beams had RSSI slightly above the noise level in random positions.

The tests showed that the system is capable of aligning to the best possible beam and the direction of the found beam correlates with the rotation and with the expected beam direction. Ideally, the lens antenna should find only one strong beam almost like in Figure 42. However, in some of the tests, the neighboring beams of the found beam had signal strength above the –55 dBm, and beams with signal strength slightly above the noise level was found in random positions. The observed non-idealities might be caused by several reasons for instance by the wider beam width of the horn in comparison with the lens antenna, strong side lobes of the neighboring beams, reflection from the surrounding or by the reflections and leakages inside the antenna system.

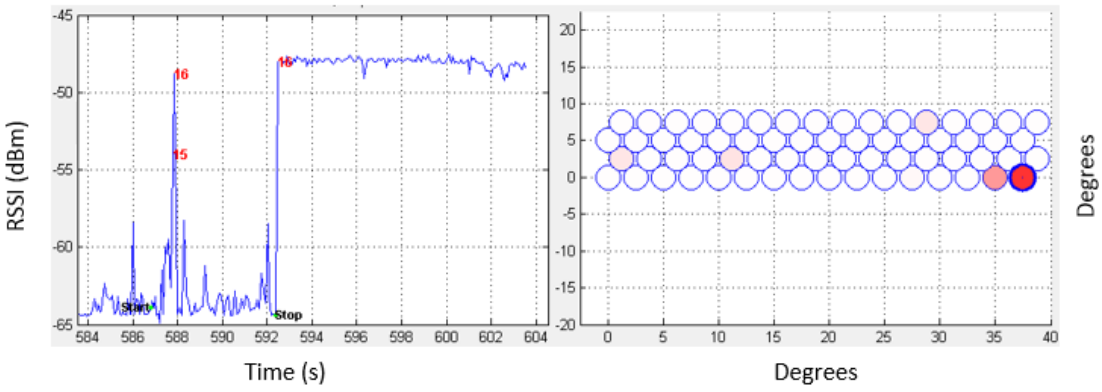

Figure 42: First automatic link alignment test.

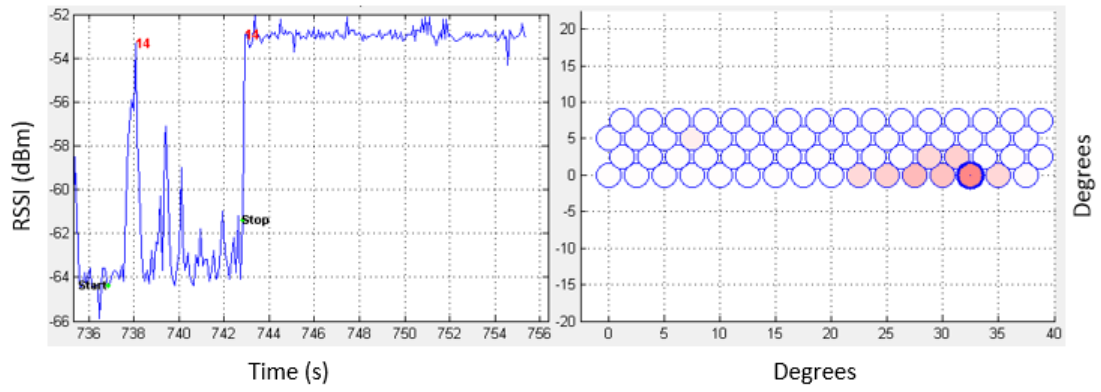

Figure 43: Second automatic link alignment test.

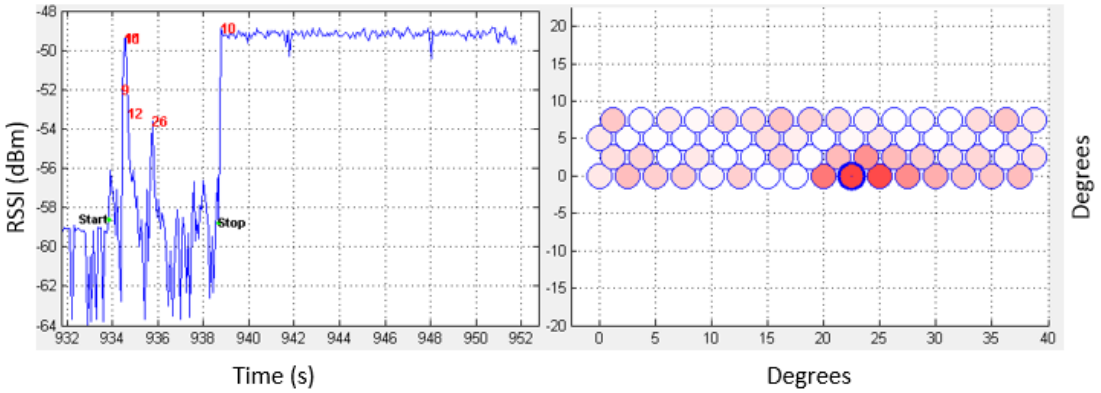

Figure 44: Third automatic link alignment test.

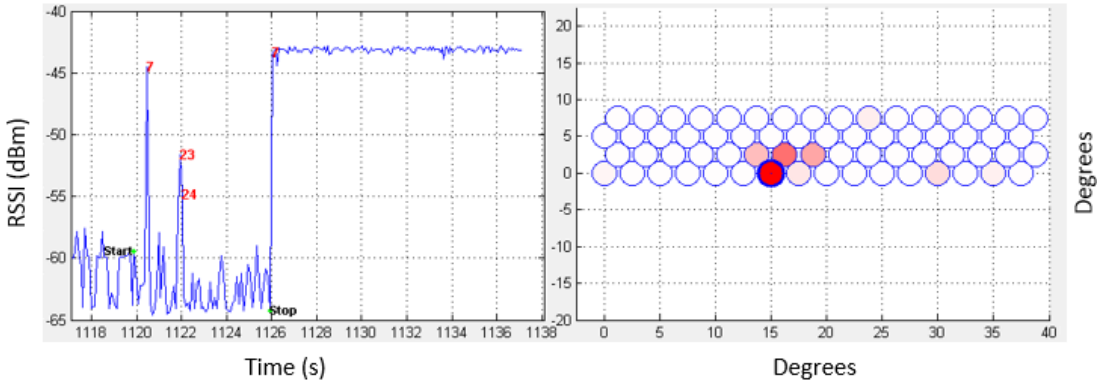

Figure 45: Fourth automatic link alignment test.

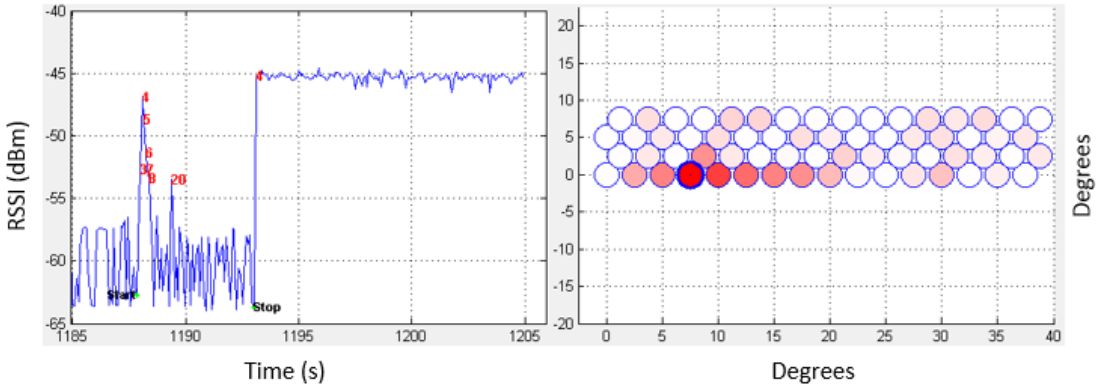

Figure 46: Fifth automatic link alignment test.

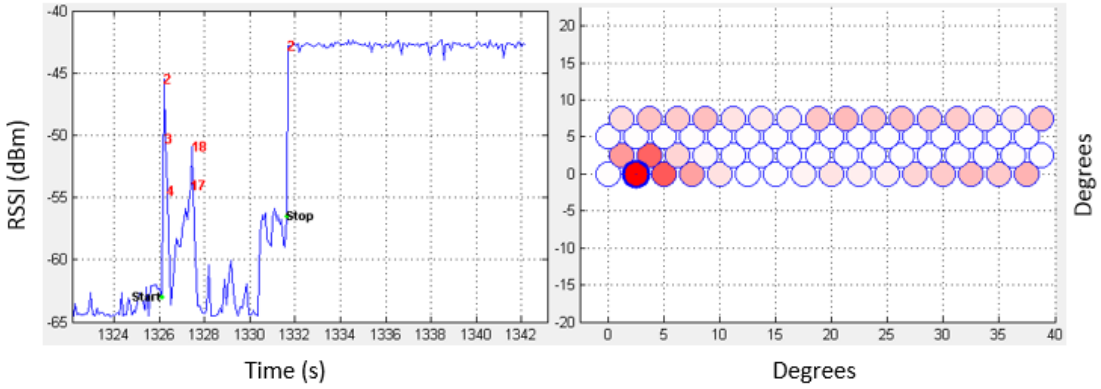

Figure 47: Sixth automatic link alignment test.

6.2.2 Vibration compensation

The tests were carried out by vibrating the device manually from side to side. Therefore, the tests are not exactly the same for all of the methods and the results cannot be interpreted precisely rather taken as suggestive results. Due

to the inadequate gain of the beams in the upper rows, the transmitting horn antenna was pointed towards the lowest row of the lens antenna. Therefore, the beam steering took place between the beams 1 and 16. The test results are presented in Figures 48 to 50.

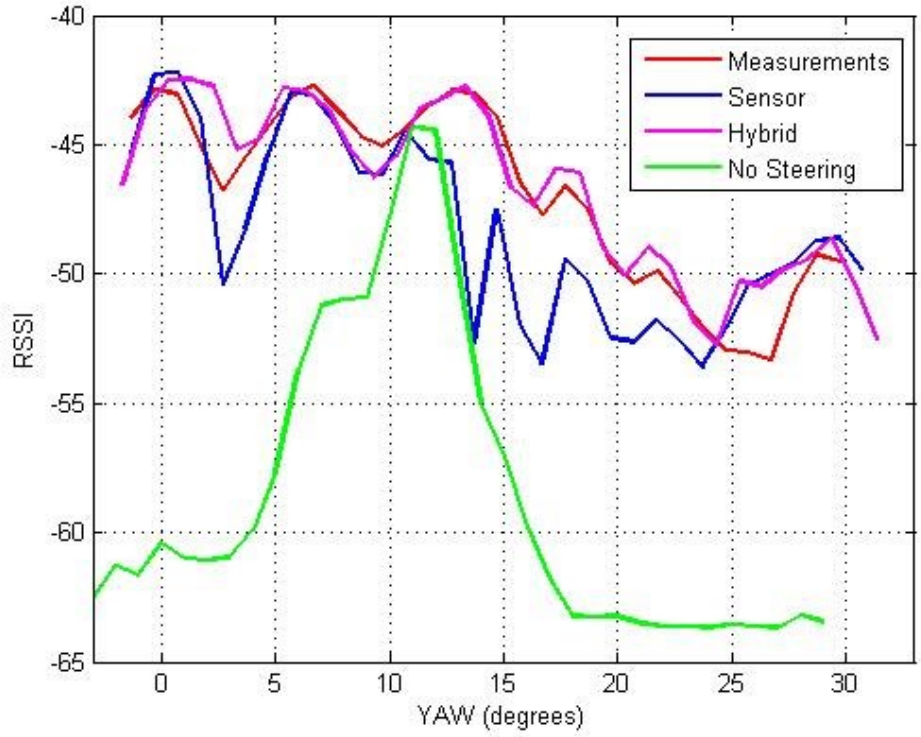

Figure 48: Average RSSI of the vibration compensation methods with different orientations.

Figure 48 demonstrates a graph where the orientation angle yaw is on the x-axis and the average RSSI of the corresponding angle is on the y-axis. The yaw value of zero degrees is approximately the orientation for the beam number 1 and the yaw value of 30 correspond approximately the beam number 16. The green graph is the test without vibration compensation showing high RSSI at the direction of the selected beam. The graphs of the vibration compensation methods show significant improvement in comparison with the no-steering test. The hybrid vibration compensation method shows the best performance with slightly better graph than the RSSI measurement methods graph. The orientation sensor method has the worst behavior; even so, the performance is reasonably good. Additionally, the tests show similar results as the automatic

link alignment tests; the RSSI decreases with the higher beam numbers, excluding the beam number 16.

Figure 49 demonstrates the probability density function of the observed RSSI. The x-axis shows the measured RSSI and the y-axis shows the probability of the corresponding RSSI level. The results show that the RSSI of the methods is distributed around good signal level. Based on the PDF graphs, an accurate performance comparison between the methods is not possible due to the inaccuracy of the tests and similarity of the graphs. However, the graph of the test without vibration compensation shows that the RSSI is distributed around the noise level confirming that the vibration compensation methods have achieved some gain.

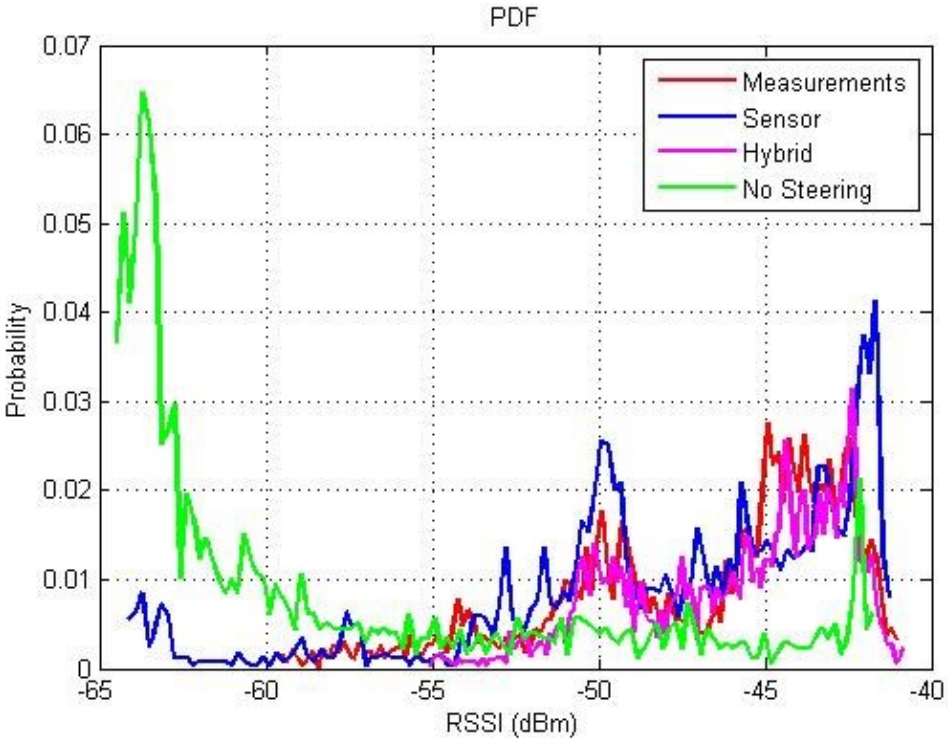

Figure 49: Probability density functions of the vibration compensation tests.

Figure 50 shows the cumulative distribution functions (CDF) of the measurements. The x-axis shows the RSSI and y-axis shows the probability that the RSSI is below the corresponding RSSI. As with the previous figures, the vibration compensation methods show significant improvement in comparison

with the test without vibration compensation. Similarly than in Figure 46, the hybrid method provides the best performance and the RSSI measurement method has the second best performance. The CDF graphs show that with the hybrid method the RSSI is always above the -55 dBm which is considered as a threshold for good signal strength. With the RSSI measurement method, the RSSI is above the threshold approximately 95 percentage of time and with the sensor steering method the time is approximately 90 percentages.

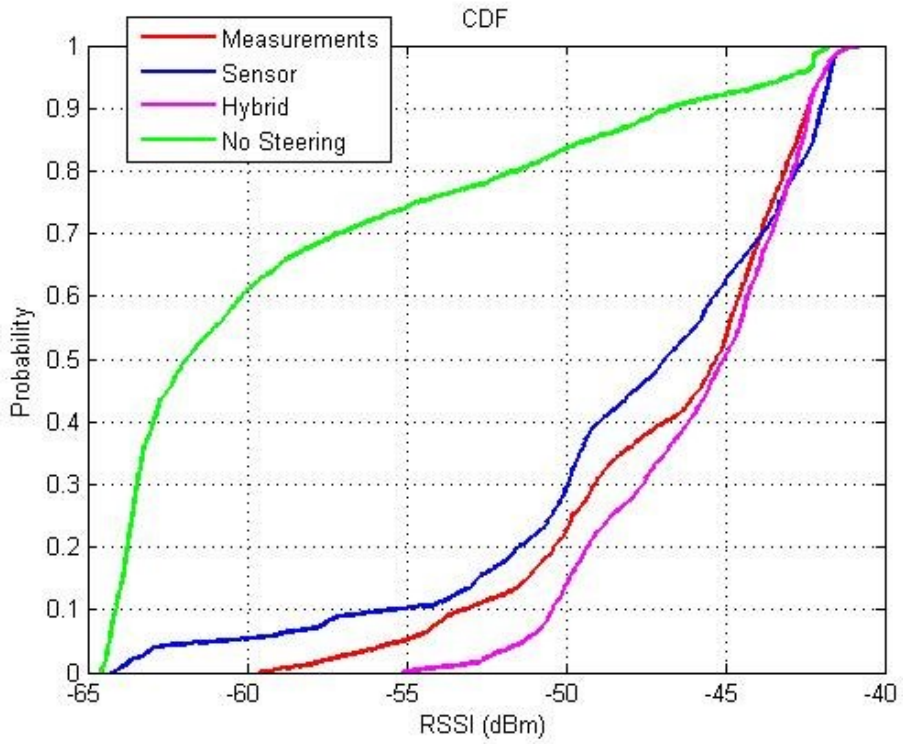

Figure 50: Cumulative distribution functions of the vibration compensation tests.

Due to the inconsistency between the tests, the test results provided by the figures 48, 49 and 50 cannot be interpreted precisely to make definitive conclusions on the goodness of the methods. However, during the measurements different problems were identified that confirm the interpretation of the test results. The next sub-section analyzes the problems and the performance of the system and the methods.

6.2.3 Analysis of the methods

Orientation estimation method: The biggest problem for the orientation estimation method is to define the exact direction of the other devices transmission. For instance, when the automatic link alignment finds the best beam, the exact point where the beam of the other device is directed can be anywhere inside the selected beam. Additionally, the implemented procedure estimating the direction of the radio link includes errors. Therefore, the orientation estimation can lead to wrong decisions. The problem is illustrated in Figure 51. The red x-sign is the selected beam and the black arrows are the estimated direction of the movement with different estimates of the point where the other devices beam is directing. The figure shows that with the same orientation estimation the beam switching decision can lead to different beams thus resulting errors for the vibration compensation. Moreover, the probability of a wrong decisions increases with the inaccuracies from the orientation sensor, the pole sway model and beam positions. Additionally, overcoming these inaccuracies increases the complexity of implementing a reliable vibration compensation solely based on the orientation estimation.

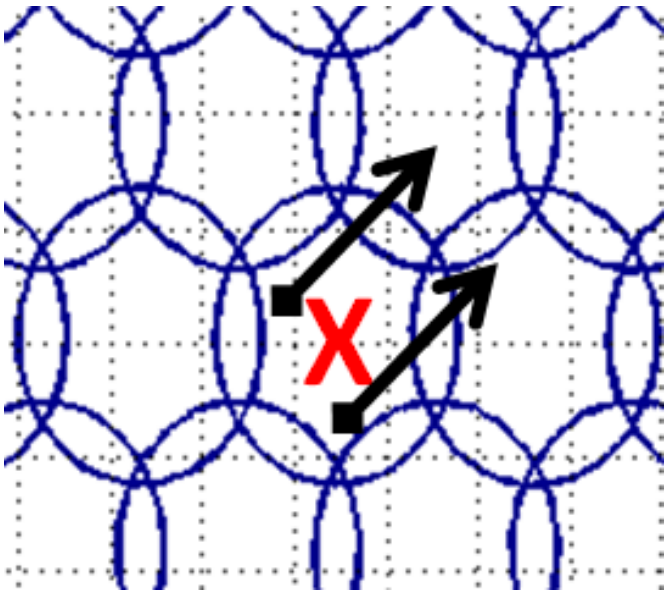

Figure 51: The estimation problem with the orientation estimation method.

Additionally, it was noted during tests that the inequality between the beam gains showed some problems for the implemented method. The problems are

demonstrated in Figure 52 showing the RSSI graph in the time domain. In the demonstration, the device is moved to achieve vibration compensation from beam number 16 towards the beam number 1. From the beam number 16 to beam number 10 the method shows good performance. However, after the method switches to beam number 9 the method detects that the previous beam was better and switches back to beam number 10. A similar problem occurs when the method jumps between the beams 6 and 7. Again, with the beams 4 and 3, the method jumps between the beams that cause a significant RSSI reduction. The switching between the beams is caused by the inaccuracy of determining the beam center and inequality between the beam gains. For instance, from Figure 40 it is visible that the beam number 3 has lower antenna gain than beam number 4 thus causing the jumping between the beams. The jumping reduces the overall signal quality thus decreasing the throughput.

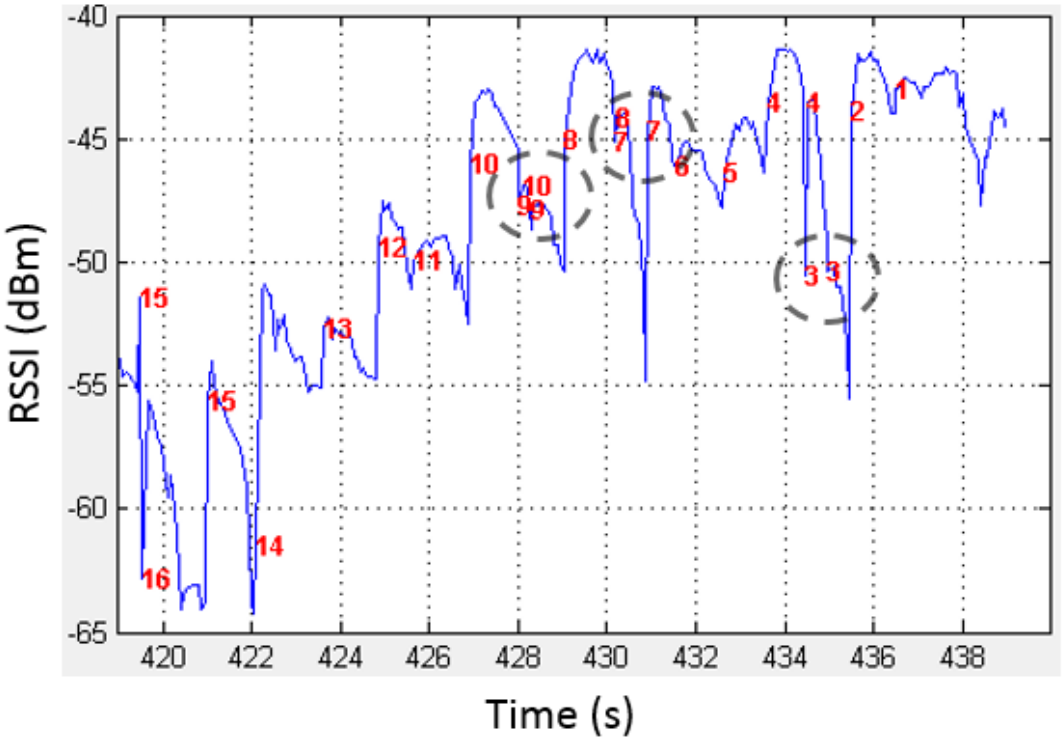

Figure 52: RSSI graph in time domain of the orientation estimation method.

RSSI measurement method: The RSSI measurement method does not have the same problem as the orientation estimation method, which is the inaccuracy of determining the precise beam direction. However, as only the neighboring

beams are measured the method can switch the beam in the wrong direction due to a strong side lobe of a beam. In addition, a weak beam between two good beams can break the communication. For instance, the method might not be able to get over a bad beam between two good beams as only the adjacent beams are measured. The performance of the RSSI measurement method is demonstrated in Figure 53. The example is similar than in Figure 52, where the device is moved to achieve vibration compensation from beam number 16 towards the beam number 1. The method overcomes the jumping between the beams that were discovered with the orientation estimation method. For instance, the beam is not switched from 10 to 9 until the beam number 9 have better RSSI. The beam number 3 is known to have low antenna gain in relative to its adjacent beams. The switching from beam number 4 to 3 almost broke the communication or at least reduced the performance. After switching to beam number 3 the beam number 2 is discovered instantly. This happens regarded that the beam number 2 could have provided better signal quality sooner.

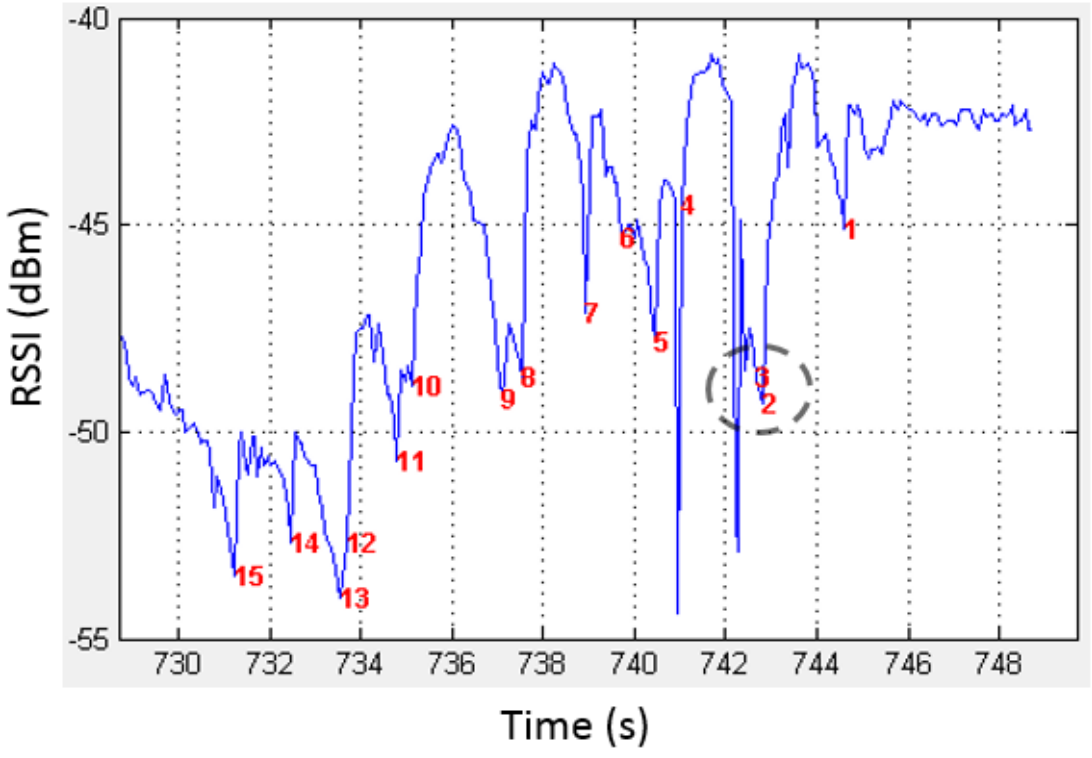

Figure 53: RSSI graph of the RSSI measurement method.

Hybrid method: The hybrid method was noted to overcome the problems faced with the other methods. For instance, the orientation estimation of the hybrid method can tolerate errors because only the approximate direction of the movement is needed. The performance of the hybrid method is provided in Figure 54, where the device is rotated from the beam number 16 towards the beam number 1. The graph does not show any jumping between beams as with the orientation estimation method. Additionally, the other methods had problems with the beam number 3 due to its low antenna gain. However, as the hybrid method measure the beams in the estimated direction of the movement, the method managed to skip the bad beam.

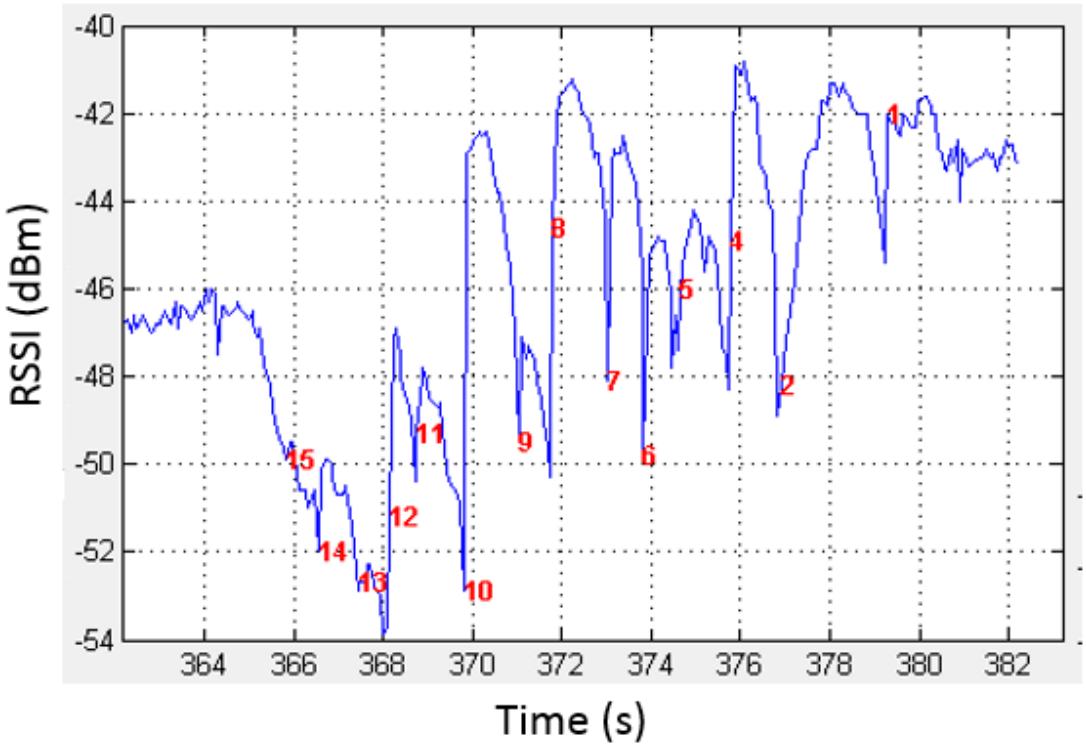

Figure 54: RSSI graph of the hybrid method.

6.3 Discussion and future work

Due to the inconsistency of the tests, the test results provided in 6.2.2 was noted to give only suggestive figures for the performance evaluation of the vibration compensation methods. However, further investigation in 6.2.3 showed consistency with the performance differences of the test results; the hybrid

steering has the best performance, the RSSI measurement method provided the second best performance, leaving the orientation estimation method with the worst performance. The problems of the orientation estimation method suggest that the vibration compensation should be implemented by applying measurements. The RSSI measurement method faced some problems due to the inequality between different beams that is caused by the poor antenna hardware used in the tests. The problems would most likely vanish with a better performance of the antenna system. However, even with the properly functioning antenna hardware the continuous measurements decrease the capacity of the radio link. Therefore, a method utilizing the measurements only when necessary would decrease the total time used for the measurements thus enhancing the throughput of the system in comparison with continuous measurements. Not only the hybrid method was discovered to have the best performance, the method also applies the measurements only during the movement of the device thus providing the suggested kind of a measurement scheme. However, the method has a down side in comparison with the implemented RSSI measurement method. Even though, the orientation estimation of the hybrid method tolerates some levels of errors, the orientation estimation still requires knowledge of the installations sites structure. Therefore, the RSSI measurement method would provide installation site independent vibration compensation. By modifying the RSSI measurement method in order to detect a movement, the measurements could be carried out only when necessary. For instance, the orientation sensor could be used only for detecting the vibration. However, utilizing the measurements in the direction of the movement would provide more reliable vibration compensation. With a method estimating the direction of the movement with reasonable accuracy for the variety of differently vibrating installation cases, a method like the hybrid method might be the most efficient way to implement the vibration compensations.

From the system point of view, the next development step of the system would be to implement the automatic link alignment and vibration compensation

methods with the HLP. The automatic link alignment procedure is controlled by the HLP and the BSP needs to follow the commands provided by the HLP. The vibration compensation methods that utilize the measurements require modifications to the HLP or to the physical layer of the modem. If the measurement periods are coordinated by the HLP, dummy data slots for instance could be transmitted during the measurement periods. If the measurement periods are provided by modem, the physical layer protocols should be modified to support the measurement. Another task for the future work is to implement a feedback procedure to support the measurement. For instance, the BSP could request the other end of the radio link to allocate every nth frame for the measurements. Therefore, the device performing the vibration compensation executes the neighbor beam measurements during these predefined frames. When the device decides to stop the measurements, a command is send. By implementing the feedback procedure in the system, the vibration compensation methods could be further developed to have variety of different features. For instance, the frequency of the measurement periods could be adjusted dynamically depending on the magnitude of the vibration. Another task for the future work is to investigate the sufficient frequency for the measurements periods. For instance, by measuring vibrations of the potential installation structures of the small cells, suggestive figures could be found to estimate the number of measurement periods needed for the vibration compensation.

6.4 Summary

This chapter described the tests and provided the analysis of the test results for the proof-of-concept system introduced in Chapter 5. The tests included the automatic link alignment tests and vibration compensation tests for the implemented methods. Two devices were used in the tests. The other device had the beam steering hardware while the other device was equipped with a horn antenna transmitting in a fixed direction at 70 GHz. The lens antenna device included the MATLAB application that recorded the data during the tests for later analysis. Due to the early stage of the project, hardware limitations

limited the testing of the system with the described configuration. For instance, the HLP is excluded from the tests, the TDD scheme of the modem is modified and the measurement periods of the vibration compensation methods are artificial. Additionally, due to the known fault of the antenna hardware, the beams on the lowest row of the antenna-array, denoting the beams from 1 to 16, have substantially higher antenna gain than the rest of the beams. Therefore, the beam steering tests are carried out with the beams at the lowest row.

Due to the hardware limitations, the HLP was not included in the tests. Therefore, the automatic link alignment was implemented by scanning through all the beams similarly like with the HLP. The automatic link alignment test was carried out by changing the positions of the lens antenna device and the automatic link alignment was started with the different orientations of the device. Overall, the test results showed that the system was capable of finding the best beam in the expected direction, as it was designed to do. The tests also showed that in some cases high RSSI values were found in the adjacent beams of the found beam. Additionally, RSSI values slightly above the noise level were found in random beams. The reason for the observed non-idealities might be caused by several reasons, including the wide beam width of the horn antenna, faults on the antenna hardware and reflections.

The vibration compensation tests were carried out by vibrating the lens antenna device from side to side resulting beam steering between the beams from 1 to 16. The tests showed that the hybrid method had the best performance while the RSSI measurement method provided the second best performance, leaving the orientation estimation method with the worst performance. During the tests, several problems were identified explaining the performance differences between the methods. The biggest problem for the orientation estimation method is to estimate the exact direction where the beam of the other device is pointing. In addition, the gain and positions of the beams include variations. Due to the inaccuracies, wrong beam steering decisions could be made. The problems for the RSSI measurement method included the strong side lobes of the adjacent beams and unequal antenna gain

between the beams. The method might select a side lobe of the adjacent beam in a wrong direction or stuck to a beam due to a bad beam between two good beams. The hybrid method was noted to overcome the problems faced with the other two methods. As the hybrid method performs the measurements on the direction of the movement, the method can tolerate more errors in the orientation estimation and can jump over the bad beams. Moreover, the hybrid method performs the measurement only when necessary thus reducing the overhead generated by the measurements.

The test results of the vibration compensation tests suggest that a reasonable way to implement the vibration compensation is to apply measurements. Additionally, the measurements should be carried out only when necessary. The next step for the development of the vibration compensation methods is to implement the measurement periods by the HLP or by the modem. Vibration compensation utilizing measurements during desired periods requires a feedback procedure, between the communicating devices, to decide the time instants of the measurement periods. For instance, the HLP could transmit dummy data slots during the requested measurement periods, or the modems physical layer protocols could be modified to support the measurements. Additionally, an adequate frequency for the measurements should be investigated with vibration measurements on the potential installation sites of the small cells.

7 Summary and conclusions

The mobile data volumes have been increasing during the past year. Various data forecasts suggest that the mobile data volumes experience an exponential growth in the near future. Although the mobile networks have evolved from the 1G circuit switched voice networks towards the emerging 4G all-IP broadband networks, further enhancements are required to fulfill the future demands.

One source of better network performance is the cell densification. The closely placed base stations are also known as small cells. In a typical small cell scenario, the small cell base stations are located in city areas of high demands where the base stations are installed on structures like building walls, lamp posts and often utility poles. The high number of small cell base stations in unconventional locations sets new challenges and requirements for the backhaul. Traditionally, the backhaul denotes the transport infrastructure from the base station to the core network. In the context of small cells, the backhaul denotes the first mile access from the small cell base station towards the core network. As the provisioning of a traditional wired backhaul to a typical small cell location might be unreasonable, the wireless solutions come in question. Rather than having an optimal solution, the small cell backhaul includes a set of different solutions.

The most important requirements for the small cell backhaul are the low cost of deployment and high capacity. Millimeter-wave frequencies provide great potential to fulfill these requirements. In the context of small cell backhaul, the millimeter-wave frequencies denote the 60 and 70/80 GHz frequencies also known as the V- and E-band. These frequency bands provide several gigahertz of unlicensed or lightly licensed spectrum, fulfilling the low cost and high speed requirement. Another significant feature of these frequencies is the high signal attenuations caused by the free space path loss, atmospheric absorption and rain. To overcome the attenuations, antenna gain around 30 to 40 dBi is required reducing the beam width of the antenna to less than a few degrees. The

narrow beam millimeter-wave signals do not produce much interference for the nearby devices as the signal do not travel far beyond its intended destination. The downside of the millimeter-wave frequencies is that the narrow beams have to be carefully aligned at both ends of the radio link. Additionally, wind or other external forces can vibrate the installation structure causing temporary misalignments. To overcome these disadvantages, beam steering is needed to automatically align the radio link and to compensate the vibrations.

Beam steering denotes that the direction of the narrow antenna beam can be changed. Technologies that provide the beam steering capabilities include for instance beamforming and integrated lens antennas with feed-array. Beamforming utilizes an array of antennas. The directivity and gain are achieved by adjusting the gain and phases between the antennas. For instance, the WLAN standard 802.11 ad utilizes beamforming at 60 GHz to automatically align the radio link. Another potential technology is the integrated lens antenna with a feed array. The lens has an elliptical or hemispherical shape that collimates the radiation from the feed array. Only one antenna element is used at a time and beam steering is achieved by switching between the antenna elements. The direction of the beam depends on the location of the active antenna element.

The main scope of this master's thesis was to implement beam steering functionalities into a proof-of-concept millimeter-wave small cell backhaul system developed by Nokia Solutions and Network. The main author's contribution was the development and implementation of the beam steering methods to the beam steering processor. The implemented beam steering methods included automatic link alignment and three different vibration compensation methods developed by the author. Additionally, a MATLAB GUI and its functions were developed by the author for the development and testing of the system. The beam steering of the system is realized by an integrated lens antenna with 4x16 feed-array. Thereby, the system has 64 beams in total, 16 beams on each of the four rows. The beam widths of the antennas are around 2.5 degrees. The beam steering of the system is handled by a beam steering

processor that selects the active beam. The automatic link alignment method of the system is predefined by the higher layer protocols of the system and the beam steering processor makes the beam switching decisions based on the commands of the higher layer protocols. The vibration compensation methods developed by the author included the orientation estimation method, the RSSI measurement method, and a hybrid of the methods. The orientation estimation method is implemented based on the author's derived pole sway calculations in Chapter 4. The method uses the orientation estimations provided by an orientation sensor to calculate the current beam. The RSSI measurement method measures the signal strength of the neighboring beams during predefined time frames and switches a beam if a better beam is found. The hybrid method utilizes similar neighbor measurements in the direction of the movement when the orientation estimation suggests switching a beam.

The tests conducted by the author included the automatic link alignment test and vibration compensation tests for the implemented methods. As the development of the system is in a very early stage, hardware limitations prevented the testing of the system and methods in their final form. Due to the inequality between the beam gains, the test setups were organized to induce beam steering with the beams in the lowest row of the antenna array. Additionally, the automatic link alignment tests were carried out without the higher layer protocols simply by scanning through all of the beams like with the higher layer protocols.

The automatic link alignment test was carried out by starting the procedure with different orientations of the device. The automatic link alignment tests demonstrated that the system is capable of aligning to a beam in the expected direction. The vibration compensation tests were carried out by vibrating the device from side to side. The vibration compensation tests showed that the orientation estimation method had the worst performance, due to the difficulty of estimating the exact point where the beam of the other device is pointing inside the selected beam. With other discovered non-idealities including the inaccuracy of the pole sway model, orientation estimation and beam positions,

implementing a vibration compensation method solely based on orientation estimation might not be a reasonable solution. The RSSI measurement method provided the second best performance thus having problems with strong side lobes and unequal antenna gain between the beams. The method might select a side lobe of the adjacent beam in a wrong direction or stuck to a beam due to a bad beam between two good beams. The hybrid method demonstrated the best performance by overcoming the problems of the two other methods. Because the hybrid method measures the RSSI in the direction of the movement, the method can tolerate more errors in the orientation estimation as the method solely based on orientation estimation.

Overall, the test of the proof-of-concept system showed promising results. Despite the non-idealities of the system still under development, the automatic link alignment test and the vibration compensation tests demonstrated that the system has potential to fulfill the final objectives of the project. The author's suggestion for the future development would be to continue the development of a measurement based vibration compensation method and study the necessity of the orientation sensor due to the discovered inaccuracies. Before anything, the vibration compensation method cannot depend on the vibration characteristics of the installation site. Another future task would be to implement the measurement periods requiring a feedback procedure to notify the start and stop instances of the measurement periods. The measurement periods should be implemented into the higher layer protocols or the physical layer protocols of the modem should be modified to support the measurements. With the feedback mechanism implementing the measurement periods, the vibration compensation methods could be further developed to have a variety of different features. Moreover, the vibration characteristics of the potential installation sites of small cells should be studied to identify the required amount of measurements per seconds.

References

[1] 4G Americas, "Mobile Broadband Explosion The 3GPP Wireless Evolution," August 2013.

[2] Nokia Siemens Networks, ”2020: Beyond 4G Radio Evolution for the Gigabit Experience,” 2011.

[3] Ericsson, ”Ericcson Mobility Report on the Pulse of the Network Society,” June 2013.

[4] Cisco, ”Cisco Visual Networking Index: Global Mobile Data Traffic Forecast Update, 2012–2017,” 2013.

[5] ABI Research, ”Small Cell Backhaul,” 2013.

[6] NGMN Alliance, ”Small Cell Backhaul Requirements,” 2012.

[7] Small Cell Forum, ”Backhaul technologies for small cells Use cases, requirements and solutions,” 2013.

[8] G. Nan, Q. Rober C, M. Shamoin S and T. Kazuaki, "60-GHz Millimeter-Wave Radio: Principle, Technology, and New Results," *EURASIP Journal on Wireless Communications and Networking,* vol. Volume 2007, p. 8, 2006.

[9] ITU-R, *Recommendation ITU-R P.676-10: Attenuation by atmospheric gases,* 09/2013.

[10] Loea Corporation, ”Understanding Millimeter Wave Wireless Communication,” San Diego, 2008.

[11] S. Hur, T. Kim, D. J. Love, J. V. Krogmeier, T. A. Thomas and A. Ghosh, "Millimeter Wave Beamforming for Wireless Backhaul and Access in Small Cell Networks," *IEEE Transaction on Communications, Vol. 61, No. 10,* no.

October 2013.

[12] J. Salmelin ja E. M. Metsala, Mobile backhaul, Wiley, 2012.

[13] A. R. Mishra, Fundamentals of Cellular Network Planning and Optimisation : 2G/2. 5G/3G- Evolution To 4G, Hoboken, NJ, USA: Wiley, 2004.

[14] M. Sauter, From GSM to LTE : An Introduction to Mobile Networks and Mobile Broadband, Hoboken, NJ, USA: Wiley, 2010.

[15] M. R. Bhalla ja A. V. Bhalla, ”Generations of Mobile Wireless Technology: A Survey,” *International Journal of Computer Applications (0975 – 8887),* 2010.

[16] A. Kumar, D. Y. Liu, D. J. Sengupta and Divya, "Evolution of Mobile Wireless Communication Networks: 1G to 4G," *IJECT,* vol. 1, no. 1, 2010.

[17] Tektronix Communications, ”LTE Networks: Evolution and Technology Overview,” October 2010.

[18] Alcatel Lucent, ”The LTE Network Architecture,” 2009.

[19] 4G Americas, ”Meeting the 1000x challenge: The Need for Spectrum, Technology and Policy Innovation,” October 2014.

[20] CBNL (Cambridge Broadband Networks), ”Small cell backhaul: the big picture. An update on small cell backhaul market progress, requirements and solutions,” 2013.

[21] Ericsson Research, ”Small-Cell Wireless Backhauling, A Non-Line-of-Sight Approach for Point-to-Point Microwave Links”.

[22] Tellabs, ”Small Cell Backhaul: What, Why & How?,” 2012.

[23] Ericsson, ”It all comes back to backhaul,” 2012.

[24] ITU-R, *Recommendation ITU-R P.838-3: Specific attenuation model for rain for use in prediction methods.*

[25] ITU-R, *Recommencation ITU-R PN.837-1: Characteristics of precipitation for propagation modeling.*

[26] A. Karttunen, Doctoral Disseration: Millimetre and submillimetre wave antenna design using ray tracing, Aalto University publication series, 2013.

[27] J. Ala-Laurinaho, A. Karttunen, J. Säily, A. Lamminen, R. Sauleau ja A. V. Räisänen, ”MM-Wave Lens Antenna with an Integrated LTCC Feed Array for Beam Steering,” tekijä: *Antennas and Propagation (EuCAP)*, April 2010.

[28] A. Artemenko, A. Mozharovskiy, A. Maltsev, R. Maslennikov, A. Sevastyanov and V. Ssorin, "2D Electronically Beam Steerable Integrated Lens Antennas for mmWave Applications," in *42nd European Microwave Conference (EuMC)*, 2012.

[29] A. Artemenko, A. Mozharovskiy, A. Sevastyanov, V. Ssorin ja R. Maslennikov, ”High Gain Lens Antennas for 71-86 GHz Point-to-Point Applications,” tekijä: *43rd European Microwave Conference*, 2013.

[30] B. Li, Z. Zhou, H. Zhang and A. Nallanathan, "Numerical Optimization Based Efficient Beam Switching for 60GHz Millimeter-wave Communications," in *International Confrence on Communications in China(ICCC): Wireless Communication Systems (WCS)*, 2013.

[31] S. Hur, T. Kim, D. J. Love, J. V. Krogmeier, T. A. Thomas and A. Ghosh, "Multilevel Millimeter Wave Beamforming for Wireless Backhaul," in *The Second GlobeCom 2011 Workshop on Femtocell Networks*.

[32] ”Digilent,” [Online]. Available: https://digilentinc.com/Products/Detail.cfm?NavPath=2,892,894&Prod=

CHIPKIT-MAX32.

[33] ”Microchip Technology,” Microchip, [Online]. Available: http://www.microchip.com/wwwproducts/Devices.aspx?product=PIC32MX795F512L.

[34] Pololu: Robotics & Electronics, [Online]. Available: http://www.pololu.com/product/1256.

[35] Sparkfun, [Online]. Available: https://www.sparkfun.com/products/759.

[36] Sparkfun, [Online]. Available: https://www.sparkfun.com/products/9568.